

**SIMULTANEOUS GAS ABSORPTION
AND CHEMICAL REACTION**

SIMULTANEOUS GAS ABSORPTION
AND
LIQUID PHASE CHEMICAL REACTION

By

KWOK-HING PANG, B.A.Sc.

A Thesis
Submitted to the Faculty of Graduate Studies
In Partial Fulfilment of the Requirements
for the degree of
Master of Engineering

McMaster University
March 1965

MASTER OF ENGINEERING (1965)
(Chemical Engineering)

McMASTER UNIVERSITY
Hamilton, Ontario

TITLE: Simultaneous Gas Absorption and Liquid Phase
Chemical Reaction

AUTHOR: Kwok-Hing Pang, B.A.Sc. (University of British Columbia)

SUPERVISORS: Dr. A. I. Johnson and Dr. A. E. Hamielec

NUMBER OF PAGES: 152

SCOPE AND CONTENTS:

The present apparatus was used to obtain rate data for the absorption of oxygen in a catalysed liquid phase reaction with acetaldehyde. The effects of several system parameters, namely, acetaldehyde concentration, catalyst concentration, partial pressure of oxygen and temperature on the rate of absorption were studied.

An attempt was made to correlate absorption rates and product distribution with mathematical models based on the film theory and existing kinetic models proposed by Bolland and Bawn. Absorption rates predicted by these semi-empirical correlations are compared with experimental values.

The differential equations involving diffusion with chemical reaction were solved on the digital computer IBM 7040 and the analog computer PACE TR10

NOMENCLATURE

A	oxygen
A_e	constant in Arrhenius Equation
A_{-}	area, ft^2
AMP	acetaldehyde monoperacetate
B	acetaldehyde = ACH
C	peracetic acid = ACOOH
C_A	concentration of oxygen in liquid, gm-moles/ft^3
C_{Ai}	interfacial concentration of oxygen in liquid, gm-moles/ft^3
C_{Ao}	initial bulk concentration of oxygen in liquid, gm-moles/ft^3
C_{AL}	bulk concentration of oxygen in liquid, gm-moles/ft^3
C_{AMP}	concentration of AMP in liquid, gm-moles/ft^3
C_B	concentration of acetaldehyde in liquid, gm-moles/ft^3
C_{BL}	bulk concentration of acetaldehyde in liquid, gm-moles/ft^3
C_C	concentration of peracetic acid in liquid, gm-moles/ft^3
C_{CL}	bulk concentration of peracetic acid in liquid, gm-moles/ft^3
C_{Ca}	concentration of cobaltous ion in liquid, gm-moles/ft^3
C_I	intensity of light
$C_{BZ_2O_2}$	concentration of benzoyl peroxide in liquid, gm-moles/ft^3
C_{RO_2H}	concentration of hydroperoxide in liquid, gm-moles/ft^3
C_n	concentration of component n in liquid, gm-moles/ft^3
D_A	diffusivity of oxygen in ethyl acetate, ft^2/hr
D_B	diffusivity of acetaldehyde in ethyl acetate, ft^2/hr
D_C	diffusivity of peracetic acid in ethyl acetate, ft^2/hr

D_n	diffusivity of component n in ethyl acetate, ft^2/hr
F	gas flow rate, ft^3/hr
H	step function, ft^3/hr
k_1^b, k_2^b k_1^w, k_2^w k_1^l, k_2^l k k_n k_{Co} k_{cl} k_n''	} reaction rate constants defined by individual rate equations
k_L	mass transfer coefficient in the liquid phase, ft/hr
k_L^*	mass transfer coefficient with chemical reaction in liquid phase, ft/hr
k_g	mass transfer coefficient in the gas phase, $\text{gm-moles}/\text{ft}^2\text{-hr-atm}$
K_L	overall liquid mass transfer coefficient, ft/hr
K_L^*	overall liquid mass transfer coefficient with chemical reaction, ft/hr
K	equilibrium constant = $C_B C_C / C_{AMP}$
m	Henry's constant = P_2/X_2 atm/mole-fraction
N_A	rate of absorption per unit area, $\text{gm-moles}/\text{ft}^2\text{hr}$
P_2	partial pressure of gas, atm
P_2^o	vapor pressure of gas, atm
P_g	partial pressure of oxygen in the gas phase, atm.
P_o	partial pressure of organic vapor in the gas, atm.
P_R	reduced pressure
P_T	total pressure, atm.
r	rate of initiation

r_L	correlation coefficient
R	gas constant, litre-atm/moles ^o K
RH	hydrocarbons
ROOH	hydroperoxide
$R' =$	$T_v(22400)/273$, ml.
$R'' =$	$T_b(22400)/273$, ml.
S	interfacial concentration gradient of A, gm-moles/ft ⁴
t	time, minutes
T	temperature, ^o C.
T_b	temperature in the gas burette, ^o K
T_R	reduced temperature
T_v	temperature in the vessel, ^o K
x	depth of the liquid from the interface, ft
$X_R = X_A$	reaction zone, ft
X_L	film thickness for physical mass transfer, ft
X_2	solubility of the gas in liquid, mole fraction
V_A	molal volume of component A at normal boiling point, c.c.
V_{AS}	volume of gas to saturate a given amount of liquid = $C_{A1} \times V_R \frac{T_b}{273} (22400)$, ml
V_g	volume of gas space in vessel, ml
V^l	molal volume of the liquid, ml
V_R	volume of liquid in vessel, ml
V_{A1}	volume of oxygen in vessel at time t , ml
Y_{A1}	mole fraction of oxygen in vessel at time t
Y_{OB}	mole fraction of oxygen in gas burette
Z	compressibility factor

Ψ	association parameter
η	viscosity, ' cp.
δ	solubility parameter
Φ	enhancement factor
ΔE	activation energy, Kcal/gm-mole
ρ	chain length of a chain reaction
$[\]$	concentration
ΔH	enthalpy of vaporization Kcal/gm-mole
ΔH_{app}	apparent enthalpy of vaporization, Kcal/gm-mole

TABLE OF CONTENTS

	PAGE
I INTRODUCTION	1
II LITERATURE SURVEY	3
II.1 Chemistry and Kinetics of Autoxidation	3
II.2 Theory of Mass Transfer with Chemical Reaction	4
II.2.1 Steady State Mass Transfer	4
II.2.1.1 Mass Transfer With Chemical Reaction Following Bolland's Mechanism	7
II.2.1.2 Mass Transfer with Chemical Reaction Following Bawn's Mechanism	8
II.2.2 Unsteady State Mass Transfer with Chemical Reaction of Zero th Order	10
III SCOPE	13
IV EXPERIMENTAL DETAILS	14
IV.1 Description of Apparatus	14
IV.2 Advantages and Disadvantages of Apparatus	17
IV.3 Experimental Procedure	18
V RESULTS AND INTERPRETATIONS	20
V.1 Physical Mass Transfer	20
V.2 Effect of General Variables on Mass Transfer With Chemical Reaction	21
V.2.1 Acetaldehyde Concentration	22
V.2.2 Catalyst Concentration	24
V.2.3 Partial Pressure of Oxygen	26
V.2.4 Temperature	27
V.3 Unsteady State Mass Transfer Studies	29
V.4 Effect of Product Distribution and Mathematical Models for Steady-State Mass Transfer	32
V.4.1 Mathematical Model Using Bawn's Reaction Mechanism	33
V.4.2 Mathematical Model Using Bolland's Reaction Mechanism	34
VI CONCLUSIONS AND RECOMMENDATIONS	38
VII EXPERIMENTAL ERRORS AND STATISTICAL EVALUATION	41

VIII LITERATURE CITED	PAGE 43
ACKNOWLEDGEMENT	45

APPENDIX

I LITERATURE SURVEY	46
I I.1 Chemistry and Kinetics	46
I.1.1 Kinetics and Mechanism	46
I.1.2 Side Reactions	52
I.1.3 Formation and Decomposition of A.M.P.	53
I.1.4 The Role of Catalyst	54
I.2 Theory of Diffusion with and without Chemical Reaction	55
I.2.1 Physical Mass Transfer and Enhancement Factor	55
I.2.2 Steady-State Mass Transfer in Stagnant Film of Finite Thickness	56
I.2.2.1 First Order with Respect to Component A	59
I.2.2.2 Second Order with Respect to A and B	62
I.2.2.3 Reaction Mechanism of Complex Nature	64
I.2.2.4 Kinetic Equations and Hydrodynamics in the Film	66
I.2.3 Unsteady-State Diffusion in Stagnant Liquid of Semi-infinite Thickness	67
I.2.3.1 First Order with Respect to Component A	69
I.2.3.2 Zeroth Order	71
II EXPERIMENTAL DETAILS	78
II.1 Description of Apparatus	78
II.2 Some Illustrations of Hydrodynamic Conditions and Limitations	80
II.3 Leakage	80
II.4 Preliminary Studies on the Effect of Several Variables On Mass Transfer	81
II.4.1 Acetaldehyde Concentration	82
II.4.2 Catalyst Concentration	82
II.4.3 Partial Pressure of Oxygen	82
II.4.4 Temperature	83
II.5 Unsteady-state Mass Transfer Studies	83
II.6 Steady-State Mass Transfer Studies	83
II.7 Mass Transfer Without Chemical Reaction	84
III DERIVATION OF WORKING EQUATIONS AND SAMPLE CALCULATIONS	85
III.1 Mass Transfer Coefficient Without Chemical Reaction	85
III.2 Mass Transfer Coefficient with Chemical Reaction and Enhancement Factor	86
III.3 Mass Transfer Coefficient with Chemical Reaction at Various Partial Pressure of Oxygen	88

	PAGE
III.4 Reaction Rate Constants from Unsteady-State Absorption Data	93
IV TABLE OF EXPERIMENTAL OBSERVATIONS	96
V EXPERIMENTAL ERRORS AND STATISTICAL EVALUATION	105
V.1 Estimation of Experimental Errors	105
V.2 Statistical Evaluation of the Correlations	107
V.2.1 Linear Correlation of Two Variables by the Least Squares Method	107
V.2.2 Statistical Evaluation of First Correlation (Bawn's Reaction Mechanism)	109
V.2.3 Statistical Evaluation of Second Correlation (Bolland's Reaction Mechanism)	109
VI DERIVATION OF REACTION RATE EQUATIONS	111
VI.1 Bolland's Rate Equation for the Oxidation of Hydrocarbons	111
VI.2 Bawn's Rate Equation for the Oxidation of Acetaldehyde	113
VII SOLUBILITY OF OXYGEN IN ETHYL ACETATE	117
VIII ESTIMATION OF DISPLACEMENT TIME	122
IX ANALYTICAL METHODS	124
IX.1 Peracetic Acid	124
IX.2 Acetic Acid	125
IX.3 Acetaldehyde	125
IX.4 Acetaldehyde Monoperacetate	126
IX.5 Precision of Analytical Methods	127
X ESTIMATION OF REACTION RATE CONSTANT FROM BAWN'S EXPERIMENTAL DATA	128
XI ESTIMATION OF DIFFUSIVITIES OF LIQUIDS	129
XII PRELIMINARY STUDIES ON PRODUCTION OF PERACETIC ACID BY VERTICAL COCURRENT REACTOR	130
XII.1 Summary	130
XII.2 Apparatus and Experimental Details	132
XII.3 Results	133
XII.4 Discussions of Results	136
XIII DIGITAL COMPUTER PROGRAMS	138

	PAGE
XIII.1 Correlation Using Bolland's Mechanism	138
XIII.2 Diffusion with Second Order Chemical Reaction	141
XIII.3 Computer Program for Statistical Evaluation	141
XIV ANALOG COMPUTER CIRCUIT	148
LITERATURE CITED	150

APPENDIX II

FIGURE INDEX

<u>Figures in Main Body</u>	PAGE
1 Concentration Profiles in the Film	9
2 Simplified Diagram of Apparatus	15
3 Detailed Diagram - Reaction Vessel	16
4 Effect of Acetaldehyde Concentration on Enhancement Factor	23
5 Enhancement Factor Versus Catalyst Concentration	25
6 Mass Transfer Coefficient versus Acetaldehyde Concentration at Various Temperatures	28
7 $\log(k_{Co})$ versus $1/T$	31
8 Comparison of Theoretical and Experimental Results (Modified Bawn's Mechanism)	35
9 Extent of Oxidation	35
10 Comparison of Theoretical and Experimental Results (Bolland's Modified Mechanism)	36
 <u>Figures in Appendices</u>	
1A Simplified Picture of Simultaneous Steady-State Diffusion and Chemical Reaction in Liquid Film	58
2A Van Krevelen's Solution of the Diffusion with Fast Second Order Reaction Equation	58
3A Simplified Picture of Simultaneous Unsteady-State Diffusion and Chemical Reaction	68
4A Concentration Profiles of Solute in Liquid ($C_{AO} > 0$)	75
5A Concentration Profiles of Solute in Liquid ($C_{AO} = 0$)	75
6A Absorption of Oxygen in Ethyl-Acetate	87
7A Absorption of Oxygen in Acetaldehyde Solution	89

	PAGE
8A Material Balance Around Gas Space	89a
9A $\log (V_{oi} - T_v/T_b(1-Y_{oB})V_L)$ Versus Time	95
10A Unsteady-State Absorption of Oxygen	95
11A Schematic Diagram of Vertical Cocurrent Reactor	131
12A Weight % of Products and Reactant Versus Time	134
13A % Yield of Peracetic Acid and Acetic Acid Versus Catalyst Concentrations	135
14A RKK Versus RK	140
15A Algorithm -- Digital Computer Programme	148
16A Analog Computer Circuit	150

TABLE INDEX

Tables in Main Body

	PAGE
1 Mass Transfer Coefficient Without Reaction	21
2 Effect of Partial Pressure on Mass Transfer	27
3 Comparison of Reaction Rate Constants	30
4 Estimated Experimental Errors	41
5 Precision of Analytical Methods	41
6 Statistical Evaluation	42

Tables in Appendices

1A Relative Magnitude of k_3 and k_6	50
2A Multiplication Constants for Calculating k_L^* at Various Partial Pressures of Oxygen	93
3A Mass Transfer Coefficient Without Chemical Reaction	96
4A Mass Transfer Coefficient and Enhancement Factor at Various Acetaldehyde Concentrations	97
5A Mass Transfer Coefficient and Enhancement Factor at Various Catalyst Concentrations	98
6A Mass Transfer Coefficient and Enhancement Factor at Various Temperatures and Acetaldehyde Concentrations	99
7A First Order Reaction Rate Constants from Unsteady-State Absorption Data	100
8A Zero th Order Reaction Rate Constants from Unsteady-State Absorption Data	100
9A Reaction Rate Constants using Bawn's Mechanism	101
10A Predicted Absorption Rates Using First Correlation (Bawn's Reaction Mechanism)	102

	PAGE
11A Product Distribution and Absorption Rates	103
12A Predicted Absorption Rates Using Second Correlation (Bolland's Reaction Mechanism)	104
13A Comparison of Solubility of Oxygen in Ethyl Acetate by Various Methods	119
14A Solubility of Oxygen in Ethyl Acetate by Winkler's Method	119
15A Vapor Pressure of Oxygen	120
16A Solubility Parameters by Equation (155A)	120
17A Displacement Time	123
18A Precision of Analytical Methods	127
19A Diffusivities of Liquids	129
20A Analytical Results of a Typical Experiment	133
21A Yield of Peracetic Acid and Acetic Acid at Various Catalyst Concentrations	136
22A Equilibrium Constant	136
23A Concentrations and Concentration Gradient Versus Distance from Interface	142
24A Maximum Values of Variables	148

I INTRODUCTION

In recent years, an increased emphasis has been placed on solving the problem of predicting the effect of a simultaneous chemical reaction on the rate of gas absorption. This is due, in part, to the increasing number of industrial applications of gas - liquid reactions in chemical processes; it is also due to the possibility that studying the effect of a chemical reaction may offer a means of inferring the kinetics of the reaction and the mechanism of the absorption process.

Direct oxidation by molecular oxygen is a widespread phenomenon. It has given rise to several important modern processes in the chemical industry, such as, the production of phenol from cumene, acetic acid from light paraffins, and peracetic acid from acetaldehyde, which is the primary concern of this study.

In these processes, a direct contact of the gas with the liquid is necessary. As the design of contacting equipment for absorption requires a knowledge of rates of transfer, the purposes of this research are two - fold:

- (1) to make preliminary studies of the effect of several variables on the rate of absorption;
- (2) to attempt to correlate absorption rates with product distribution by a mathematical model based on the film theory.

Apart from the fact that it is simple to construct and to operate, the stirred vessel was chosen for this investigation, because

the interfacial area was known and the absorption rates were fast enough to build up a sufficient concentration of the product within a reasonable period of time for analysis using simple titration methods.

II LITERATURE SURVEY

II.1 Chemistry and Kinetics of the Autoxidation of Acetaldehyde

The basic theory of liquid--phase oxidation of organic materials was elucidated by Bolland, Gee and Garner (1,2). It was found that many of these oxidations are chain reactions and because of their characteristic of producing hydroperoxide which further accelerates the reaction, they are often referred to as autocatalytic.

The oxidation of cumene was studied by Twigg (3). The simplicity of this oxidation is due to the activation of the tertiary hydrogen atom adjacent to the benzene ring. The mechanism leading to the production of hydroperoxide is believed to be the same in the case of acetaldehyde which also possesses a hydrogen atom activated by a carbonyl group.

Based on his studies of hydrocarbon oxidation, Bolland (1) has outlined a possible reaction scheme which, Twigg (3) believed, can be applied equally well to aldehydes. Using Cobalt salts as catalyst, the resulting simplified rate equation is as follows:

$$-\frac{dC_A}{dt} = k C_C^{\frac{1}{2}} C_{Ca}^{\frac{1}{2}} C_B \quad (1)$$

where C_A , C_{Ca} , C_B , C_C are the concentrations of oxygen, catalyst, acetaldehyde and peracetic acid respectively; k is the reaction rate constant.

Bawn and Williamson (4) were the first workers to investigate experimentally the kinetics of the oxidation of acetaldehyde using

cobaltous acetate as catalyst. They have concluded that the rate of oxidation is proportional to both the acetaldehyde and the catalyst, but independent of peracetic acid concentration. The rate equation is:

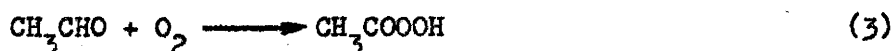
$$\frac{-dC_A}{dt} = k^1 C_B C_{Ca} \quad (2).$$

where k^1 is the reaction rate constant.

The oxidation of acetaldehyde when catalysed by traces of metal salts also gives rise to a number of products, the distribution of which is governed critically by temperature.

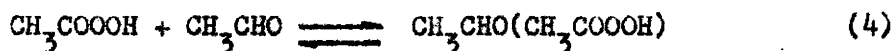
Generally, at temperatures between 0° and 20°C . the reaction can be said to proceed in three well-defined stages:

- (1) the oxidation of acetaldehyde to peracetic acid



- (2) the reaction of peracetic acid with acetaldehyde to give an addition compound acetaldehyde monoperacetate (AMP) which is

in equilibrium with its components



- (3) the reaction of acetaldehyde with peracetic acid to form acetic acid



II.2 Theory of Mass Transfer with Chemical Reaction

II.2.1 Steady - State Mass Transfer

Mathematical models for predicting the effect of chemical reaction on the rate of gas absorption were first developed by Hatta (5,6).

and Davis and Crandall (7) based on the assumption that the resistance to diffusion is concentrated within a thin liquid film adjacent to the gas - liquid interface, while the main body is so thoroughly mixed that no concentration gradient exists within it.

The assumption of two such films, one in the gas and one in the liquid, is the basis of Whitman's (8) two - film theory and the resulting concept of resistances in series which can be expressed as:

$$\frac{1}{K_L^*} = \frac{1}{mk_g} + \frac{1}{k_L^*} \quad (6)$$

or

$$\frac{1}{K_g^*} = \frac{1}{k_g} + \frac{m}{k_L^*} \quad (7)$$

where K_L^* and K_g^* are overall mass transfer coefficients based on the liquid and the gas; k_g and k_L are mass transfer coefficients of the gas and the liquid respectively; * indicates mass transfer with reaction.

The rate of absorption is given by:

$$N_A = k_L^* (C_{A1} - C_{AL}) \quad (8)$$

$$= K_L^* (C_{Ag} - C_{AL}) \quad (9)$$

where C_{Ag} is the hypothetical concentration of oxygen in equilibrium with its partial pressure in the gas phase; C_{AL} is the concentration of oxygen in the bulk of the liquid.

However, it is useful to express the effect of chemical reaction on gas absorption in terms of an enhancement factor, E which is defined as

$$E = \frac{k_L^*}{k_L} \quad (10)$$

where k_L^* and k_L are obtained under almost identical hydrodynamic conditions. It is hoped that by introducing ϕ the effect of the complex hydrodynamics of the experimental system on k_L^* and k_L may be cancelled out.

In order to simplify the situation so that the idealized model may be applied to interpret experimental data the following assumptions are necessary:

- (1) The gas phase resistance is negligible compared to the liquid so that $K_L^* \doteq k_L^*$ and $C_{Ai} \doteq C_{Ag}$
- (2) The liquid surface is continuously saturated with the gas.
- (3) The concentration of the dissolved gas in bulk of the liquid is zero or nearly zero when reaction occurs.
- (4) Hildebrand's semi - empirical equation (9) for the estimation of the solubility of oxygen in ethyl - acetate is applicable.
- (5) The gas phase is saturated with acetaldehyde and peracetic acid vapors so that there is no transfer of these materials across the interface.
- (6) The liquid contains mostly ethyl acetate and thus the effect of bulk flow in multi-component systems can be considered negligible.
- (7) All physical properties including diffusivities, densities and viscosities are virtually constant throughout the liquid.

With the above assumptions the film theory differential equation can be derived for component n as:

$$D_n \frac{d^2 C_n}{dx^2} = \text{rate of change of concentration of component n} \quad (11)$$

where D_n is the diffusivity of component n in the liquid.

The right - hand - side of equation (11) derived from the kinetics

of the reacting system may be a function of the concentrations of reactants or products. ~~W~~ Equations analogous to equation (11) can be written for n components and solved simultaneously subjected to known boundary conditions.

II.2.1.1 Mass Transfer With Chemical Reaction Following Bolland's Mechanism

Adopting Bolland's reaction mechanism for the autoxidation of acetaldehyde, taking into account the side reaction of acetaldehyde and peracetic acid to form acetic acid and keeping C_{Ca} constant, equation (11) can be written for various components as

$$D_A \frac{d^2 C_A}{dx^2} = k_1^b C^{\frac{1}{2}} C_B \quad (12)$$

$$D_B \frac{d^2 C_B}{dx^2} = k_1^b C^{\frac{1}{2}} C_B + k_2^b C C_B \quad (13)$$

$$D_C \frac{d^2 C_C}{dx^2} = -k_1^b C^{\frac{1}{2}} C_B + k_2^b C C_B \quad (14)$$

where $k_1^b = k C_{Ca}^{\frac{1}{2}}$ and k_2^b is the reaction rate constant for the reaction given by equation (5).

The boundary conditions are:

$$(1) \text{ at } X = 0, \quad C_A = C_{Ai}, \quad \frac{dC_A}{dx} = S, \quad \frac{dC_B}{dx} = 0, \quad \frac{dC_C}{dx} = 0 \quad (15)$$

(assumption (5))

where S , according to Fick's First Law, is given by: $S = -NA/DA$

$$(2) \text{ At } X_R \leq X \leq X_L, C_A = 0, \frac{dC_A}{dx} = 0, \text{ no reaction} \quad (16)$$

(Assumption (3))

where X_R is defined as the reaction zone and X_L is the film thickness.

Furthermore, as $C_A = 0$ the first reaction term in equation (13) and (14) vanishes and hence

$$D_B \frac{d^2 C_B}{dx^2} = k_2^b C_C C_B \quad (17)$$

$$D_C \frac{d^2 C_C}{dx^2} = k_2^b C_C C_B$$

$$(3) \text{ At } X = X_L, C_B = C_{BL}, C_C = C_{CL} \quad (18)$$

The resulting concentration profiles in the film are shown in figure 1.

II.2.1.2 Mass Transfer With Chemical Reaction Following Bawn's Reaction Mechanism.

Combining Bawn's rate equation and equation (11), keeping C_{Ca} constant and assuming that

$$\frac{d(AMP)}{dt} = 0^*$$

the following equations can be written for various components as:

$$D_A \frac{d^2 C_A}{dx^2} = k'' C_B \quad (19)$$

* See Appendix VI

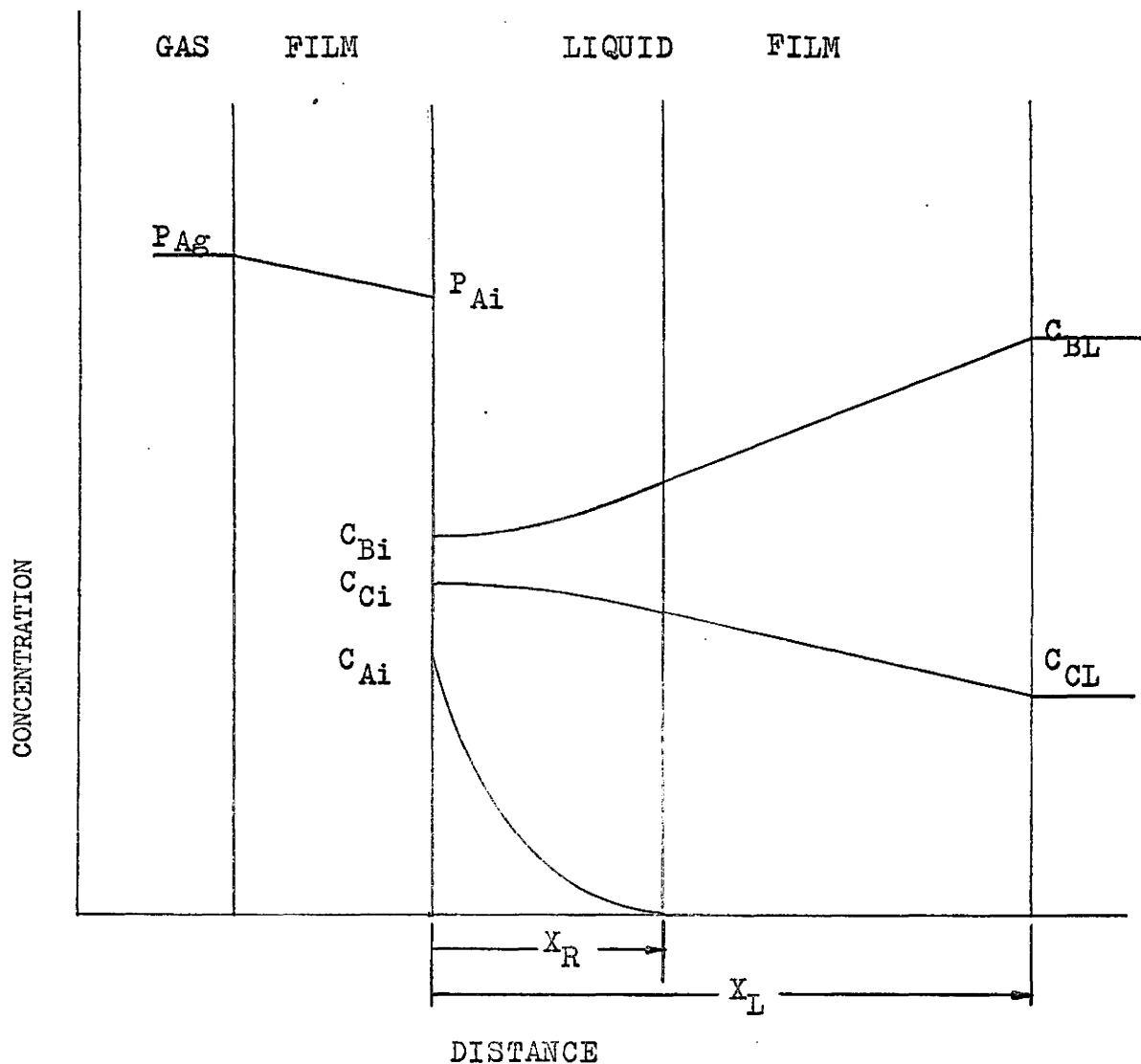


FIGURE 1 CONCENTRATION PROFILES IN THE FILM

$$x=0, C_A=C_{Ai}, \frac{dC_B}{dx}=0, \frac{dC_C}{dx}=0;$$

$$x=X_R, C_A=0; x \geq X_R, \text{ NO REACTION}$$

$$x=X_L, C_B=C_{BL}, C_C=C_{CL}$$

$$D_B \frac{d^2 C_B}{dx^2} = k'' C_B^2 / C_C \quad (20)$$

$$D_C \frac{d^2 C_C}{dx^2} = -k'' C_B \quad (21)$$

where $k'' = k' C_{Ca}$.

The boundary conditions are the same as the previous case except when $X_R \leq X \leq X_L$ the right - hand - side of equations (19) (20) and (21) completely vanishes.

III.2.2 Unsteady Mass Transfer

As truly stagnant films are hardly conceivable in industrial absorbers, Higbie (21) was one of the first to suggest the application of the unsteady - state diffusion concept to the process of gas absorption with chemical reaction. Danckwerts (10) has described and solved equations for the rate of absorption of the solute gas into a semi - infinite medium with which the gas undergoes a first order or pseudo - first order reaction. Brian, Hurley, and Hasseltine (11) have solved the unsteady - state diffusion equations with reactions of second order. Brian (12) in his recent paper has extended his solution to cases where the reaction is n^{th} and m^{th} order with respect to the gas and the liquid. However, the kinetics for many gas - liquid systems, such as the oxidation of hydrocarbons, cannot be explained by the existing theories. It was not until recently that Van de Vusse (13) started to deal with this type of reaction by assuming it zeroth order, that is, the rate of reaction is no longer dependent on the concentration of the reactants nor the

products. A rigorous mathematical treatment of the problem was given by Astarita and Marrucci (14). The unsteady - state diffusion involving zeroth - order chemical reaction is represented by the following differential equation:

$$D_A \frac{\partial^2 C_A}{\partial x^2} = \frac{\partial C_A}{\partial t} + k_{Co} H(C_A), \quad (22)$$

where the function $H(C_A)$ is defined as:

$$H(C_A) = 1, \text{ when } C_A > 0 \quad (23)$$

$$H(C_A) = 0, \text{ when } C_A = 0 \quad (24)$$

and k_{Co} is the zeroth order reaction rate constant.

The liquid medium is assumed infinitely deep, and the boundary conditions are:

$$\begin{aligned} t = 0, \quad X > 0, \quad C &= C_{AO} \\ t > 0, \quad X = 0, \quad C &= C_{Ai} \\ t > 0, \quad X \rightarrow \infty, \quad C &= \max(C_{AO} - k_{Co}t, 0) \end{aligned} \quad (25)$$

where $\max(C_{AO} - k_{Co}t, 0)$ is equal to the larger of $C_{AO} - k_{Co}t$ and 0.

For the special case, where $C_{AO} = 0$ equation (22) cannot be solved analytically. However, for values of $\frac{k_{Co}t}{C_{Ai}} > 1$ an approximate

solution was given by Astarita and Marrucci as

$$C_A = \frac{k_{Co}}{D_A} \frac{x^2}{2} - \left(\frac{k_{Co}}{D_A} \sqrt{\frac{2C_{Ai}D_A}{k_{Co}}} \right) x + C_{Ai} \quad (26)$$

Equation (26) is independent of t indicating that a steady - state has been reached. Differentiating equation (26) one obtains:

$$\left. \frac{dC_A}{dx} \right|_{x=0} = - \sqrt{\frac{2k_{Co} C_{Ai}}{D_A}} \quad (27)$$

$$\text{and } N_A = - D_A \left. \frac{dC_A}{dx} \right|_{x=0} = \sqrt{2 D_A k_{Co} C_{Ai}} \quad (28)$$

III SCOPE

The purposes of the experimental work were two-fold:

(1) to study the effect of several variables, namely, acetaldehyde concentration, catalyst concentration, partial pressure of oxygen and temperature on the rate of absorption

(2) to attempt to correlate absorption rates with product distribution by a mathematical model based on the film theory just reviewed.

IV EXPERIMENTAL DETAILS

IV.1 Description of Apparatus

The apparatus used by Akehata (15) was adopted for some preliminary studies. It was later modified to eliminate contamination by rubber, to enable long runs to be made with less attention and to minimize back - diffusion. The modified apparatus and the reaction vessel are shown in Figures(2) and (3).

The essential feature of the apparatus is an open cylindrical glass vessel, (Fisher Standard Reaction Kettle) 4 inches I.D. and 8 inches high. The lid of the vessel has four ground glass junctions leading separately to a gas burette, feeding funnel, mercury seal and a bleeding stopcock. The lid and the vessel are jointed by ground glass contact and brought tightly together by stainless - steel clamps. At the bottom of the vessel is a delivering tube for draining and sampling. The mercury seal allows the introduction of the stirrer and at the same time seals the vessel from the atmosphere. The apparatus is immersed in a thermostatted ethylene - glycol - water bath which is kept below room temperature by a cooling coil. Agitation in the vessel is obtained by a stirrer with three blades so that both the gas and the liquid phases are well - mixed.

By means of a three - way stopcock the vessel connects either to the gas burette or the gas storage tank. The gas burette is

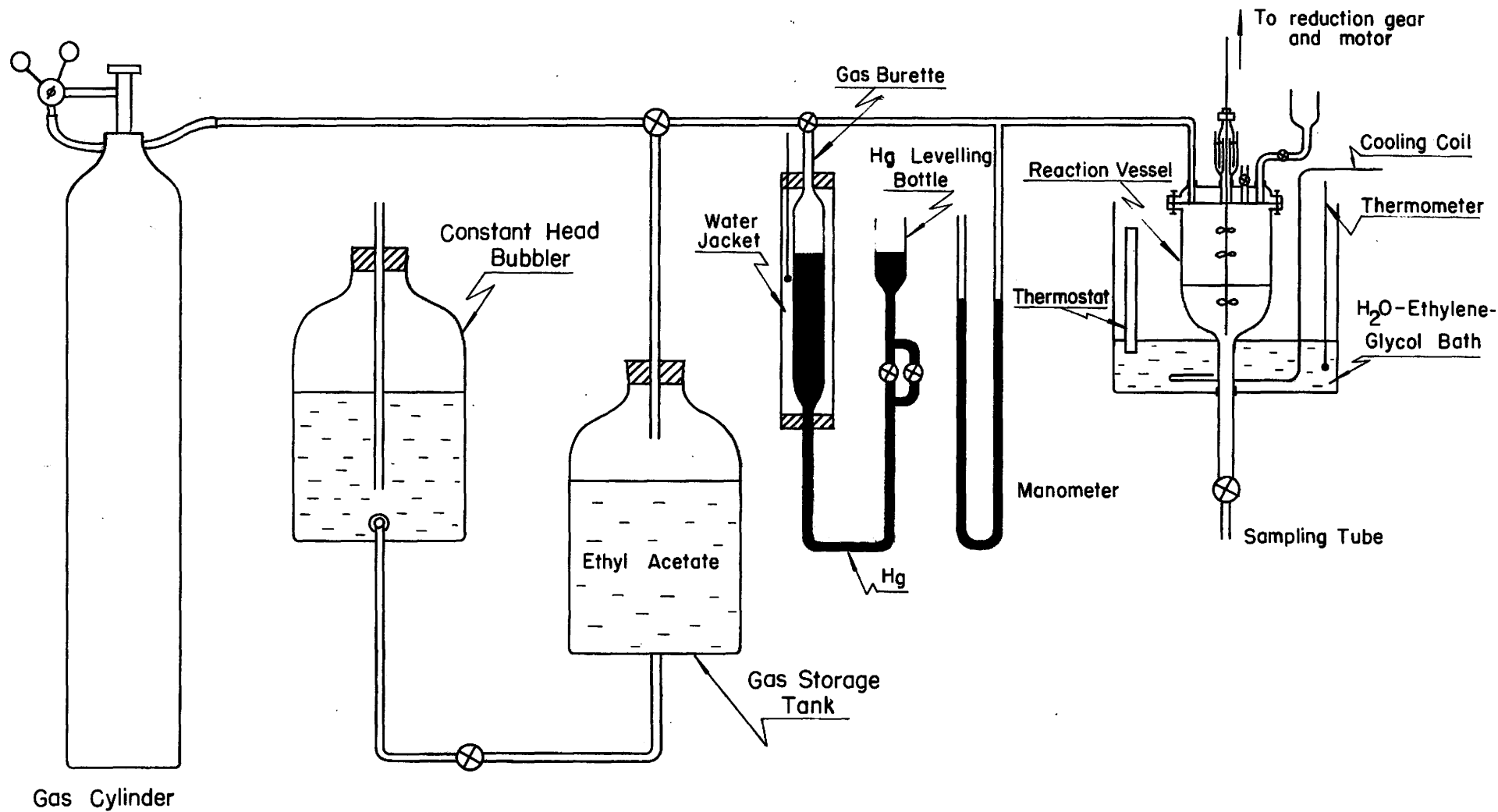


FIGURE 2

SIMPLIFIED DIAGRAM OF APPARATUS

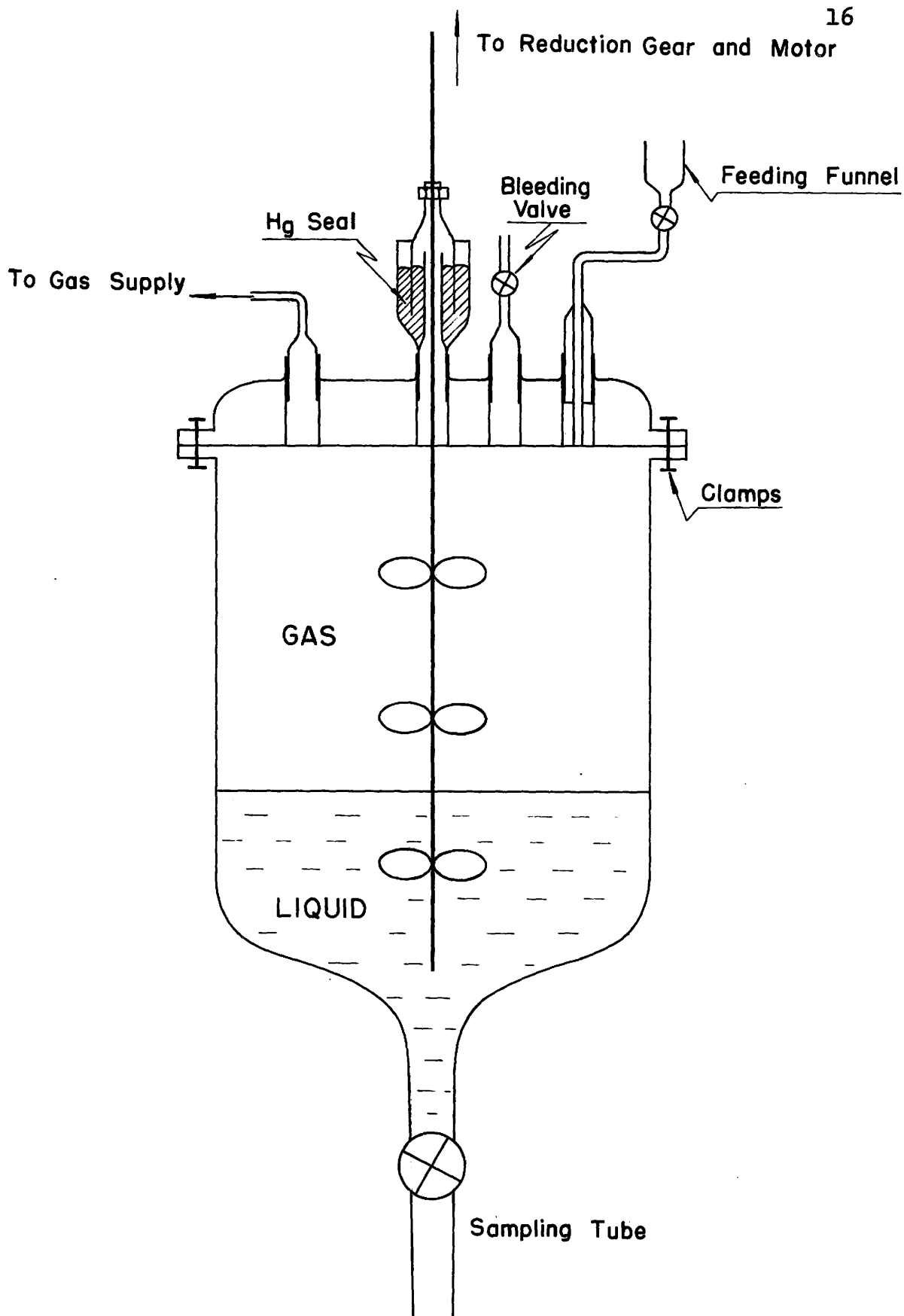


FIGURE 3 DETAILED DIAGRAM - REACTION VESSEL

jacketed by water at room temperature. The gas tank is connected to a constant head bubbler.

Atmospheric pressure is maintained in the gas burette and in the reaction vessel by means of a mercury levelling bottle. Pressure inside the vessel is indicated by a manometer.

IV.2 Advantages and Disadvantages of Apparatus

Apart from the fact that it is simple to construct and to operate the apparatus has the following advantages over packed or plate columns which are often engaged in gas absorption studies.

First, the interfacial area is known.

Second, although the hydrodynamic condition at the interface is not well defined, it may be assumed laminar if the stirrer speed is low.

Third, with the stirrer at low speeds the liquid surface is plane and the main body of the liquid is thoroughly mixed. The existence of a very thin film of liquid at the interface, where reaction and resistance to diffusion are concentrated, may be conceivable. However, without the stirrer the liquid layer is stagnant and of semi-infinite thickness. Mass transfer of an unsteady-state nature is likely to occur.

Fourth, sufficient concentration of the product can be built up within a reasonable period of time for analysis using simple titration methods.

The above characteristics of the apparatus enable the data to be interpreted in terms of the film theory or in terms of an unsteady - state diffusion equation when there is no stirring in the liquid phase.

However, the apparatus has its limitation in measuring low rates of absorption, especially, in the case where no chemical reaction occurs. Because of the presence of the mercury seal and the ground glass joints the apparatus can only be used for pressures slightly higher or lower than atmospheric.

IV.3 Experimental Procedure

The purposes of the experimental work were two-fold:

- (1) To study the effect of several variables namely, acetaldehyde concentration, catalyst concentration, partial pressure of oxygen and temperature on the rate of absorption.
- (2) To correlate the product distribution with the rate of absorption.

Hence, the first set of experiments consisted of measuring the initial rates of absorption while varying the above parameters. The second set involved the determination of product concentrations as well as absorption rates.

The general procedure for all experiments was as follows:

At the start of each run the ethylene - glycol - water bath was maintained at the desired temperature by adjusting the flow rate of the coolant. The gas tank and the burette were then filled with oxygen or an oxygen - nitrogen mixture. The reactor ~~was flushed with the same gas~~ until air was completely displaced. A mixture of acetaldehyde, ethyl acetate and freshly made cobaltous acetate standard solution was fed into the vessel which was then connected to the gas tank. The stirrer and the stop clock were started simultaneously. To measure the rate of

absorption the gas supply from the storage tank was shut off and the burette was connected to the reactor. By means of a levelling bottle the pressure in the reactor could be adjusted to atmospheric while burette readings were taken at convenient intervals.

The concentrations of peracetic and acetic acid, A.M.P and unreacted acetaldehyde were determined by simple titration methods as described in Appendix IX.

V RESULTS AND INTERPRETATION

V.1 Physical Mass Transfer

It was shown in equation (8) that $N_A = k_L(C_{A1} - C_{AL})$.

If there is no dissolved oxygen in the liquid at the start of an experiment, C_{AL} at time t can be related to the volume of oxygen absorbed. Assuming the gas phase resistance is always negligible so that C_{A1} is practically equal to C_{Ag} , which can be estimated from the solubility of the gas in pure solvent, it can be shown that k_L is given by

$$k_L t = 2.303 \frac{V_L}{A_F} \log \left(\frac{C_{AL}}{C_{A1} - C_{AL}} \right) \quad (29)$$

$\log (C_{A1} - C_{AL})$ was plotted against t . The method of least squares was used to find the slope of the resulting straight line and k_L was calculated using equation (29).

The mass transfer coefficients at various experimental conditions are tabulated in Table 1. It indicates that the mass transfer coefficient increases markedly with stirring speed and gradually with temperature. Increasing stirring speed would tend to make the liquid film thinner thus steepening the concentration gradient at the interface. An enhancement in mass transfer is then expected.

The increase of diffusivities with temperature is believed to be the cause of the effect of temperature on the mass - transfer coefficient.

Expt. No.	Stirring Speed r.p.m.	Apparatus	Temperature $\pm 0.3^\circ \text{C}$.	k_L $\frac{\text{ft}}{\text{hr}} \times 10^2$	Average $k_L \times 10^2$
6	509	Akehata	4	7.62	8.32
7	509	"	4	9.60	
9	509	"	4	7.13	
13	509	"	4	8.80	
14	509	"	4	8.50	
102	395	"	0	4.10	4.13
98	395	"	0	4.16	
103	395	"	4	4.12	4.36
104	395	"	4	4.60	
95	395	"	10	4.55	4.69
99	395	"	10	4.83	
123	120	modified	5	3.90	4.00
35A	120	"	5	4.10	

$$\begin{aligned}
 A_r (\text{Akehata}) &= .0475 \text{ ft}^2 \\
 A_r (\text{Modified}) &= .0873 \text{ ft}^2 \\
 V_R &= 5.66 \times 10^{-3} \text{ ft}^3
 \end{aligned}$$

TABLE 1 MASS TRANSFER COEFFICIENT
WITHOUT REACTION

V.2 Effect of Several Variables On Mass Transfer with Chemical Reaction

It was assumed, when reaction occurs that all of the dissolved oxygen in the bulk of the liquid was reacted and its concentration was zero. Then,

$$\begin{aligned}
 N_A &= k_L^* C_{Ai} \quad \text{and} \\
 &= K_L^* C_{Ag} \quad \text{and} \quad \bar{\phi} = \frac{k_L^*}{k_L} = \frac{N_A}{C_{Ai} k_L}
 \end{aligned}$$

V.2.1 Acetaldehyde Concentration

Figure 4 illustrates the effect of acetaldehyde concentration on the ratio K_L^*/k_L which increases sharply at low concentrations, then gradually, and eventually approaches a constant value at high concentrations.

This behaviour can be explained by applying the two - film theory and the resulting concept of resistances in series which can be expressed by equation (7).

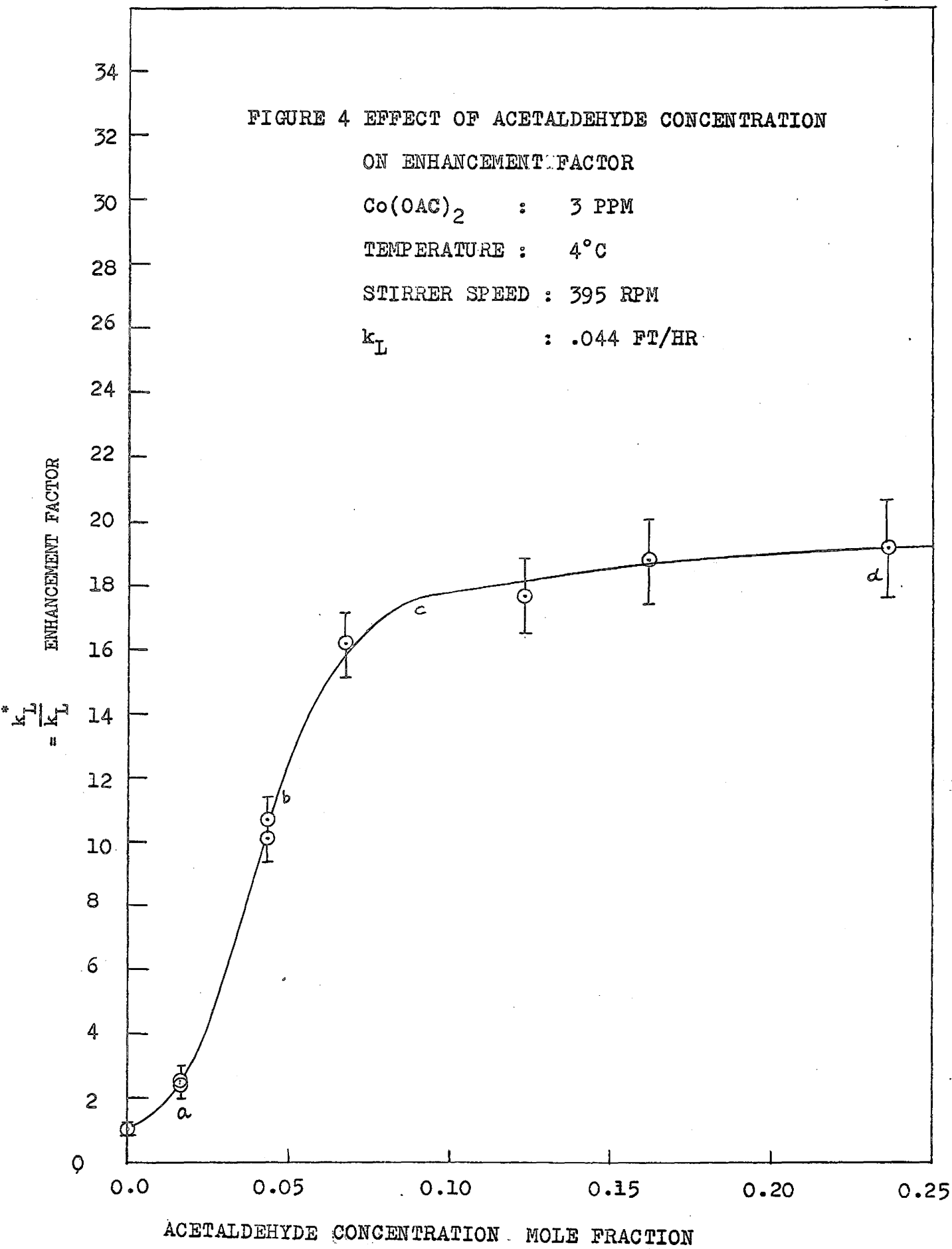
It was shown in Section I.1 that the rate of reaction and hence the oxygen uptake is proportional to acetaldehyde concentration. Consequently, at low concentrations reaction is slow and $k_L^* \ll mk_g$; K_L^* is then equal to k_L^* . The ordinate will represent \bar{E} which is dependent on acetaldehyde concentration (region ab, Figure 4). However, as the concentration increases, k_L^* is so large, and furthermore, acetaldehyde vapor content in the gas phase becomes so high that the gas phase resistance is no longer negligible. When this occurs the ordinate will not represent \bar{E} but a smaller value $\frac{K_L^*}{k_L}$ (region bc, Figure 4).

As concentrations further increases k_L^* becomes much larger than mk_g . In this case $K_L^* \doteq mk_g$. The absorption rate will only depend on the partial pressure of oxygen (region cd, Figure 4) and is given by

$$N_A = mk_g C_{Ag} = k_g P_g.$$

The same behavior was observed also in later work when this set of experiments was repeated at various temperatures and by Hatta in his CO_2 - NaOH absorption studies (5).

In order to illustrate the effect of chemical reaction on mass transfer the concentration of acetaldehyde was confined to region a - b for subsequent experiments.



V.2.2 Catalyst Concentration

Figure 5 illustrates the effect of catalyst concentration on the enhancement factor which increases markedly to a maximum and then decreases gradually.

It was reviewed in literature (1,2,3,4) that the initiation of reaction is due to the decomposition of hydroperoxide by the catalyst and thus the overall reaction is a function of catalyst concentration. The relation according to Bawn (4) is first order.

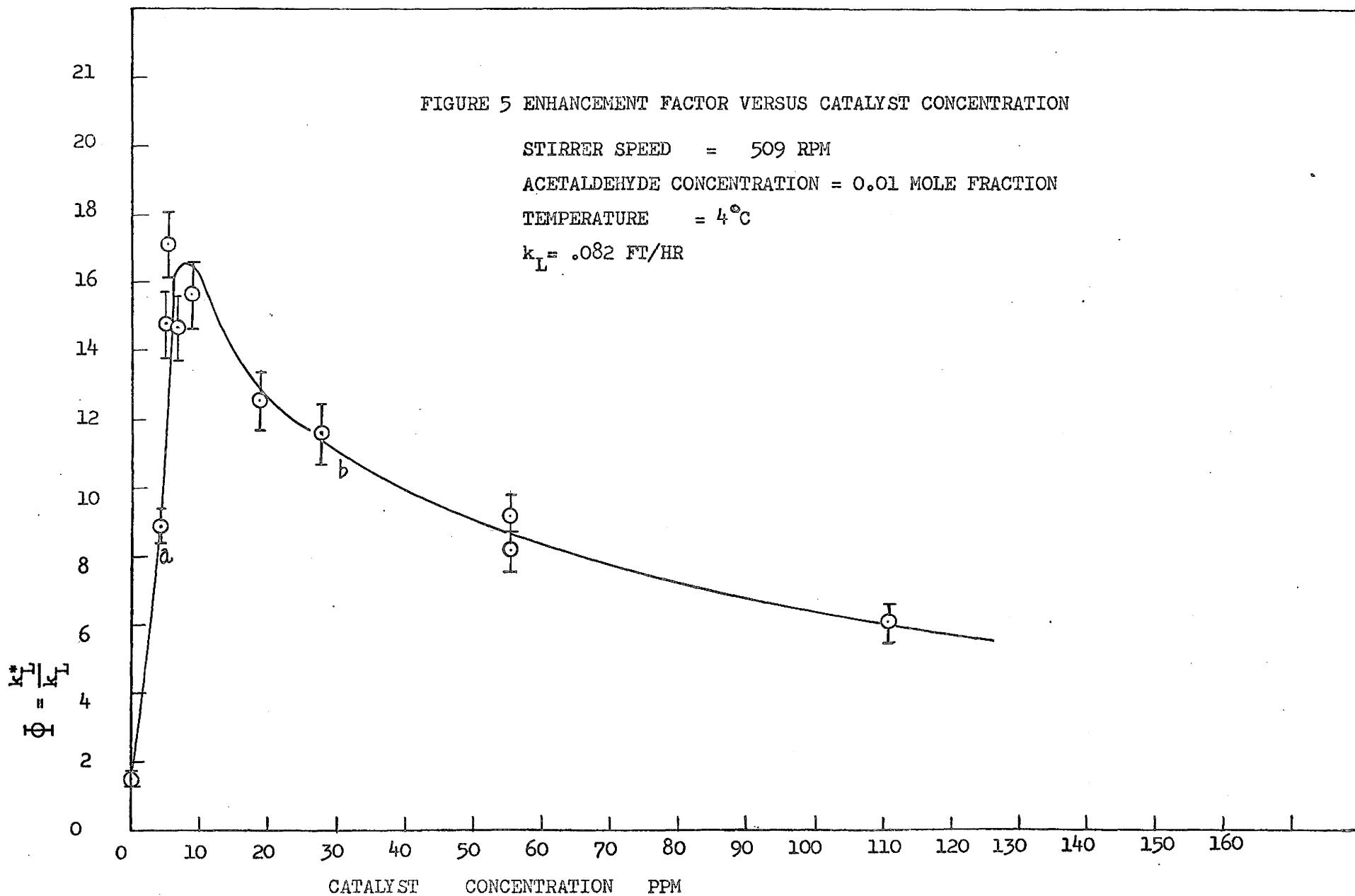
However, the occurrence of the maximum in Figure (5) may be explained by the following hypotheses (16).

- (1) The hydroperoxide has a "steady - state" concentration when the rate of its formation by oxidation is equal to the rate of decomposition to free radicals by the catalyst.
- (2) The catalyst may form inactive micelles (16).
- (3) The catalyst may take part in both the initiation and the termination of the chain reaction (16).

Hence, further increase of catalyst concentration may not have any catalytic effect, but rather kills the reaction by decomposing the peroxide to inactive products, such as acetic acid and acetic anhydride.

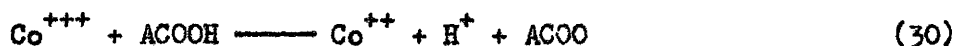
It was also shown in the "Preliminary studies on peracetic - acid production in a cocurrent flow reactor" (see Appendix XII) that the yield of peracetic acid decreased with increase in catalyst concentration after a maximum was reached. The increase in the production of acetic acid after the maximum also supported the hypothesis.

It was noted that the retardation effect of the catalyst at high concentrations has also been observed in industrial processes.



The range of catalyst concentration used in commercial processes as reported in several patents (17, 18, 19, 20) lies between 5 and 30 ppm (region ab in Figure 5).

It was observed that the cobaltous - acetate solution originally pink in color turned green as soon as contacted with acetaldehyde and remained green throughout the experiment. This behaviour can be explained by considering the initiation reaction.



where AC represents $\text{CH}_3\text{CO} \cdot$.

Equations (31) and (32) show that the cobalt ions undergo a constant change of state. However, if reaction (32) predominates, the ions will appear to remain in the higher state and the solution is green throughout the reaction.

V.2.3 Partial Pressure of Oxygen

The mass transfer coefficient at various partial pressures of oxygen and stirring speeds were tabulated in Table 2. When k_L^* was plotted against partial pressure for r.p.m. = 206 the slope of the resulting straight line estimated by the least squares method was - .0087.

Hence, at certain stirring speeds k_L^* did not vary with partial pressure of oxygen between .21 - .95 atmosphere.

The constancy of k_L^* as the gas changes from air to pure oxygen has justified the assumption that the gas phase resistance is negligible ($mkg \gg k_L^*$) for concentrations of acetaldehyde below the value used in this experiment.

Expt. No.	Stirring Speed r.p.m.	Mole Fraction of Oxygen	k_L^* ft./hr.
52	206	.21	.532
46	"	.50	.490
47	"	.50	.503
48	"	.75	.545
49	"	.75	.540
55	"	.75	.569
53	"	1.00	.505
54	"	1.00	.492
58	363	.50	.662
56	"	.75	.642
57	"	1.00	.643
59	509	.21	1.14
66	"	.21	1.36
60	"	.50	1.40
65	"	.50	1.36
61	"	.75	1.03
64	"	.75	1.36
63	"	1.00	1.47

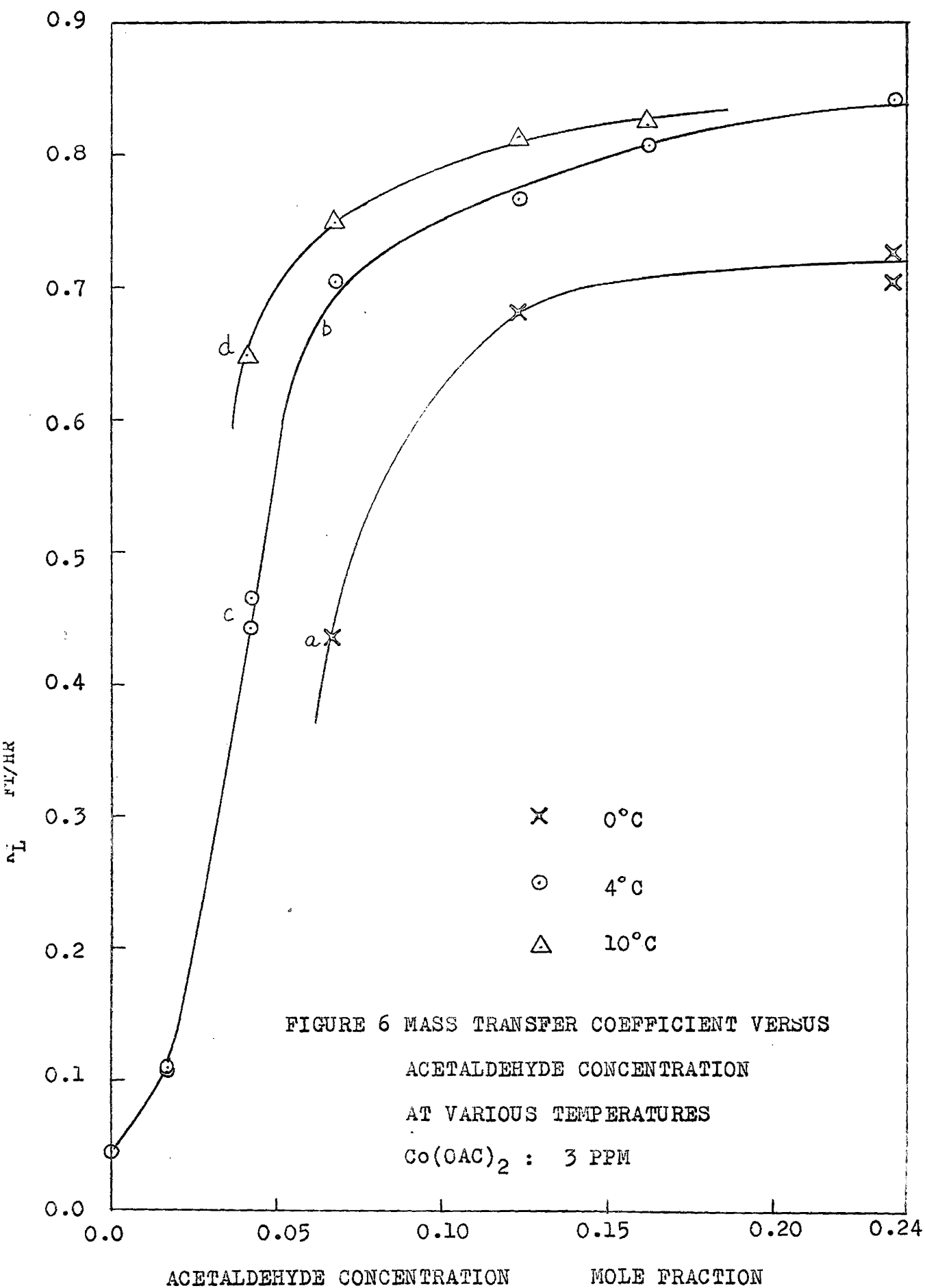
Catalyst Concentration = 6.0 ppm

TABLE 2 EFFECT OF PARTIAL PRESSURE ON MASS TRANSFER

It also indicates that interfacial turbulence, which should show different effects on the mass transfer for different partial pressures of oxygen, if it exists in this system, is not noticeable (22).

V.2.4 Temperature

The mass transfer coefficient K_L^* was plotted against acetaldehyde concentration for three different temperatures 0°, 4° and 10°C in Figure (6). It was shown that K_L^* in general increased with



temperature. As the effect of temperature on reaction rates is generally expressed by the Arrhenius equation as follows:

$$k_c = A e^{\frac{-\Delta E}{RT}}, \quad (33)$$

thus K_L^* , which is equal to k_L^* at lower acetaldehyde concentrations, becomes a strong function of temperature. Even at such a small range ($0^\circ - 10^\circ\text{C}$) the effect is pronounced as indicated by the distances a - b and c - d.

At high acetaldehyde concentrations, when $K_L^* \neq mk_g$, the effect of temperature is reduced as k_g is generally taken as proportional to T^n , where n is approximately $3/2$.

V.3 Unsteady-State Mass Transfer Studies

Some preliminary experiments with stirring only in the gas phase were run. That the rate of absorption was independent of stirring speed further justified the assumption that the gas phase resistance was negligible compared to the liquid at low acetaldehyde concentrations.

Results also indicated that the absorption rate was constant throughout each experiment. Hence it may be assumed that steady - state had been reached a few minutes after the start of the experiment.

Analysis of acetaldehyde before and after each run showed no essential difference in concentration. Thus the reaction, which is first order with respect to acetaldehyde according to Bawn, may be assumed pseudo - zeroth order. k_{Co} for various temperatures were

calculated from the absorption rates using equation (28). With these values of k_{Co} it was estimated that the absorption rate had reached a steady - state value after approximately 1.2 minutes for all the experiments. Thus the previous assumption was justified.

$\log (k_{Co})$ versus $\frac{1}{T}$ was then plotted in Figure (7) and the activation energy was estimated to be 5.05 Kcal/moles from the slope of the resulting straight line.

When the graph was extrapolated to 25°C., at which Bawn's experiment was carried out, a value for k_{Co} was obtained and a comparison could be made in the following way.

Using Bawn's data k'' was estimated by letting it equal to $k'C_{Ca}$.

For the present study k'' is equal to k_{Co}/C_B .

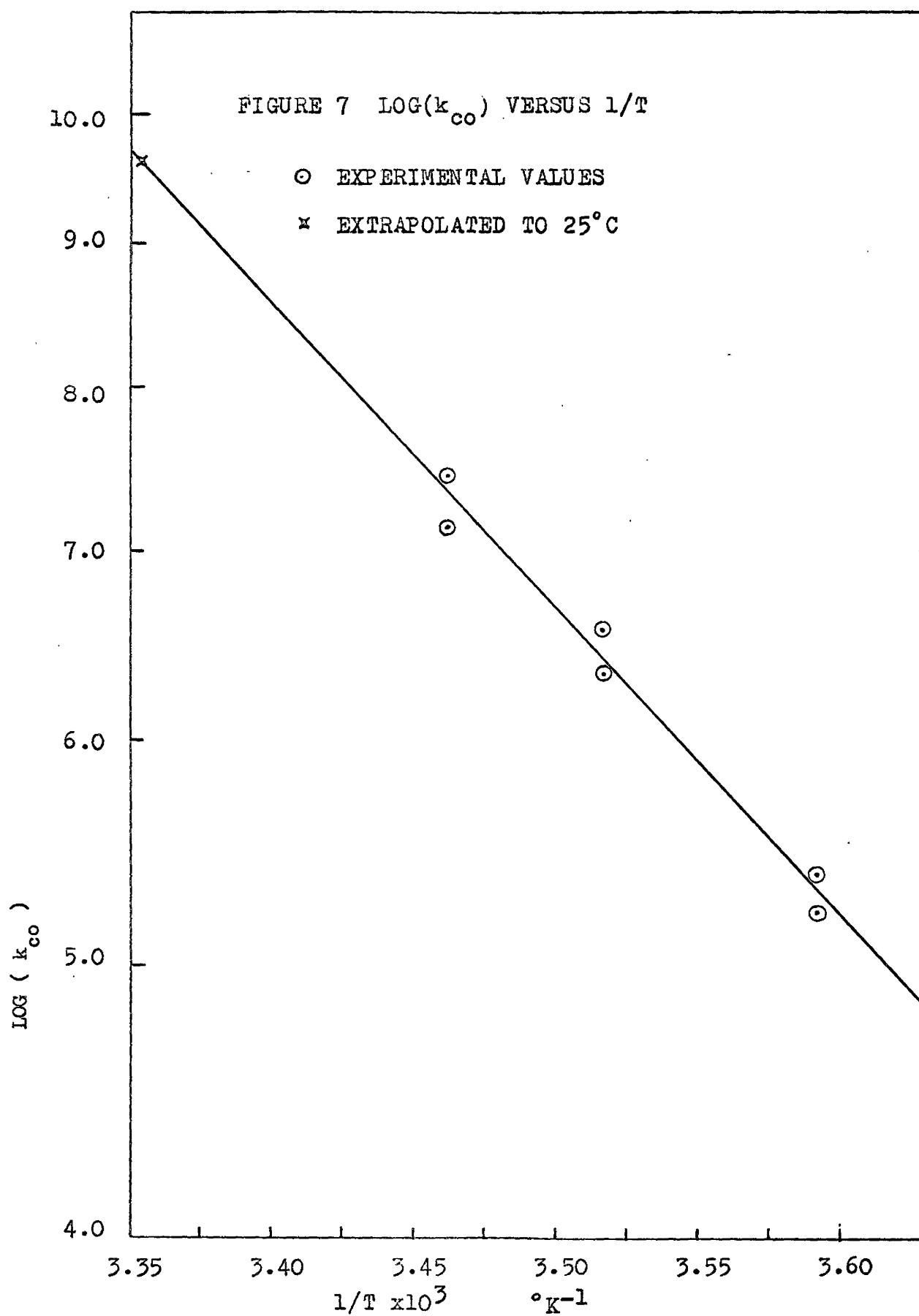
Table 3 includes a comparison of k'' and the catalyst concentration.

	Catalyst Concentration (ppm)	k'' (hr) ⁻¹
Bawn result	9.0	1.54
Present Study	3.0	.96

TABLE 3 COMPARISON OF REACTION RATE CONSTANTS

The magnitude of k'' in both cases is of the same order. The higher catalyst concentration in Bawn's experiment probably accounts for the higher k'' .

* Detailed calculation are found in "Estimation of reaction constant from Bawn's data".



There is no data on the activation energy of this particular reaction.

The oxidation of hydrocarbons with benzoyl peroxide as the catalyst has an overall activation energy ranging from 20 to 25 Kcal/ moles (2). three quarters of which, however, were reported to come from the dissociation of peroxide in the initiation step.

V.4 Effect of Product Distribution and Mathematical Models for Steady - State Mass Transfer

This part of the experimental work was to determine the effect of rate of mass transfer on product distribution. Mathematical models were built to correlate the product distribution with absorption rates.

The concentration of AMP was found comparatively small in all experiments and was neglected. A material balance of the loss of acetaldehyde by reaction with the formation of peracetic and acetic acid showed that the maximum percentage gain or loss of acetaldehyde was 6%.

Now, the film theory diffusion equations (12), (13), (14), (18), (20), (21) and the significance of their boundary conditions were re-considered. Referring to Figure 1 which shows typical concentration profiles in the film, X_R is defined as the reaction zone beyond which oxygen concentration is zero; X_L , called the film thickness for mass transfer without chemical reaction, is equal to D_A/k_L . Physically, it can be defined as the distance from the interface to the place where the stirrer cuts the concentration profiles, so that beyond this point the liquid is well mixed and all the concentration gradients become zero.

As only one stirring condition was used X_L could be considered the same for both cases with and without chemical reaction.

Here S , the concentration gradient of oxygen at the interface, can be related to the rate of absorption by Fick's First Law as

$$N_A = - D_A \left. \frac{dC_A}{dx} \right|_{x=0} \quad (34)$$

Diffusivities were estimated by Wilke's Equation (see Appendix XI)

V.4.1 Mathematical Model Using Bawn's Reaction Mechanism.

With known values of C_{BL} , C_{GL} and N_A , equations (19), (20) and (21) were solved simultaneously for k'' using an analog computer. The values of k'' evaluated for different bulk concentrations and the corresponding rates were not constant, but varied linearly with acet-aldehyde concentration. k'' was then plotted against C_{BL} , an empirical equation was obtained as follows :

$$k'' = - 44.4 + 15.85 C_B \quad (35)$$

Equation (35) was substituted into the diffusion equations which become

$$D_A \frac{d^2 C_A}{dx^2} = - 44.4 C_B + 15.95 C_B^2 \quad (36)$$

$$D_B \frac{d^2 C_B}{dx^2} = - 44.4 \frac{C_B^2}{C_c} + 15.95 \frac{C_B^3}{C_c} \quad (37)$$

$$D_C \frac{d^2 C_C}{dx^2} = + 44.4 C_B - 15.95 C_B^2 \quad (38)$$

Using these empirical equations and the bulk concentrations the concentration profiles in the film were predicted, and from equation (34) the absorption rates were estimated. These predicted rates were plotted against the experimental values in Figure 8. A least - squares line was drawn through these points. The slope is $1.078 \pm 2.228 (.0936)$.

A statistical evaluation of the correlation is given in Section VII

V.4.2 Mathematical Model using Bolland's Reaction Mechanism

According to Bolland (1,2) and Twigg (3) the rate of reaction is also a function of peracetic acid. Hence, at the beginning of an experiment the rate of absorption increased as more peracetic acid was built up. Later on, as acetaldehyde was depleted the rate of absorption started to decrease. Figure 9 shows a typical reaction curve.

A peracetic acid concentration term was built into the reaction rate expression.

Taking into account also the reaction of peracetic acid and acetaldehyde to acetic acid, a new correlation represented by the following equations fit the data with reasonable accuracy.

$$D_A \frac{d^2 C_A}{dx^2} = 1.134 C_B C_C^{1.9} \quad (39)$$

$$D_B \frac{d^2 C_B}{dx^2} = 1.134 C_B C_C^{1.9} + .20 C_B C_C \quad (40)$$

$$D_C \frac{d^2 C_C}{dx^2} = -1.134 C_B C_C^{1.9} + .20 C_B C_C \quad (41)$$

FIGURE 9 EXTENT OF OXIDATION

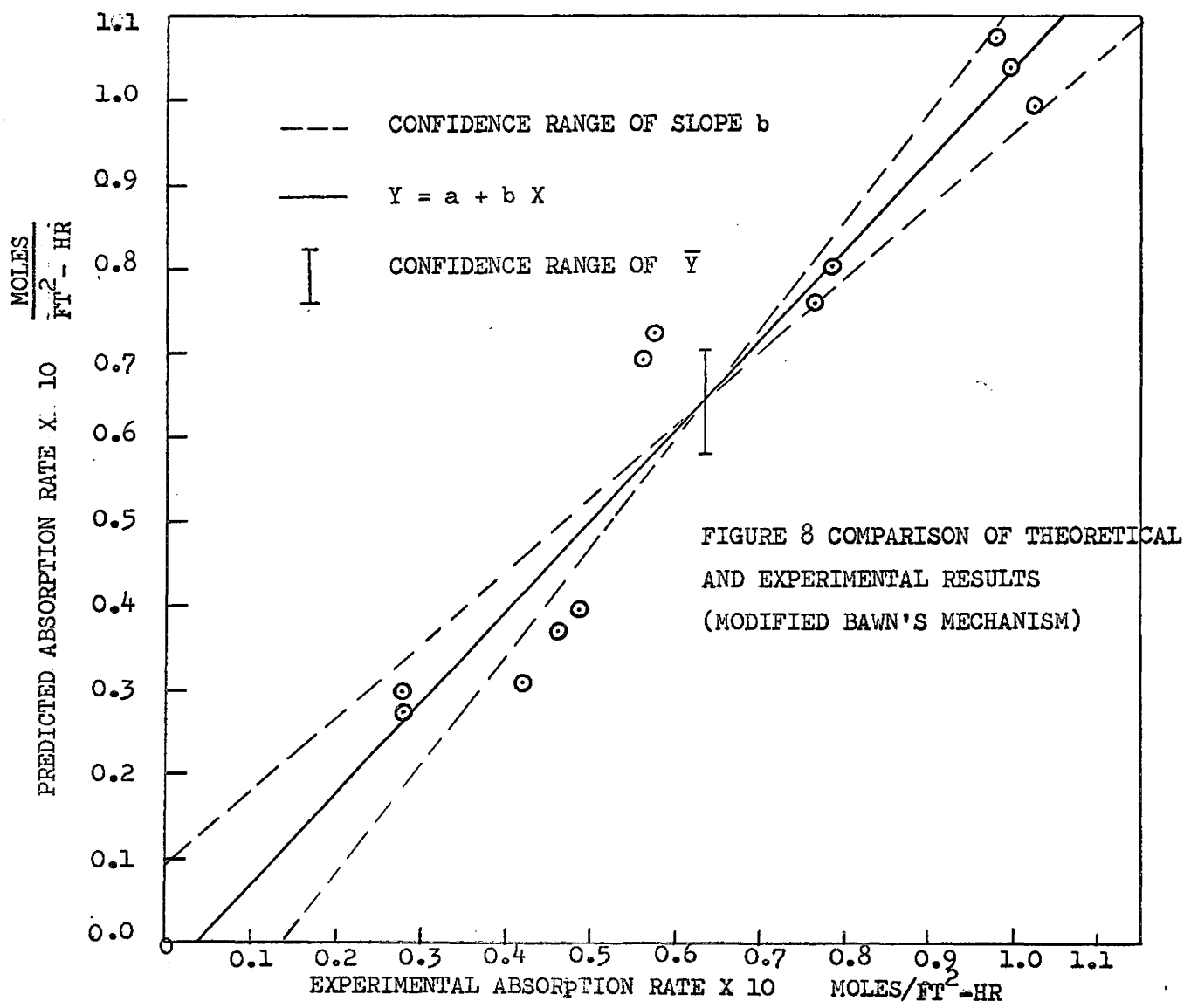
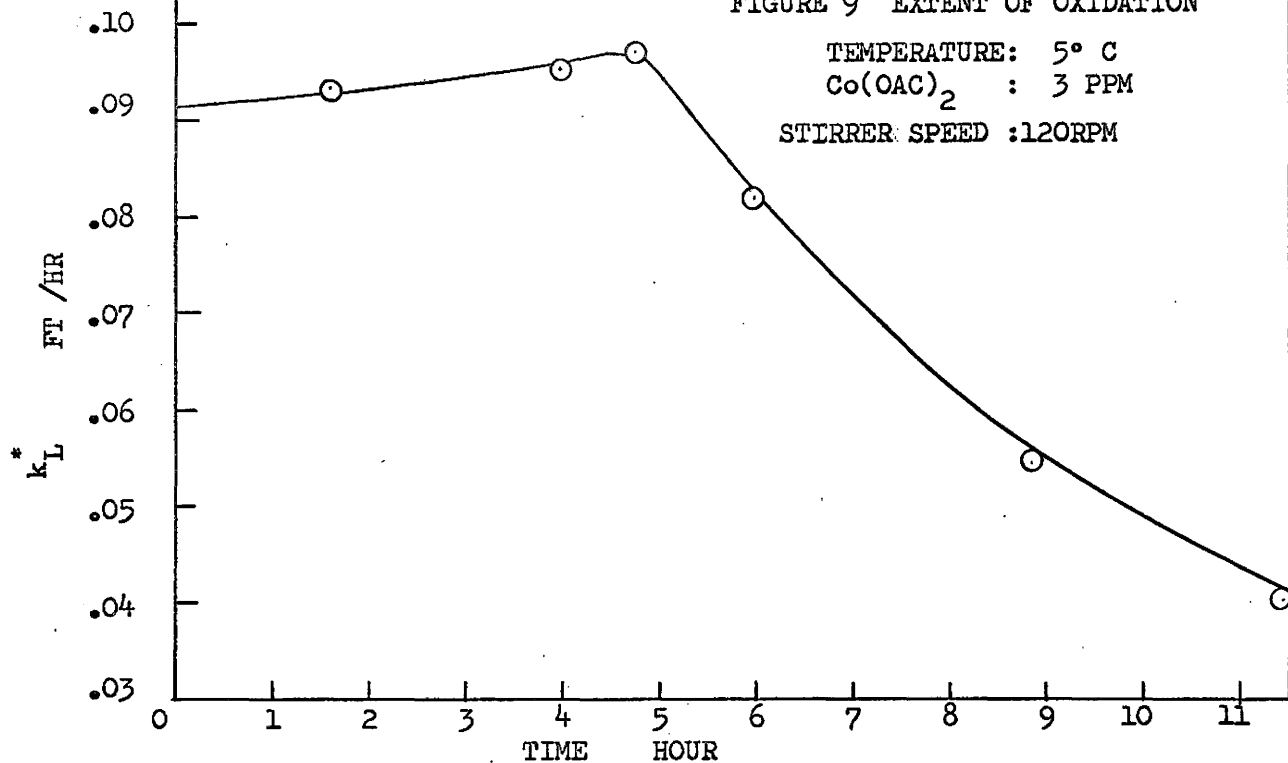
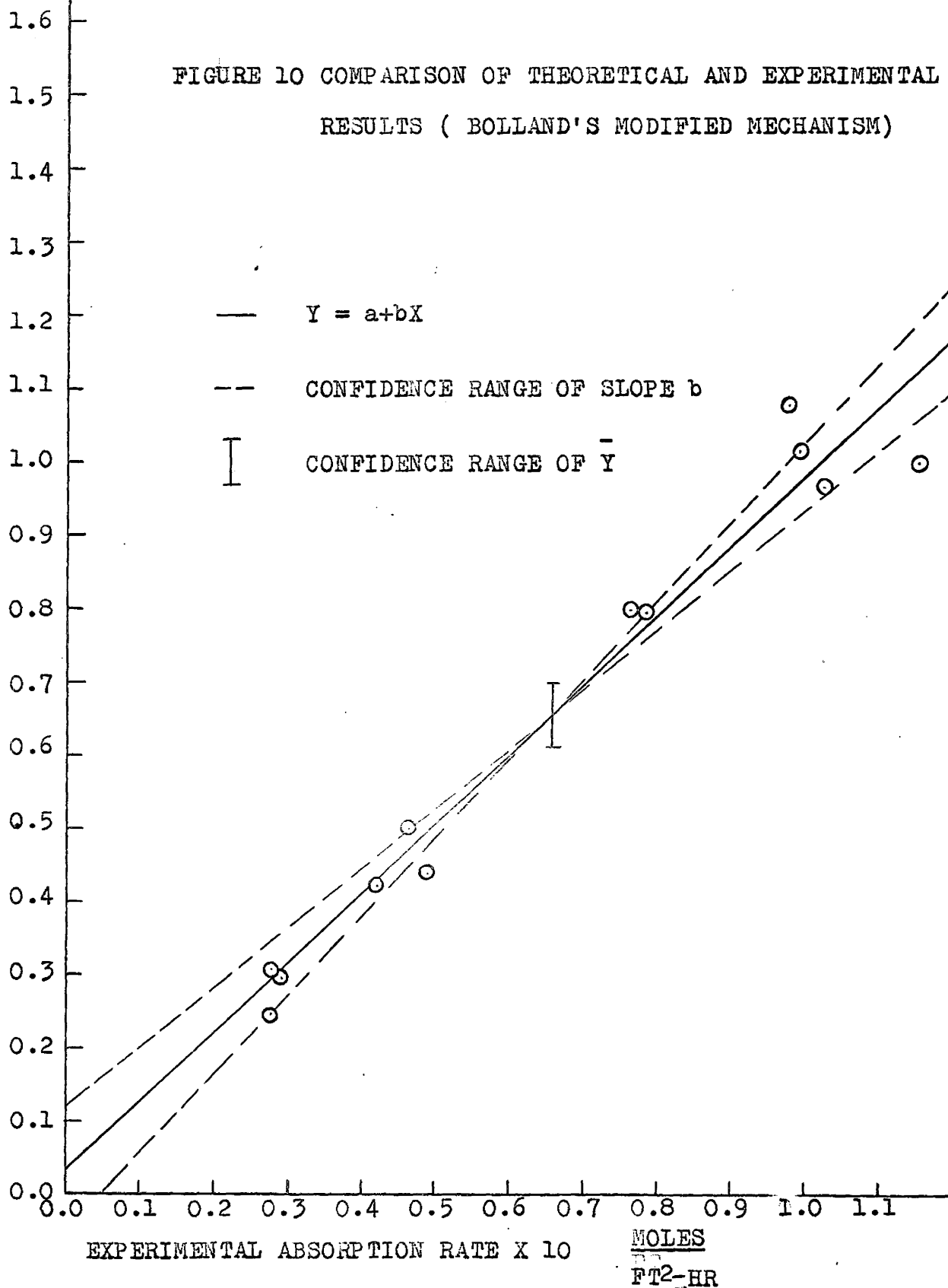


FIGURE 10 COMPARISON OF THEORETICAL AND EXPERIMENTAL
RESULTS (BOLLAND'S MODIFIED MECHANISM)

MOLES
PREDICTED ABSORPTION RATE X 10
FT²-HR



Predicted absorption rates were obtained as in the last section and plotted against the experimental values in Figure 10. A least squares line was drawn through these points. The slope is $.948 \pm 2.228$ (0.592). A statistical evaluation of the correlation is given in Section VII.

VI CONCLUSIONS AND RECOMMENDATIONS

A simple apparatus has been used to obtain rate data for the absorption of oxygen in a catalysed liquid phase reaction. The effects of several system parameters have been studied and reported graphically and the following observations have been made:

(1) The range of acetaldehyde concentrations studies was from .017 to .24 mole fraction. The rate of absorption was controlled by the rate of reaction at the lower range but limited by the partial pressure of oxygen in the gas phase at the higher range.

(2) The effect of cobaltous acetate concentration ranging from 0 to 110 p.p.m. was studied. The highest absorption rate occurred at concentrations from 5 to 10 p.p.m.

(3) The rate of absorption increased with temperature. The effect was more pronounced at lower acetaldehyde concentrations. The range of temperature studied was from 0°C. to 10°C.

(4) The suspected effect of driving force, which was varied by a factor of five, on interfacial tension change and thus on mass transfer coefficient was not found.

The present apparatus can still be used for further investigations of the effect of other parameters, such as, solvent and catalyst other than ethyl acetate and cobaltous acetate.

Mathematical models based on the film theory and on previous

kinetic models in the literature have been applied to the data. The following conclusions may be made:

(1) Using the mathematical models the rate of oxygen absorption under the present experimental conditions can be predicted, provided that the product distribution and a coefficient of mass transfer without reaction are known.

(2) Bawn's mechanism is not adequate to interpret the present experimental data. The empirical model based on the modified reaction mechanism predicts absorption rates within $\pm 30\%$ of the experimental values.

(3) The mathematical model based on Bolland's rate equation predicts absorption rates within $\pm 15\%$. However, this correlation is also a semi-empirical one as the exponent of C has a higher value than that derived theoretically.

A better agreement between the theoretical prediction and experimental measurements is hard to obtain. This is due, in part, to the uncertainties about the complex liquid and gas flow patterns and about some system parameters, such as, the diffusivity and viscosity of the liquid, which change as reaction proceeds; it is also due to the uncertainty about the reacting system, for example, the kinetics and chemical equilibrium of the reactions, and the stability of the product.

It is therefore, recommended that a kinetic study should be made to develop a complete kinetic model taking into account all the possible reactions in the temperature range concerned. Then a more rigorous treatment of the problem of diffusion with reaction can be made.

The apparatus has also been used to obtain data for the

absorption of oxygen with no stirring in the liquid phase. The major advantage is that the hydrodynamics in the liquid are better defined. However, as the absorption rate was slow there was insufficient concentration of the product being built up for analysis.

It is therefore suggested that by using high pressure cells, higher absorption rates and better yield of peracetic acid may be obtained.

The present study of the effect of several parameters on the rate of absorption has not yet provided enough information for the design of reactors or other contacting equipment, however, it has prepared a sound starting ground for further mathematical correlations. It has also established^a range of catalyst concentration (between five and ten parts per million) which gives the highest absorption rate. The mathematical models may now be tested in other experimental systems and consequently may be used to predict the performance of bench scale and industrial gas absorbers.

VII EXPERIMENTAL ERRORS AND STATISTICAL EVALUATION

The estimated experimental errors are summarized in the following tables. Detailed calculations are given in Appendix V.

Δk_L ft/hr	Δk_L^* ft/hr		$\Delta \bar{x}$	
$k_L = .041$	$k_L^* = .1$	$k_L^* = 1.0$	$\bar{x} = 2.50$	$\bar{x} = 25.0$
$\pm .003$	$\pm .005$	$\pm .008$	$\pm .20$	± 3.13

TABLE 4 ESTIMATED EXPERIMENTAL ERRORS

Compound	No. of Sample	Maximum Deviation From Mean
acetaldehyde	10	$\pm 2\%$
acetic acid	10	$\pm 10\%$
peracetic acid	10	$\pm 2\%$

TABLE 5 PRECISION OF ANALYTICAL METHODS

The statistical evaluation of the experimental data is referred to "Volk, Applied Statistics for Engineers".

When predicted values are plotted against experimental values, the resulting straight line is expressed by:

$$\hat{y} = a + bx \quad (42)$$

where a is the intercept and b , the slope of the straight line.

The confidence ranges of the slope and the mean as well as the correlation coefficient of the correlations are tabulated in Table 6.

	b	a	$b \pm ts(b)$	$\bar{y} \pm ts(\bar{y})$	r
First Correlation	1.078	-.00390	.863 - 1.293	.0429 - .0775	.962
Second Correlation	.948	.00299	.816 - 1.080	.0613 - .0697	.981

$$r_{10,.001} = .823$$

$$b \text{ (prescribed)} = 1.0$$

$$a \text{ (prescribed)} = 0.0$$

TABLE 6 STATISTICAL EVALUATION

VIII LITERATURE CITED

1. Bolland, J. L. and G. Gee, Trans Fara Soc., Vol. 42, 236 (1946).
2. Bolland, J. L. and P. ten Have, ibid., vol. 43, 201 (1947).
3. Twigg, G. H., Symposium - Oxidation Process in Chemical Manufacture, Sept., (1961) Soc. Chem. Ind. (London).
4. Bawn, C. E. Williamson, J. B., Trans. Fara. Soc., Vol. 47, 721 (1951).
5. Hatta, S. Techol. Rept. Tohoku Imp. Univ., 8, 1, (1928).
6. Hatta, S., ibid., 10, 118 (1932).
7. Davis, H. S. and Crandall, G. S., J. Am. Chem. Soc., 52, 3757, 3709 (1930).
8. Whitman, W. G., Chem. and Met. Eng., 29, No. 4, July 23, 1923.
9. Hildebrand, J. H., "Solubilities of non-electrolytes" Amer. Chem. Soc. Monograph Series, Reinhold Publishing Corp., 3rd Ed., p. 244, 425.
10. Danckwerts, P. V., Trans. Fara Soc. 46, 300, (1950).
11. Brian, P. L. T., Hurley, Hasseltine, E. H., A. I. Ch. E. J. 7 (2), 226, June (1961).
12. Brian, P. L. T., ibid., 10 (1), 5, Jan (1964).
13. Van de Vusse, J. G., Chem. Eng. Sci., 16, 21, (1961).
14. Astarita, G. and Marrucci, G., I & EC Fundamentals, Vol. 2, 4, Feb. (1963).
15. Akehata, T., "Absorption of Ethylene in Chlorine-water", to be published in Can. J. Chem. Eng..
16. Kimiya et al. and Ingold, Can. J. Chem., 41 2020 (1963).
17. U. S. Patent 2833814, May 6, 1958.
18. U. S. Patent 2804473, August 27, 1957.
19. U. S. Patent 2804473, August 27, 1957.
20. Phillips, B., Starcher, P. S., Frostick, F. C. Jr, J. Org. Chem., 26, 3568-71 (1961).

21. Higbie, R. Trans. Am. Inst. Chem. Engrs., 31, 365-89, (1935).
22. Sternling, C. R., Scriven, L. E., A.I.Ch.E. J. Vol. 5, No. 4, Dec. (1959).

ACKNOWLEDGEMENT

The author is gratefully indebted to Dr. A. I. Johnson and Dr. A. E. Hamielec for their guidance and assistance throughout the course of this work. He also wishes to acknowledge the financial assistance obtained through McMaster University and the National Research Council.

APPENDIX I LITERATURE SURVEY

1.1 Chemistry and Kinetics

1.1.1 Kinetics and Mechanism

The basic theory of liquid phase oxidation of organic materials was elucidated by Bolland, Gee and Farmer (37, 38). It was found that many of these oxidations are chain reactions. Because of their characteristic of producing hydroperoxide which further accelerates the reaction, they are often referred to as autocatalytic. These reactions are decelerated by traces of impurities, such as phenols and amines or some organic compounds, and accelerated by certain metal ions. The primary product of oxidation is hydroperoxide, the stability of which depends on the structure and stoichiometry of the oxidized material (39).

The oxidation of cumene was studied by Twigg (27) and his colleagues. The simplicity of this oxidation is due to the activation of the adjacent tertiary hydrogen atom by benzene ring. The mechanism leading to the production of peroxide is believed to be the same in the case of acetaldehyde which also possesses a hydrogen atom activated by a carbonyl group.

Based on his studies of hydrocarbon oxidation, Bolland (37, 38) has outlined a possible reaction scheme which, Twigg believed, can be applied equally well to aldehydes.

The general scheme of oxidation (37) comprises of three steps

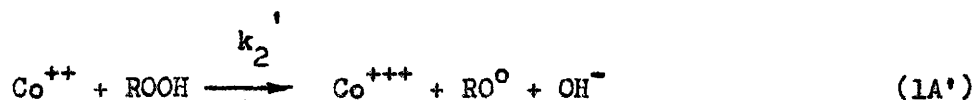
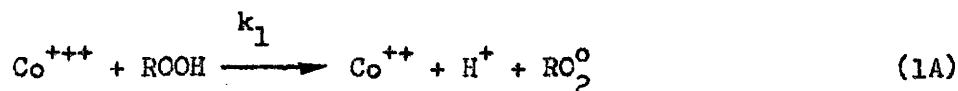
- 1) Initiation 2) Propagation 3) Termination

1) Initiation

In the initiation, free radicals are produced in several ways:

- a) by radiation which splits the molecule into radicals
- b) by the thermal decomposition into radicals of the hydroperoxide already present prior to the start of reaction.
- c) by the reaction of metal catalysts with the hydroperoxide to form radicals.

As the last method is widely used in industry, it was also used in this study. The initiation step can be written for a cobalt catalyst as:



2) Propagation

The two propagation steps are



3) Termination

The chains are terminated by the combination of radicals.



A complete kinetic analysis, allowing for all three termination reactions gives no simple explicit rate equation. However, an approximate treatment is possible by assuming $k_5 = k_4^{1/2} k_6^{1/2}$ whereupon it may be shown that the rate of oxidation is given by:

$$\frac{dC_A}{dt} = r^{1/2} \frac{k_3}{k_6^{1/2}} \frac{C_{RH} \cdot k_2 k_6^{1/2} C_A}{k_3 k_4^{1/2} C_{RH} + k_2 k_6^{1/2} C_A + k_4^{1/2} k_6^{1/2} r^{1/2}} \quad (7A)$$

where $r = k_1 C_a C_c$ is the rate of initiation; the k 's are the reaction rate constants.

The chain length is defined as the number of molecules of oxygen taken up per initiation

$$\rho = \frac{1}{r} \left(\frac{-dC_A}{dt} \right) \quad (8A)$$

At the start of the reaction when peroxide concentration is low the chain length is long, and the third term in the denominator of equation (7A) can be neglected. Furthermore if the oxygen pressure is sufficiently high the expression can be approximated to

$$\frac{-dC_A}{dt} = \frac{r^{1/2} k_3 C_{RH}}{k_6^{1/2}} \quad (9A)$$

Equation (9A) explains the shape of the absorption curve (see Figure 9). At the beginning, with little or no peroxide, the reaction is slow and then accelerates as the peroxide builds up. The rate of reaction reaches a maximum after which it starts to decrease because of the depletion of the oxidizable material. Bolland and his colleagues have carried out the oxidation of ethyl linoleate by three separate processes: (1) benzoyl peroxide catalysis (42); (2) photo - oxidation (41); (3) autoxidation (42). The rate of initiation was found to be proportional to $C_{BZ_2O_2}$, $C_I^{1/2}$ and C_{RO_2H} for the three cases respectively. However, the three rate equations derived from experimental data can be reduced to a common form,

$$\frac{-dC_A}{dt} = r^{1/2} k_3 C_{RH} \frac{C_A}{k_6 C_{RH} + C_A} \quad (10A)$$

where $r = k'_b C_{BZ_2O_2}$ for case (1)

$= k''_b C_I^{1/2}$ for case (2)

$= k'''_b C_{RO_2H}^2$ for case (3)

The similarity between equations (7A) and (10A) showed a close correspondence between the experimental and theoretical results. It is generally accepted that the decomposition of peroxide formed during various types of oxidation plays an essential role in the initiation of

the reaction. The decomposition of tetralin hydroperoxide was studied and the rate of decomposition was found to be first order (33). While in the oxidation of ethyl linoleate, the peroxide decomposition was second order (33, 37).

Kinetic investigations (33) of the thermal decomposition of hydroperoxide derived from low molecular weight saturated hydrocarbons have shown that the reaction is actually concurrent first and second order.

Comparing the experimental rate equations with the theoretical and assuming the rate of initiation is the rate of decomposition of hydroperoxides, composite quantities $k_3 k_6^{1/2}$ and $k_2 k_4^{1/2}$ can be evaluated. Bateman and Gee (41) have estimated k_3 and k_6 separately by the "rotating sector techniques". Results are summarized in the following table.

Olefin	Temp. °C	mol ⁻¹ l sec ⁻¹	
		k_3	$k_6 \times 10^{-6}$
Cyclohexane	15	0.6	0.9
Methyl - cyclohexane	15	1.1	0.5
Ethyl linoleate	11	5.7	0.5
Dihydromyrene	15	0.4	0.6

TABLE 6 RELATIVE MAGNITUDE OF k_3 and k_6 (33)

The conclusions which have been arrived at are:

- 1) The rate at which two RO_2 radicals react is quite insensitive to the structure of "R" in the radical.
- 2) The comparison of k_1 , the bimolecular rate constant of the peroxide

decomposition process throughout a series of olefins show that any variations are relatively trivial.

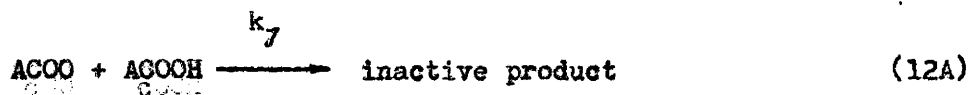
3) Consequently, the rate of autoxidation is mainly controlled by k_3 the propagation reaction which is very markedly dependent on the structure of the material being oxidized.

Bawn and Williamson (25) were the first workers to investigate experimentally the kinetics of the oxidation of acetaldehyde using cobalt acetate as catalyst.

They have concluded that the rate of oxidation is proportional to both the acetaldehyde and the catalyst concentration. The rate equation is

$$\frac{-dC_A}{dt} = k' C_B C_{ca} \quad (11A)$$

This relation can be accounted for by a chain reaction mechanism which differs from Bolland and Twigg's only in the nature of the termination reaction. Bawn's termination step may be represented by one of the following.



Equation 11A indicates that the rate of oxidation is not a function of peroxide concentration as contrasted to equation (9A). Bawn suggested at the beginning of the reaction where there is little peroxide, termination is by the interaction of two $ACOO$ radicals. As peroxide builds up, $ACOO$ begins to react with $ACOOH$ forming inactive products. Assuming equations 1A, 2A and 3A represent the initiation and propagation

reaction, the resulting rate equations for the two stages are:

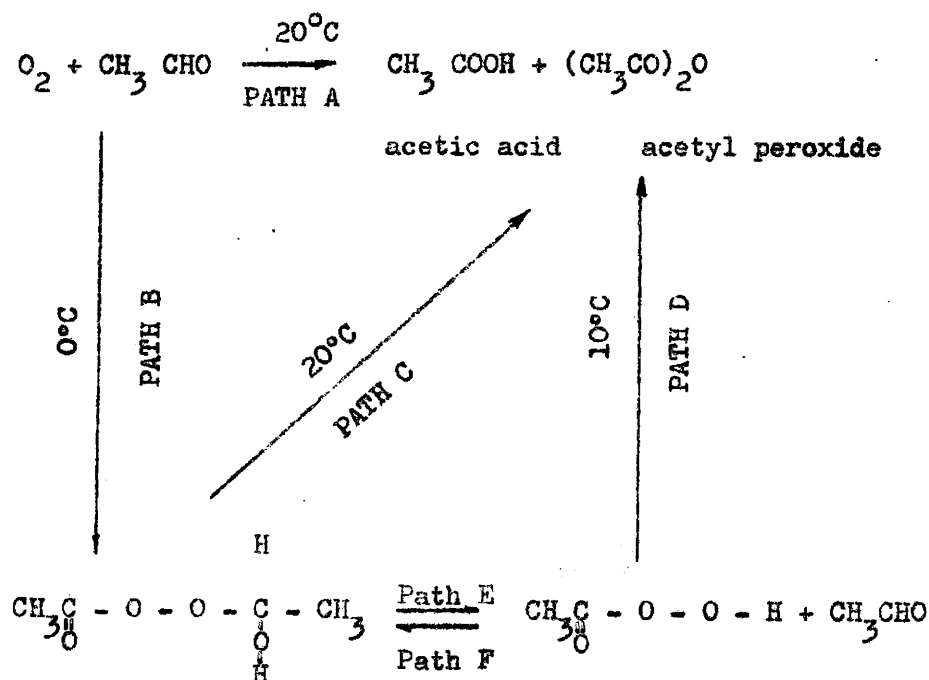
$$\frac{-dC_A}{dt} = k_3 C_B \sqrt{\frac{k_1}{k_6} C_B C_{ca}} \quad (14A)$$

$$\frac{-dC_A}{dt} = \frac{k_1 k_3}{k_7} C_{ca} C_B = k' C_{ca} C_B \quad (15A)$$

However, as the initial accelerating period is short, equation (15A) can be considered as the overall rate equation.

I.1.2 Side Reactions

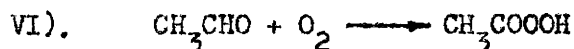
The oxidation of acetaldehyde by molecular oxygen, when catalysed by traces of iron, copper, and cobalt salts gives rise to several products the distribution of which is governed critically by temperature. Paths of reaction are shown in the following diagram (26)



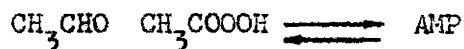
These reaction paths are also governed by the type and the amount of catalyst employed.

Generally, at temperatures between 0° and 20°C the oxidation of acetaldehyde can be said to proceed in three well-defined stages:

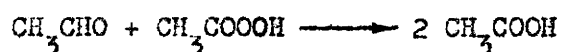
- a) the oxidation of acetaldehyde to peracetic acid (See Appendix



- b) the reaction of peracetic acid with acetaldehyde to give an addition compound AMP which is in equilibrium with its components.



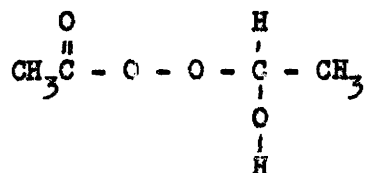
- c) the reaction of acetaldehyde with peracetic acid to form acetic acid



1.1.3 Formation and Decomposition of A.M.P.

Galitzenstein and Mugdan (44) have prepared A.M.P. by the oxidation of acetaldehyde with molecular oxygen. Temperature had to be kept low and certain impurities, particularly manganese and water, had to be excluded.

Careful analytical investigation of A.M.P. was made by Losch (43) who postulated that it is an addition compound of acetaldehyde and peracetic acid having a structure



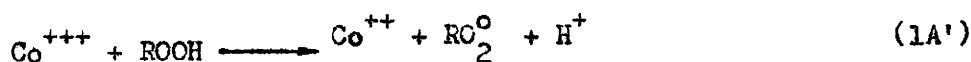
However, when the decomposition of the compound in water was

followed, it was found that the compound has a structure which corresponds to $(\text{ACH}.\text{ACOOH})\text{ACH}$ where the aldehyde outside the bracket is said to be the aldehyde of crystallization.

Bawn (25) has shown experimentally that the decomposition of A.M.P. in the absence of catalyst obeys a first order law. The rate is accelerated by the presence of cobalt acetate and other metal salts. This behaviour is consistent with that of hydrocarbon peroxides.

I.1.4 The Role of the Catalyst

A number of heavy metals, particularly those that possess two or more valency states with suitable reduction and oxidation potentials, such as cobalt, iron and copper, decompose hydroperoxides giving rise to free radicals which can initiate a chain reaction. The metallic ion can act either as a reductant or an oxidant.



Thus the rate of oxidation of organic materials, initiated by the above reaction, increases with the concentration of the metal salt. However, the catalytic effect reaches a maximum, so that further increase in concentration may, on the other hand, slow down the reaction. Kimiya and Ingold (45) have summarized the various opinions explaining the phenomenon of this maximum rate of oxidation.

Firstly, the concentration of hydroperoxide may have reached a steady - state when the rate of its formation by oxidation is equal to its rate of decomposition to free radicals by catalysts. Further

increase of catalyst concentration may not have any effect on the rate of oxidation but rather on some undesirable side reactions. This theory was first proposed by Tobolsky (46, 48) and supported experimentally by Woodward and Mesrobian (47).

Secondly, metal salts of organic acid, at high concentrations may associate into inactive micelles. Once the critical concentration has been passed further increase in catalyst will tend to cause an increase in the size and number of micelles rather than an increase in the amount of active catalyst (45).

Thirdly, George et al. (49) suggested that the metal catalyst may take part in both the initiation and the termination of the free radical chain reaction.

Finally, the catalyst may react with the hydroperoxide to form inactive products. Bawn and Williamson (25) in their work on the oxidation of acetaldehyde have shown that the rate of decomposition of peroxides is first order with respect to the catalyst. Hence an increase in catalyst concentration may cause further decomposition of peroxide, and the rate of reaction may be greatly reduced.

I.2 Theory of Diffusion with and without Chemical Reaction

I.2.1 Physical Mass Transfer and Enhancement Factor

Generally, the rate of mass transfer of a gas into a liquid is expressed in terms of a concentration driving force and a proportionality constant, the mass transfer coefficient in the liquid and thus,

$$N_A = k_L (C_{A1} - C_{A1}) \quad (19A)$$

If the mass transfer is accompanied by chemical reaction in the

liquid phase, then k_L is replaced by k_L^* which is the mass transfer coefficient with reaction. Letting $\mathcal{E} = \frac{k_L^*}{k_L}$, where \mathcal{E} is called the enhancement factor, the rate of absorption with chemical reaction is given by

$$N_A = k_L^* (C_{Ai} - C_{AL}) = \mathcal{E} k_L (C_{Ai} - C_{AL}) \quad (21A)$$

Therefore, the effect of chemical reaction is equivalent to multiplying the liquid phase coefficient by \mathcal{E} .

1.2.2 Steady State Mass Transfer in Stagnant Film of Finite Thickness

The kinetic theory of simultaneous diffusion and chemical reaction in the liquid phase has been developed by Hatta (1,2), Davis and Crandall (3) based on the assumption that the resistance to diffusion is concentrated within a thin film adjacent to the gas - liquid interface. This film is assumed to have negligible capacity for holding the dissolved solute compared with the main body of the liquid, which is so thoroughly mixed that no concentration gradient exists within it. The assumption of two such films, one in the gas and one in the liquid, is the basis of Whiteman's (24) two - film theory and of the resulting concept of resistances in series which can be expressed as

$$\frac{1}{K_L} = \frac{1}{mk_g} + \frac{1}{k_L} \quad (22A)$$

or

$$\frac{1}{K_g} = \frac{1}{k_g} + \frac{m}{k_L} \quad (23A)$$

The mechanism of simultaneous mass transfer and chemical reaction

is briefly described as follows. The solute A diffuses from the bulk of the gas through the film to the interface where it dissolves into liquid B and is gradually consumed by reaction. Thus, only some fraction of the solute or none at all, if the reaction is fast has passed through the liquid film reaching the bulk in free state.

The reactant B diffuses from the bulk of the liquid into the film where it reacts with A to form product C which diffuses in an opposite direction back to the bulk of the liquid.

Throughout this section, the following assumptions were made in order that the derivation of equations may be simplified.

- (1) There is no variation in physical properties within the film.
- (2) The reactant B and product C are non-volatile or ~~very~~ saturated with the gas phase so that there is no mass transfer of these components across the interface.
- (3) The rate of accumulation of materials in the film is zero.
- (4) The concentration of the solute is zero in the bulk of the liquid.

In the liquid film, consider a slab of unit area and thickness dx at a distance x from the interface as shown in Figure 1A. According to Fick's law, the rate of diffusion into the slab can be expressed by:

$$N_A = - D_A \frac{dC_A}{dx} \quad (24A)$$

Similarly, the rate of diffusion out of the slab is

$$N_A + dN_A = - \left(D_A \frac{dC_A}{dx} + \frac{d}{dx} \left(D_A \frac{dC_A}{dx} \right) dx \right) \quad (24B)$$

If the solution is dilute, it essentially contains one component,

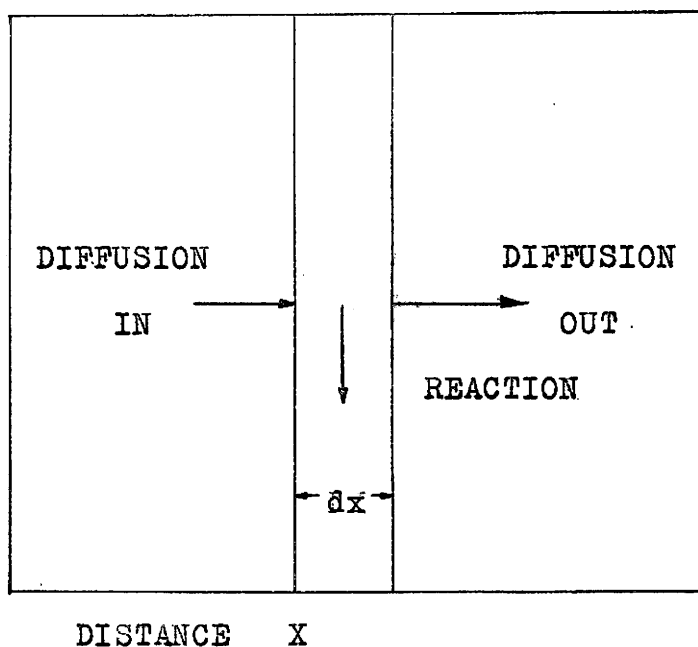


FIGURE 1A SIMPLIFIED PICTURE OF
SIMULTANEOUS STEADY STATE
DIFFUSION AND CHEMICAL REACTION

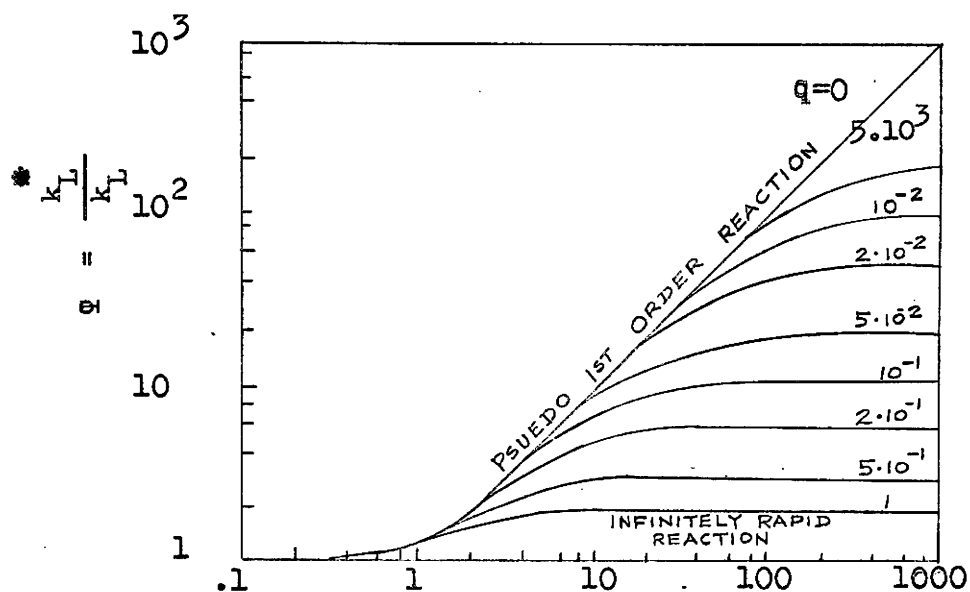


FIGURE 2A VAN KREVELEN'S SOLUTION
OF THE DIFFUSION WITH FAST
SECOND ORDER REACTION EQUATION

then the diffusivity can be assumed constant throughout the film. Thus,

$$N_A + dN_A = -D_A \left(\frac{dC_A}{dx} + \frac{d^2C_A}{dx^2} dx \right)$$

The consumption of A is then

$$N_A - (N_A + dN_A) = -dN_A = D_A \frac{d^2C_A}{dx^2} dx \quad (25A)$$

In steady state, the disappearance of A must be accounted for by chemical reaction. By material balances,

$$D_A \frac{d^2C_A}{dx^2} dx = (\text{rate of depletion of A}) \quad (26A)$$

The right hand side of equation (24A) may be a function of the concentrations of reactants or products, depending on the order and mechanism of the reaction.

Likewise, similar equations can be written for reactant B and product C as:

$$D_B \frac{d^2C_B}{dx^2} dx = \text{rate of depletion of B} \quad (27A)$$

$$D_C \frac{d^2C_C}{dx^2} dx = \text{rate of formation of C} \quad (28A)$$

I.2.2.1 First Order With Respect to Component A

If the reaction is first order with respect to component A, the rate of reaction per unit volume can be expressed as

$$\text{rate of depletion of A} = +k_{C1} C_A dx \quad (29A)$$

Substituting equation (29A) into equation (24A), the following equation is obtained

$$D_A \frac{d^2 C_A}{dx^2} = +k_{C1} C_A \quad (30A)$$

Assuming k_{C1} constant throughout the entire film at any instant, the solution for equation (30A) was obtained by Hatta (1) as:

$$C_A = A_1 e^{\alpha x} + A_2 e^{-\alpha x} \quad (31A)$$

Applying the following boundary conditions

$$X = 0, \quad C_A = C_{Ai}, \quad (32A)$$

$$X = X_L, \quad C_A = 0, \quad (32A')$$

the concentration of A in the film is given by

$$C_A = \frac{\text{Sinh } \alpha (X_L - X)}{\text{Sinh } \alpha X_L} C_{Ai}, \text{ and } \alpha = \sqrt{\frac{k_{C1}}{D_A}} \quad (33A)$$

$$\text{Therefore, } \frac{dC_A}{dx} = -\frac{\text{Cosh } \alpha (X_L - X)}{\text{Sinh } \alpha X_L} \alpha C_{Ai}$$

The rate of diffusion of A into the liquid is obtained by multiplying the slope at $X = 0$ by the diffusivity D_A . Thus,

$$\begin{aligned} N_A &= -D_A \left(\frac{dC_A}{dx} \right)_{x=0} = D_A \alpha C_{Ai} \frac{\text{Cosh}(\alpha X_L)}{\text{Sinh}(\alpha X_L)} \\ &= \frac{D_A \alpha C_{Ai}}{\text{Tanh}(\alpha X_L)} \end{aligned} \quad (34A)$$

Alternatively, the rate of mass transfer across the interface can also be expressed as equation (19A) that

$$N_A = k_L^* (C_{Ai} - C_{AL})$$

In this case, $C_A = 0$ at $X \geq X_L$

then

$$N_A = k_L^* C_{Ai} \quad (35A)$$

Equating (34) and (35),

$$k_L^* = \frac{D_A \alpha}{\tanh(\alpha X_L)} \quad (36A)$$

From equation (20A)

$$\Phi = \frac{k_L^*}{k_L} \quad \text{and letting } k_L = \frac{D_A}{X_L}$$

then

$$\Phi = \frac{(X_L \alpha)}{\tanh(X_L \alpha)} \quad (37A)$$

Examining equation (34A) a few interesting observations are made.

First, the rate of absorption should be constant if X_L governed by hydrodynamic conditions are unchanged.

Second, when (αX_L) is very small (< 0.2) due to slow reaction rate or thin film, Φ is nearly unity. In such cases the absorption is essentially by physical mass transfer. The effect of chemical reaction upon rate of absorption is negligibly small.

Third, when (αX_L) is large (> 3.0) due to rapid reaction rate or

thick film, \bar{x} is equal to (αX_L) equation (34A) then becomes

$$N_A = \sqrt{k_{c1} D_A} C_{Ai} \quad (38A)$$

In such cases, the rate of absorption is independent of film thickness or hydrodynamic conditions of the liquid phase.

I.2.2.2 Second Order with Respect to Components A and B

If the reaction is second order with respect to components A and B, the rate of reaction can be expressed as $k_{c2} C_A C_B$, where k_{c2} is the reaction rate constant. Then equations (26A) and (27A) become

$$D_A \frac{d^2 C_A}{dx^2} = k_{c2} C_A C_B \quad (39A)$$

$$D_B \frac{d^2 C_B}{dx^2} = k_{c2} C_A C_B \quad (40A)$$

Assuming that B is non-volatile and also that the concentration of B is constant throughout the bulk of the liquid, the boundary conditions are

$$X = 0, C_A = C_{Ai}, \frac{dC_A}{dx} = 0; \quad (41A)$$

$$X = X_L, C_A = 0, C_B = C_{BL}$$

Since equation (37A) and (38A) are non-linear differential equations analytical solutions are impossible. However,

$$\text{since } N_A = k_L^* C_{Ai} = -D_A \left. \frac{dC_A}{dx} \right|_{X=0}$$

$$k_L^* = \left(-D_A \frac{dC_A}{dx} \right)_{X=0} / C_{Ai}$$

$$\text{then } \bar{x} = \frac{k_L^*}{k_L} = \left(-\frac{dC_A}{dx} \right)_{X=0} \frac{X_L}{C_{Ai}} \quad (42A)$$

An approximate solution was obtained by Van Krevelen (5).

Assuming $C_B = C_{Bi}$ throughout the reaction zone, after which $C_A = 0$ and C_B increases linearly to C_{BL} at $X = X_L$ his explicit solution is expressed as:

$$\bar{\Phi} = \frac{-\sqrt{M(1-q(\bar{\Phi} - 1))}}{\tanh \sqrt{M(1-q(\bar{\Phi} - 1))}} \quad (43A)$$

Equation (43A) is plotted in Figure (2A)

where

$$M = C_{BL} R_O^2 X_L = \frac{k_{C2} C_{BL} X_L^2}{D_A}$$

$$q = \frac{D_A C_{Ai}}{D_B C_{BL}}$$

$$R_O^2 = \frac{k_{C2}}{k_L}$$

It is noteworthy to consider equation (43A) in some limiting cases

- (1) When M approaches zero $\bar{\Phi}$ tends to unity. This condition is met if either the rate of reaction is slow or the film is thin. In such cases, physical absorption prevails.
- (2) When M approaches infinity, then

$$\lim_{M \rightarrow \infty} \bar{\Phi} = \frac{\lim_{M \rightarrow \infty} \sqrt{M(1-q(\bar{\Phi} - 1))}}{1} \quad \text{as}$$

$$\tanh(\infty) = 1.$$

Since $\bar{\Phi}$ must be finite

$$\lim_{M \rightarrow \infty} \sqrt{1 - q(\bar{\Phi} - 1)} = 0 \quad (44A)$$

Consequently,

$$\bar{\Phi} = 1 + \frac{1}{q} = 1 + \frac{D_B C_{BL}}{D_A C_{Ai}} \quad (45A)$$

Equation (45A) was also derived by Hatta (7) for absorption with second order fast reactions.

For any gas - liquid reacting system, if the reaction rate is fast or the film is thick the rate of absorption is independent of k_{c2} and X_L but increases linearly with C_{BL} .

(3) When q approaches zero, equation (41A) becomes:

$$\Phi = \frac{\sqrt{M}}{\tanh \sqrt{M}} = \frac{X_L \sqrt{\frac{k_{c2} C_{BL}}{D_A}}}{\tanh X_L \sqrt{\frac{k_{c2} C_{BL}}{D_A}}} \quad (46A)$$

which is identical to equation (43A) for first order reaction provided that the rate constant k_{c1} is now replaced by $(k_{c2} C_{BL})$. This case corresponds to a pseudo - first - order reaction in the film, that is, $C_B = C_{BL} = C_{B1}$, $X \gg 0$.

Comparing equations (36A) and (46A) it can be shown that when $M > 3.0$ equation (46A) becomes:

$$\Phi = \sqrt{M} = X_L \sqrt{\frac{k_{c2} C_{BL}}{D_A}} = \frac{k_L^*}{k_L}$$

$$\text{But } k_L = \frac{D_A}{X_L} ,$$

$$\text{hence, } k_L^* = \sqrt{(k_{c2} C_{BL}) D_A} \quad (47A)$$

1.2.2.3 Reaction Mechanism of Complex Nature

The above discussions have made the tacit assumption that the

absorption of gas A into liquid B is accompanied by reactions of simple mechanism, such as, $A + B \longrightarrow C$, in which case rate equations may be formulated by the law of mass action.

In most absorption processes the mechanism of reaction is complicated by side reactions, consecutive reactions or chain reactions. However, the film theory can still be applied if the mechanism of the reaction is known. Reaction rate expressions are first formulated according to the proposed mechanism and equated to diffusion terms. A general equation is written as

$$D_n \frac{d^2 C_n}{dx^2} = - \text{rate of change of concentration of component } n \quad (48A)$$

Equations analogous to (48A) can be written for n components and solved simultaneously by computers subjected to known boundary conditions.

The reaction of oxygen with acetaldehyde in the liquid phase follows a chain mechanism. The overall reaction is:



The following differential equations were derived to describe the concentration profiles of the components for the O_2 - ACH system

$$D_A \frac{d^2 C_A}{dx^2} = k'' C_B \quad (49A)$$

$$D_B \frac{d^2 C_B}{dx^2} = k'' C_B^2 / C_C \quad (50A)$$

$$D_C \frac{d^2 C_C}{dx^2} = k'' C_B \quad (51A)$$

Equations (49A) (50A) and (51A) were solved simultaneously by the

analog computer using the boundary conditions:

$$(1) \quad X = 0, C_A = C_{Ai}, \quad \frac{dC_B}{dx} = 0, \quad \frac{dC_C}{dx} = 0;$$

$$(2) \quad X \geq X_R, 0 < X_R < X_L, \quad C_A = 0, \quad \frac{dC_A}{dx} = 0.$$

Furthermore, when $C_A = 0$ there is no reaction and thus the right hand side of equations (49A) (50A) and (51A) vanish. Hence,

$$\frac{d^2 C_B}{dx^2} = 0, \quad \frac{d^2 C_C}{dx^2} = 0$$

$$(3) \quad X = X_L, C_B = C_{BL}, C_C = C_{cL}$$

Figure 1 has illustrated the concentration profiles that may result. The concentration of component A decreases from the interfacial concentration C_{Ai} to zero and remains zero at $X \geq X_R$. As it is assumed that B and C are non-volatile, or the gas phase is saturated with their vapors, so that there is no mass transfer across the interface, C_B and C_C both start with a zero concentration gradient. Gradually, C_B increases while C_C decreases to their bulk concentrations.

I.2.2.4 Kinetic Equations and Hydrodynamics in the Film.

Detailed derivation of kinetic equations for the reactions between oxygen and acetaldehyde are given in Appendix VI. Hydrodynamics in the film as referred to the conditions of the present system will be discussed in Section II.

I.2.3 Unsteady State Diffusion in Stagnant Liquid of Semi - Infinite Thickness

As truly stagnant films are hardly conceivable in industrial absorbers, Higbie (8) was one of first to suggest the application of the unsteady - state diffusion concept to the process of gas absorption with chemical reactions. Danckwerts (9) has derived and solved equations for the rate of absorption of solute gas into a semi - infinite medium with which the gas undergoes a first order or pseudo - first order reaction. Brian, Hurley & Hassaltine (12) and Astarita & Marrucci (10) have solved the unsteady - state diffusion equations with reactions of second and zeroth order respectively. Brian (11) in his recently published paper has extended his solution to cases where the reaction is nth order with respect to the gas and the liquid.

In all the above cases, the following assumptions have been made:

- (1) The medium has a plane surface and is of infinite depth, or for practical purpose, is of such a depth that the concentration at the bottom does not change appreciably during the period of time considered.
- (2) The surface of the liquid is continuously saturated with the gas.
- (3) All physical properties including diffusivities, densities and viscosities are virtually constant throughout the liquid.

In the liquid medium, consider a slab of unit area and thickness dx as shown in figure 3A. The rates of diffusion into and out of the slab are given by equations (24A) and (24A'). The disappearance of A is accounted for not only by reaction but also by accumulation in the slab. Thus a general equation can be set up as follows:

$$\frac{\partial C_A}{\partial t} = D_A \frac{\partial^2 C_A}{\partial x^2} - \text{rate of reaction} \quad (52A)$$

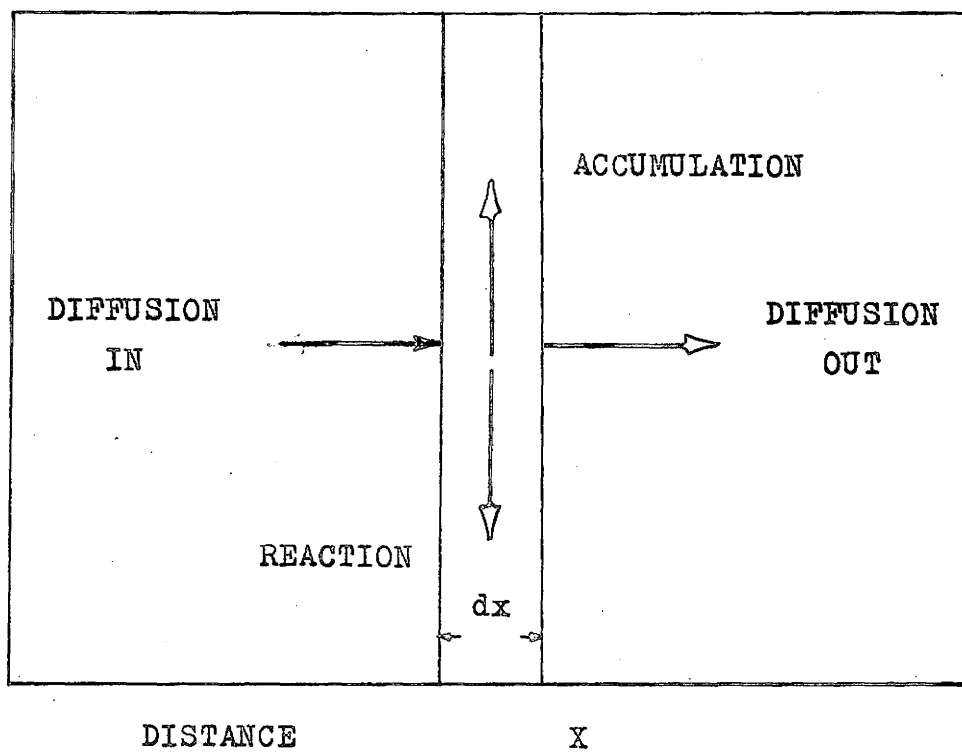


FIGURE 3A SIMPLIFIED PICTURE OF SIMULTANEOUS
UNSTEADY STATE DIFFUSION AND
CHEMICAL REACTION

I.2.3.1 First Order With Respect to Component A

If the reaction is first order with respect to the gas, equation (52A) becomes:

$$\frac{\partial C_A}{\partial t} = D_A \frac{\partial^2 C_A}{\partial x^2} - k_{cl} C_A \quad (53A)$$

With the following boundary conditions,

$$\begin{aligned} x = 0, \quad t > 0, \quad C_A &= C_{A1}; \\ x > 0, \quad t = 0, \quad C_A &= 0; \\ x = \infty, \quad t > 0, \quad C_A &= 0. \end{aligned} \quad (54A)$$

Equation (53A) may be solved (9, 54) by substituting

$$C_A = \mu e^{-\frac{k_{cl} t}{D_A}}, \quad (55A)$$

which reduces it to

$$\frac{\partial \mu}{\partial t} = D_A \frac{\partial^2 \mu}{\partial x^2}, \quad (56A)$$

With boundary conditions

$$\begin{aligned} x = 0, \quad t > 0, \quad \mu &= C_{A1} e^{-\frac{k_{cl} t}{D_A}}; \\ x > 0, \quad t = 0, \quad \mu &= 0; \\ x = \infty, \quad t > 0, \quad \mu &= 0. \end{aligned} \quad (57A)$$

Equation (56A) becomes identical to the equation for conduction of heat in a semi - infinite rod with initial temperature zero and surface temperature a function of time. Method of solution in detail is found on page 64 "Conduction of Heat in Solids" by Carslaw and Jaeger (13).

The solution to equation (53A) is,

$$\frac{C_A}{C_{Ai}} = \frac{1}{2} \exp \left(-x \sqrt{\frac{k_{cl}}{D_A}} \right) \operatorname{erfc} \left[\frac{x}{2\sqrt{D_A t}} - \sqrt{k_{cl} t} \right] + \frac{1}{2} \exp \left(x \sqrt{\frac{k_{cl}}{D_A}} \right) \operatorname{erfc} \left[\frac{x}{2\sqrt{D_A t}} + \sqrt{k_{cl} t} \right] \quad (58A)$$

where $\operatorname{erf} z = \frac{2}{\sqrt{\pi}} \int_0^z e^{-x^2} dx$;

and $\operatorname{erfc} z = 1 - \operatorname{erf} z$.

According to Fick's law the rate of absorption is given by

$$N_A = -D_A \left(\frac{\partial C_A}{\partial x} \right)_{x=0} \quad (59A)$$

Differentiating equation (58A) with respect to x and setting $x=0$ one obtains

$$\left. \frac{\partial C_A}{\partial x} \right|_{x=0} = -C_{Ai} \sqrt{\frac{k_{cl}}{D_A}} \left[\operatorname{erf} \sqrt{k_{cl} t} + \frac{e^{-k_{cl} t}}{\sqrt{\pi k_{cl} t}} \right] \quad (60A)$$

Therefore,

$$N_A = C_{Ai} \sqrt{D_A k_{cl}} \left[\operatorname{erf} \sqrt{k_{cl} t} + \frac{e^{-k_{cl} t}}{\sqrt{\pi k_{cl} t}} \right] \quad (61A)$$

When $k_{cl} t$ is sufficiently large, say > 3.0 ,

$$\operatorname{erf} \sqrt{k_{cl} t} \doteq 1$$

$$\operatorname{erf} (-\sqrt{k_{cl} t}) \doteq -1$$

and the second term in equations (58A) and (61A) vanishes, giving

$$\frac{C_A}{C_{Ai}} \doteq \exp \left(-x \sqrt{\frac{k_{cl}}{D_A}} \right) \quad (62A)$$

and

$$N_A = C_{Ai} \sqrt{D_A k_{cl}} \quad (63A)$$

Equation (63A) is identical to (38A) derived from the film theory. Thus, when the reaction is fast or time is long, the rate of absorption and the concentration at any point approach some steady-state values. When kt is small, $\text{erf } \sqrt{k_{cl} t}$ and $e^{-k_{cl} t}$ can be expanded in power series:

$$\text{erf}(z) = \frac{2}{\sqrt{\pi}} \left(x - \frac{x^3}{3} + \frac{x^5}{2 \cdot 5 \dots} \right)$$

$$e^{-z} = 1 - x + \frac{x^2}{2!} - \frac{x^3}{3!} \dots$$

Neglecting powers of $k_{cl} t$ other than the first, equations (58A) and (60A) become

$$\begin{aligned} \frac{C_A}{C_{Ai}} &= \frac{1}{2} \text{erfc} \frac{x}{2\sqrt{D_A t}} \left(e^{-x \sqrt{\frac{k_{cl}}{D_A}}} + e^{-x \sqrt{\frac{k_{cl}}{D_A}}} \right) \\ &\doteq \text{erfc} \frac{x}{2\sqrt{D_A t}} \cosh x \sqrt{\frac{k_{cl}}{D_A}} \end{aligned} \quad (64A)$$

and $N_A \doteq C_{Ai} \sqrt{\frac{D_A}{\pi t}} (1 + k_{cl} t)$

1.2.3.2 Zeroth Order

For many years the process of simultaneous absorption and chemical reaction has been studied both theoretically and experimentally by many investigators. Most workers dealt with reactions of first or pseudo-first order and second order. However, the kinetics for many gas -

liquid systems, such as the oxidation of hydrocarbons cannot be explained by the existing theories. It was not until recently that Van de Vusse (14) started to deal with this type of reaction by assuming it zeroth order, that is, the rate of reaction is no longer dependent on the concentration of the reactants. A rigorous mathematical treatment of the problem was given by Astarita and Marrucci (10). The unsteady - state diffusion involving zeroth order chemical reaction is represented by the following differential equation:

$$D_A \frac{\partial^2 C_A}{\partial x^2} = \frac{\partial C_A}{\partial t} + k_{Co} H(C_A) \quad (65A)$$

where the function $H(C)$ is defined as:

$$H(C_A) = 1, \text{ when } C_A > 0 ; \quad (66A)$$

$$H(C_A) = 0, \text{ when } C_A \leq 0 . \quad (67A)$$

and k_{Co} is the zeroth order reaction rate constant. If the liquid medium is assumed infinitely deep, then the boundary conditions are

$$t = 0, X > 0, C = C_{AO} ; \quad (68A)$$

$$t > 0, X = 0, C = C_{Ai} ; \quad (69A)$$

$$t > 0, X \rightarrow \infty, C = \max(C_{AO} - k_{Co}t, 0) . \quad (70A)$$

where $k_{Co}t$ is the amount of A depleted by reaction and $\max(C_{AO} - k_{Co}t, 0)$ is equal to the larger of $C_{AO} - k_{Co}t$ and 0.

Because the reaction is zeroth order the rate of which is independent of C_A , mathematically, when x approaches infinity reaction still continues at a constant rate in spite of the fact that C_A may be zero.

Therefore equations (66A), (67A) and (70A) are required to fulfill the physically obvious condition that the rate of reaction is zero in the absence of solute A and also that C_A is never negative.

$$(1) \text{ Solution for } t < \frac{C_{AO}}{k_{Co}}$$

In such case, nowhere in the liquid has concentration of A become zero. Then according to equation (66A) $H(C_A)$ is equal to 1 for any positive value of x and equation (65A) thus becomes:

$$\frac{\partial^2 C_A}{\partial x^2} - \frac{1}{D_A} \frac{\partial C_A}{\partial t} - \frac{k_{Co}}{D_A} = 0 \quad (71A)$$

Letting $C_A = u + C_{AO} - k_{Co}t$

equation (71A) reduces to

$$\frac{\partial^2 u}{\partial x^2} = \frac{1}{D_A} \frac{\partial u}{\partial t} \quad (72A)$$

Subject to the boundary conditions:

$$x = 0, \quad t > 0, \quad u = C_{A1} - C_{AO} + k_{Co}t; \quad (a)$$

$$x > 0, \quad t = 0, \quad u = 0; \quad (b)$$

$$x \rightarrow \infty, \quad t > 0, \quad C_A = C_{AO} - k_{Co}t,$$

$$\therefore u = 0 \quad (c)$$

Equations (72A) and (73A) are analogous to equations for heat conduction in a semi - infinite rod with initial temperature zero and surface temperature $f(t)$. The solution may be deduced by Duhamel's Theorem (16) as

$$C_A = (k_{Co}t + C_{Ai} - C_{AO} - \frac{k_{Co}x^2}{2D_A}) \operatorname{erfc} \frac{x}{2\sqrt{D_A t}} - k_{Co} \sqrt{\frac{t}{\pi D_A}} x e^{-\frac{x^2}{4D_A t}} + C_{AO} - k_{Co}t \quad (74A)$$

By differentiating equation (74A) with respect to x and letting $x = 0$, one obtains

$$\left. \frac{\partial C_A}{\partial x} \right|_{x=0} = -\sqrt{\frac{k_{Co}}{\pi D_A}} \left(\frac{C_{Ai} - C_{AO}}{\sqrt{k_{Co}t}} + 2\sqrt{k_{Co}t} \right) \quad (75A)$$

and

$$N_A = -D \left. \frac{\partial C_A}{\partial x} \right|_{x=0} = \sqrt{\frac{D_A k_{Co}}{\pi}} \left(\frac{C_{Ai} - C_{AO}}{\sqrt{k_{Co}t}} + 2\sqrt{k_{Co}t} \right) \quad (76A)$$

Equation (74A) is shown diagrammatically in Figure 4A. It is noticed that $-\left(\frac{\partial C_A}{\partial x}\right)_{x=0}$ first decreases toward a minimum value and then eventually increases to a constant for all values of C_{AO} smaller than C_{Ai} .

It should be noted that when $t = t_D$, $C_A = C_{AO} - k_{Co}t_D = 0$ at $x = x_\lambda$. When this happens equations (71A) and (76A) no longer hold.

The physical meaning of the minimum is that at very low values of t interfacial concentration gradient decreases with time because of the self-quenching effect of the diffusion process. Eventually, this effect slows down, while the chemical reaction continues at constant rate, thus steepening the concentration gradient by depleting the solute gas.

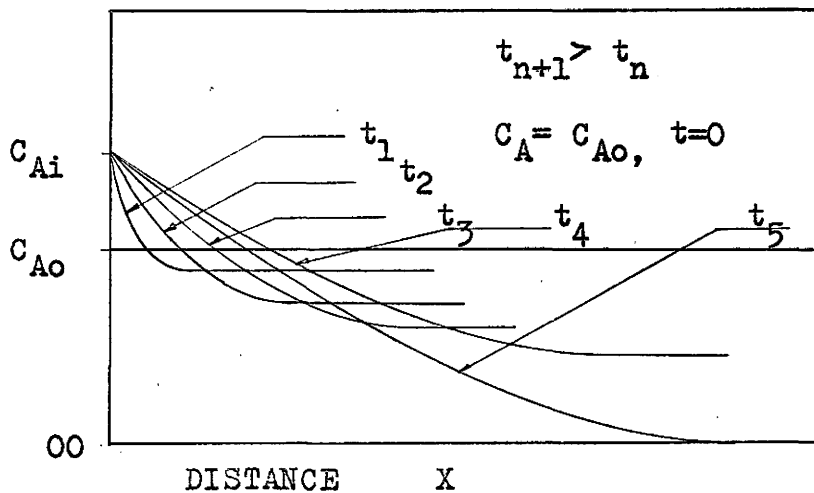


FIGURE 4A CONCENTRATION PROFILES OF
SOLUTE IN LIQUID ($C_{A0} > 0$)

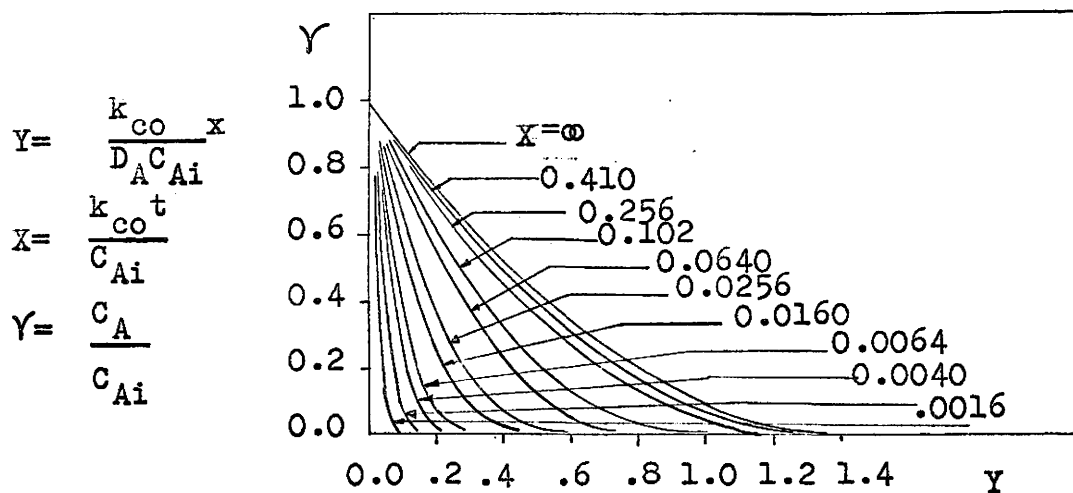


FIGURE 5A CONCENTRATION PROFILES OF
SOLUTE IN LIQUID ($C_{A0} = 0$)

(2) Solution for $t > \frac{C_{AO}}{k_{Co}}$

As soon as t reaches the value $\frac{C_{AO}}{k_{Co}}$, C_A becomes zero at x_λ whose position moves along the x - axis with time. For values of x larger than x_λ , C_A is constantly zero.

Equation (65A) subject to boundary conditions:

$$x = 0, \quad C_A = C_{Ai};$$

$$x = x_\lambda, \quad C_A = 0;$$

$$t = \frac{C_{AO}}{k_{Co}}, \quad C_A = (C_{Ai} + \frac{k_{Co}}{D_A} \frac{x^2}{2} \operatorname{erfc} \frac{1}{2} \sqrt{\frac{k_{Co}}{D_A C_{AO}}} x$$

$$- \sqrt{\frac{k_{Co} C_{AO}}{\pi D_A}} x \exp \left(\frac{-k_{Co} x^2}{4 D_A C_{AO}} \right) \quad (77A)$$

could not be solved analytically. A numerical solution using finite differences was presented by Astarita and Marrucci (10) and plotted in Figure 5A.

(3) Solution for $k_{Co} t$ approaching infinity

At very high values of $k_{Co} t$ a steady - state is reached. Equation (65A) is then reduced to

$$D_A \frac{d^2 C_A}{dx^2} = \frac{k_{Co}}{D_A} \quad (78A)$$

with the following boundary conditions

$$x = 0, \quad C_A = C_{Ai};$$

$$x = x_{\lambda\infty}, \quad \frac{dC_A}{dx} = 0, \quad C_A = 0. \quad (79A)$$

Integrating (78A) twice and using equation (79A) one obtains

$$C_A = \frac{k_{Co}}{D_A} \frac{x^2}{2} - \frac{k_{Co}}{D_A} x_{\lambda\omega} x + C_{A1} \quad (80A)$$

When $x = x_{\lambda\omega}$, $C_A = 0$.

From equation (80A)

$$x_{\lambda\omega} = \sqrt{\frac{2 C_{A1} D_A}{k_{Co}}}, \text{ and}$$

$$\left. \frac{dC_A}{dx} \right|_{x=0} = - \frac{k_{Co} x_{\lambda\omega}}{D_A} = 2 \sqrt{\frac{k_{Co} C_{A1}}{D_A}} \quad (81A)$$

$$N_A = - D_A \left. \frac{dC_A}{dx} \right|_{x=0} = 2 \sqrt{D_A k_{Co} C_{A1}} \quad (82A)$$

Equation (82A) indicates that the absorption rate is proportional only to the square root of the driving force C_{A1} .

From Figure (5A) it appears that at $\frac{k_{Co} t}{C_{A1}} = 0.4$, the steady-state is reached. Hence, equation (82A) may be a good approximation for the rate of absorption when $\frac{k_{Co} t}{C_{A1}} > 1.0$

APPENDIX II EXPERIMENTAL DETAILS

II.1 Description of Apparatus

The apparatus used by Akehata (32) was adopted for some preliminary studies. It was later modified, (A) to eliminate all the rubber joints and tubings which may easily be attacked by peracetic acid and ethyl acetate; (B) to increase the diameter of the reaction vessel and thus the area for mass transfer; (C) to decrease the size of the feeding tube to minimize back diffusion; (D) to equip with a constant - head storage tank to enable long runs to be made with less attention.

The essential components of the modified apparatus are described in the following sub - sections.

Reaction Vessel

The essential feature of the apparatus is an open cylindrical glass vessel, (Fisher's Standard Reaction Kettle) four inches I.D. and eight inches high. The lid of the vessel has four ground glass junctions leading individually to a gas burette, feeding funnel, mercury seal and a bleeding stop cock. The lid and the vessel are jointed by ground glass contact and brought together tightly by stainless steel clamps. At the bottom of the vessel is a delivery tube for draining and sampling. The mercury seal allows the introduction of the stirrer and at the same time seals the vessel from the atmosphere.

Agitation Device

Agitation in the vessel is obtained by a stirrer made of 316 stainless steel. The stirrer has three blades equally spaced so that both the bulk of the gas and liquid are well mixed even at low stirring speeds. The stirrer is driven by a variable speed motor (200 r.p.m. - 1000 r.p.m.) equipped with a 3:1 reduction gear in order that very low speeds can be obtained.

Gas Burette

Absorption rates were measured by a gas burette which connects to the reaction vessel by a three - way stopcock. The burette with a capacity of 100 ml, is graduated at 0.2 ml intervals and jacketed by water at room temperature.

Gas Storage Tank

The gas tank has a capacity of two gallons and is connected to a constant head bubbler from which ethyl acetate continuously runs into the tank under a constant pressure displacing the gas into the reaction vessel.

Pressure Control

During the measurement of absorption rates atmospheric pressure is maintained in the gas burette and in the reaction vessel by means of a mercury levelling bottle which can be raised or lowered by a crank or a micrometer for fine adjustment. Pressure inside the vessel is indicated by a manometer.

When long runs are made the reaction vessel is connected to the

gas storage tank which is maintained at approximately atmospheric pressure by the constant head bubbler.

Temperature Control

The reaction vessel is immersed in a thermostated ethylene - glycol - water bath which is kept below room temperature by a cooling coil through which a coolant from a refrigeration unit is circulated. The temperature of bath can be adjusted to the nearest $\pm .25^{\circ}\text{C}$.

II.2 Some Illustrations of Hydrodynamic Conditions and Limitation Of the Apparatus

Although the hydrodynamic conditions at the interface is not well defined it may be assumed laminar if the stirrer speed is low. The existence of the laminar layer was indicated by the flow pattern of small paper particles moving in the liquid under stirring condition.

By introducing a few drops of red ink it was indicated that the bulk of the liquid is well mixed.

The apparatus has its limitation in measuring low rates of absorption, especially, in the case where no chemical reaction occurs. In order to have a significant volume change of the gas in the burette, the length of time necessary for each run is over two hours during which a variation of 0.5 degrees in the temperature of the bath would have upset the final result by one hundred percent.

II.3 Leakage

Before each experiment, a leakage test was run. The vessel was connected to the gas burette. The reading of the mercury level was

taken when the pressure was adjusted to atmospheric. The reading was checked again after the levelling bottle was raised and lowered several times. If these readings did not differ by more than .2 ml there was no leakage.

II.4 Preliminary Studies on the Effect of Several Variables on Mass Transfer

II.4.1 Acetaldehyde Concentration

Preparation of Solutions

In every experiment, the amount of catalyst used was constant. This could be arranged by making a standard cobaltous acetate solution in acetic acid and measuring a constant volume with a pipette. Acetaldehyde solution having concentrations varying from .017 to .255 mole fraction was made from acetaldehyde and ethyl acetate by accurate weighing to the nearest .01 gm.

Choice of Stirring Speed and Catalyst Concentration

Acetaldehyde is a very volatile substance. The gas phase in the reactor therefore, contains some organic vapors, the amount of which depends on the concentration of aldehyde in the liquid. When the absorption rate is high, in the case of high acetaldehyde concentrations, and the stirrer speed is low, oxygen near the interface is used up much faster than the bulk of the gas can supply it. Then there is an existence of a significant gas phase resistance changing with time which complicates the situation. Therefore, the catalyst concentration and the stirring speed were so

adjusted that for all experiments, the absorption rate was never very high and at the same time the liquid surface always plane.

II.4.2 Catalyst Concentration

In these experiments, the acetaldehyde concentration used was always .162 mole fraction. Cobaltous acetate standard solution was made by dissolving .100 gm in 100 ml acetic acid. Although the volume of $\text{Co}(\text{OAc})_2$ solution used varied in each experiment, the total amount of acetic acid was kept constant by the addition of pure acetic acid.

At very low catalyst concentrations the absorption rates became very slow. Difficulty arose in the measurement of volume change by the gas burette.

II.4.3 Partial Pressure of Oxygen

In order to show the effect of partial pressure of oxygen on the coefficient of mass transfer, acetaldehyde and catalyst concentrations were kept constant for all experiments. Partial pressures of oxygen were varied by using enriched air, which came in cylinders of the following compositions:

	O_2	N_2
(1)	100%	0
(2)	75%	25%
(3)	50%	50%
(4)	21%	79%

In all experiments when pure oxygen was used, the partial pressure of oxygen in the vessel remained the same during the run. Thus the absorption rate was not a function of time. However, when oxygen -

nitrogen mixtures were used, the partial pressure and thus the absorption rate decreased with time. Therefore, at the start of each run there should be very little or no time delay between the introduction of the feed, the starting of the clock and reading of the gas burette.

The displacement equation (See Appendix VIII) must be reconsidered for different composition of the gas mixtures to estimate the time needed for flushing the apparatus so that 99.5% of the air in the reactor was displaced by the gas in use.

II.4.4 Temperature

As acetaldehyde boils at 20°C and the reaction changes its path at higher temperatures, it is therefore desirable to keep the temperature between $0^{\circ} - 10^{\circ}\text{C}$.

The ethylene - glycol - water bath was set at 0° , 4° , 10°C respectively. Experiments were run at each temperature for a range of acetaldehyde concentrations from .068 - .24 mole fractions.

II.5 Unsteady - State Mass Transfer Studies

The general experimental procedure was the same as in II.3 except that only the gas phase was stirred. Volume of gas absorbed V_g at time t was measured. The experiment was repeated at different temperatures and stirring speeds. Analysis of acetaldehyde was carried out before and after each run.

II.6 Steady-State Mass Transfer Studies

The general experimental procedure was the same as in II.3 except that the product distribution was determined by analytical methods.

outlined in Appendix X.

The extent of oxidation was followed by measuring absorption rates and determining product concentrations at convenient time intervals. The main part of an experiment was carried out with the reaction vessel connected to the gas storage tank, so that the run could be made continuous for a period of eight hours. Before absorption rates were measured the gas burette was connected to the vessel. The measurement should take approximately ten minutes after which a 7-ml sample was taken from the bottom delivery tube. Seven ml of fresh feed was then added through the feeding funnel. Before each addition the pressure inside the vessel must be kept slightly above atmospheric so that no air could be admitted into the system.

The sample for analysis must be kept cold with ice as acetaldehyde is volatile and peracetic acid is unstable at high temperatures

II.7 Mass Transfer Without Chemical Reaction

The experimental procedure is essentially the same as II.3 except that only pure ethyl acetate with no acetaldehyde and catalyst was used. Before each run, the ethyl acetate was double - distilled and collected in a nitrogen atmosphere, so that the solution contains no oxygen initially. The volume of gas absorbed with respect to time was measured.

APPENDIX III DERIVATION OF WORKING EQUATIONS

AND SAMPLE CALCULATIONS

III.1 Mass Transfer Coefficient Without Chemical Reaction

Derivation of Equation

It was given in equation (19A) that $N_A = k_L(C_{A1} - C_{AL})$

Assuming the gas phase resistance is always negligible so that C_{A1} is practically equal to C_{Ag} , the hypothetical concentration of oxygen in equilibrium with its partial pressure in the gas phase, C_{Ag} can be estimated from the solubility of oxygen in pure ethyl acetate. The method of calculation is given in Appendix VII.

As pure oxygen was used the partial pressure of the gas in the vessel was given by:

$$P_{Ag} = P_g - P_O,$$

where P_g is the total pressure and P_O is the pressure of the organic vapor which does not vary at constant pressure and temperature. Thus, P_{Ag} can be considered as constant throughout each experiment.

Furthermore, if there is no dissolved oxygen in the liquid at the start of an experiment and assuming the gas obeys ideal gas law, then C_A at time t can be related to the volume of oxygen absorbed by:

$$C_{AL} = \frac{273}{T_b} \left(\frac{1}{22400 V_R} \right) V_L,$$

$$C_{A1} = \left(\frac{273}{T_b} \right) \left(\frac{1}{22400 V_R} \right) V_{A1},$$

where V_{A1} is the volume of oxygen to saturate the given amount of liquid.

Therefore

$$N_A = \frac{V_R}{A_r} \frac{dC_A}{dt} = \left(\frac{273}{T_b} \right) \left(\frac{1}{22400 A_r} \right) \frac{dV_L}{dt}, \quad (83A)$$

where A_r is the interfacial area.

Equation(19A) becomes

$$\frac{1}{A_r} \frac{dV_L}{dt} = \frac{k_L}{V_R} (V_{Ai} - V_L) \quad (83A')$$

Rearranging and integrating (83A')

$$\frac{k_L A_r}{V_R} \int_0^t dt = \int_0^V \frac{dV_L}{V_{Ai} - V_L}$$

$$\frac{k_L A_r t}{V_R} = 2.303 \log \left(\frac{V_{Ai}}{V_{Ai} - V_L} \right) \quad (84A)$$

$\log (V_{Ai} - V_L)$ was plotted against t . The method of least squares was used to find the slope of the resulting straight line and k_L was given by

$$k_L = (\text{slope}) \left(\frac{-2.303 V_R}{A_r} \right) \quad (85A)$$

Sample Calculation: Experiment No. 6.

$\log (V_{Ai} - V_L)$ versus t was plotted in figure 6A slope = $-.00862 \text{ (hr}^{-1}\text{)}$

$$k_L = \frac{-.00862 (-2.303 \times .2) \ell}{.0475 \text{ ft}^2 \times 28.3 \ell(\text{hr})} \text{ ft}^3 = .0762 \frac{\text{ft}}{\text{hr}}.$$

III.2 Mass Transfer Coefficient With Chemical Reaction and Enhancement Factor at Various Acetaldehyde Concentration, Catalyst Concentration and temperature.

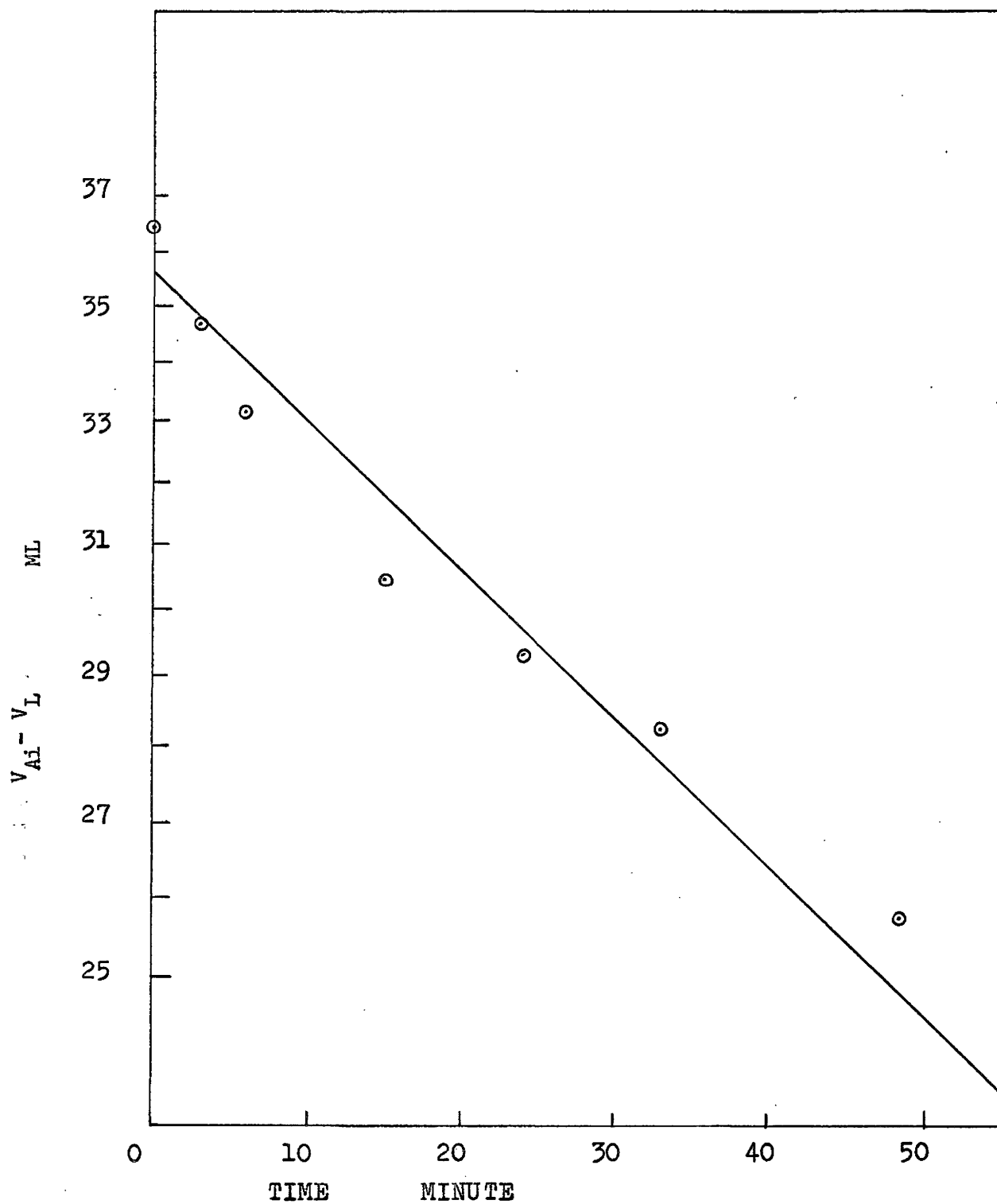


FIGURE 6A ABSORPTION OF OXYGEN IN ETHYL-ACETATE

Derivation of Equation

The rate of absorption of oxygen by acetaldehyde was given by equation (19A).

$$N_A = k_L^* (C_{Ai} - C_{AL}) \quad (19A)$$

It was assumed, when reaction occurred, all dissolved oxygen in the bulk of the liquid was reacted and its concentration became zero.

$$\text{Then } N_A = k_L^* C_{Ai} \quad (86A)$$

and

$$\bar{m} = \frac{k_L^*}{k_L} = \frac{N_A}{C_{Ai} k_L} \quad (87A)$$

N_A , the rate of absorption was determined by measuring the volume of oxygen absorbed with time. C_{Ai} was estimated in the same way as III.1.

Sample Calculation: Experiment No. 78.

Volume of oxygen absorbed versus time was plotted in Figure 7A

$$N_A = \left(\frac{\text{ml}}{\text{hr}}\right) \left(\frac{273}{277}\right) \left(\frac{\text{moles}}{22,400 \text{ ml}}\right) \frac{181}{.0473} \text{ ft}^3$$

$$= .168 \text{ moles/ft}^2 \text{ hr.}$$

$$C_{Ai} = .200 \text{ moles/ft}^3$$

$$k_L^* = \frac{.168}{.200} = .840 \text{ ft/hr.} \quad k_L = .0436 \text{ ft/hr}$$

$$\bar{m} = \frac{.840}{.0436} = 19.20$$

III.3 Mass Transfer Coefficient With Chemical Reaction at Various

Partial Pressure of Oxygen

Nomenclature

m Henry's Law Constant

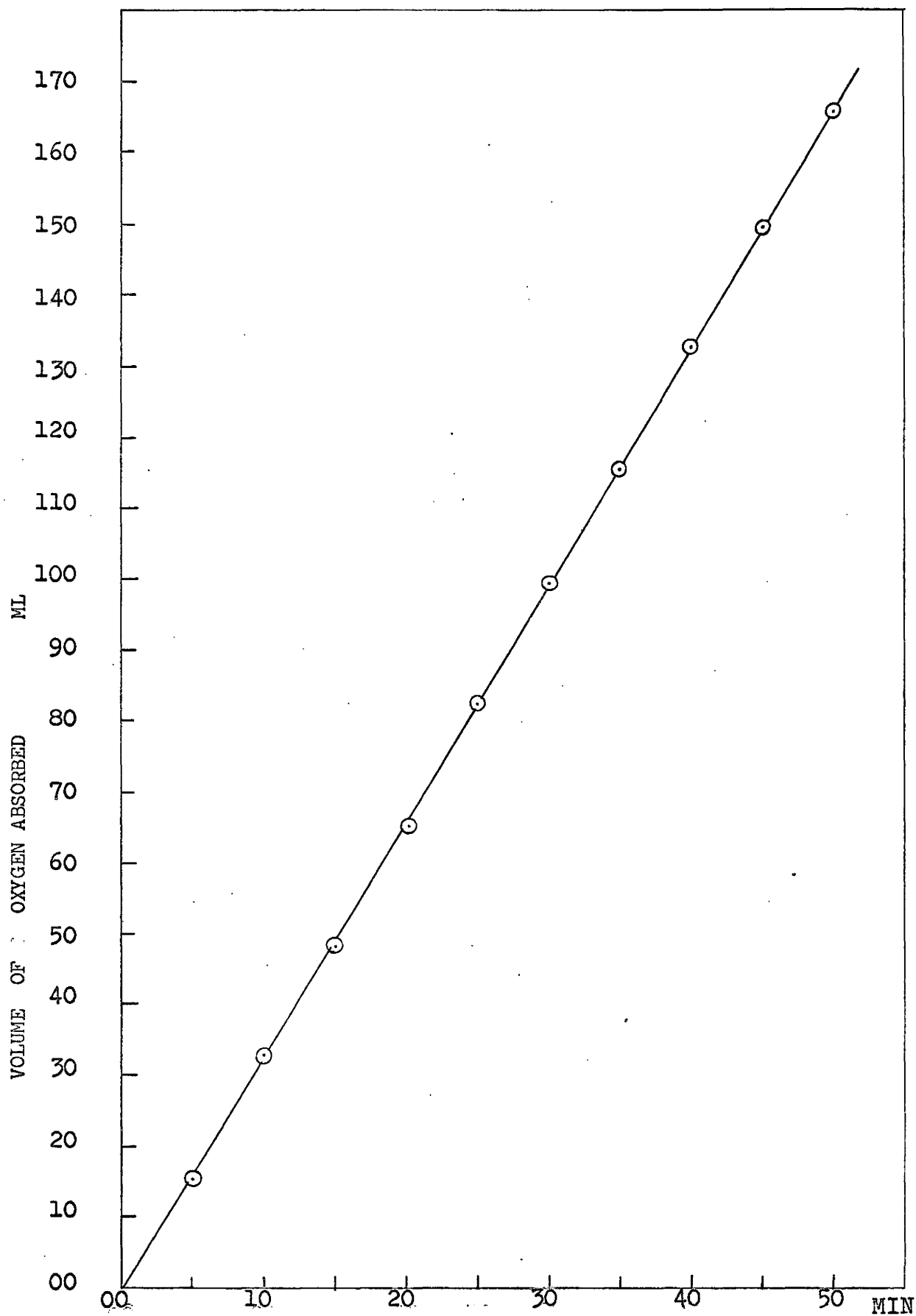


FIGURE 7A ABSORPTION OF OXYGEN IN ACETALDEHYDE SOLUTION

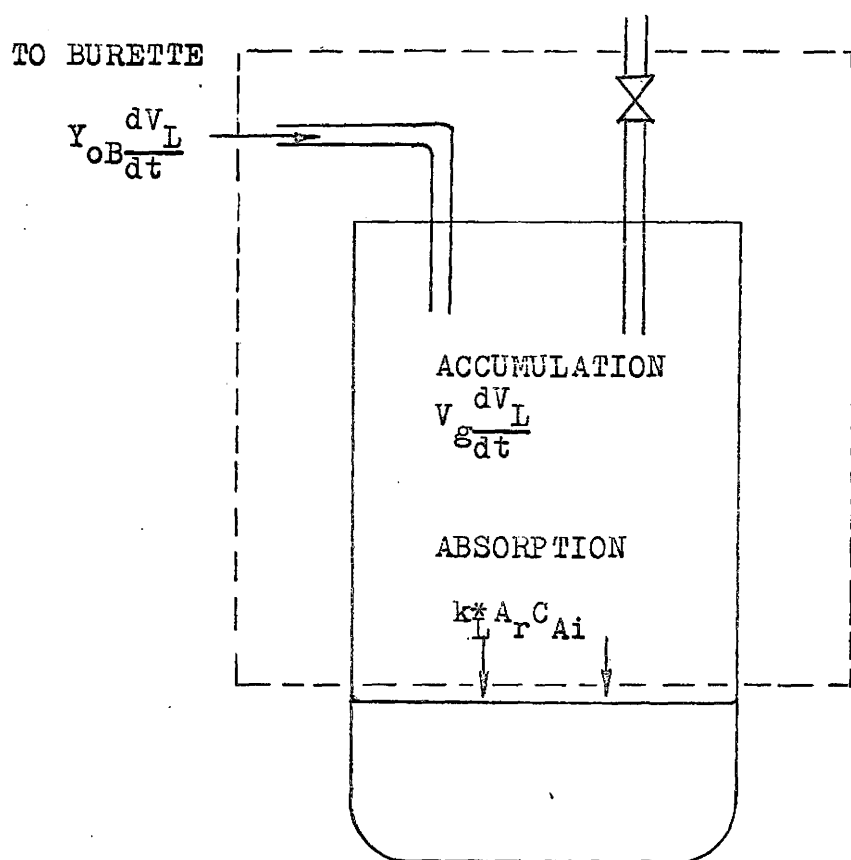


FIGURE 8A MATERIAL BALANCE AROUND GAS SPACE

R''	$T_b(22400)/273$ ml
R'	$T_v(22400)/273$ ml
T_b	temperature of burette $^{\circ}\text{K}$
T_v	temperature of vessel $^{\circ}\text{K}$
P_T	total pressure = 1 atmosphere
Y_{Ai}	mole fraction of oxygen in the gas space of the vessel at time t
Y_{OB}	mole fraction of O_2 in burette = constant
V_{Oi}	volume of O_2 in vessel at $t = 0$, ml
V_L	change of volume in burette at time t, ml
V_g	volume of gas space in the vessel, ml

Derivation of equation

A material balance of oxygen and the gas space as shown in Figure 8A consists of three terms:

$$\begin{aligned}
 \text{Rate of gas absorption} &= k_L^* A_r C_{Ai} \\
 &= \frac{k_L^* A_r Y_{Ai} P_T}{m} \\
 &= \frac{k_L^* A_r Y_{Ai} (1)}{m}
 \end{aligned} \tag{88A}$$

Rate of oxygen coming from gas burette

$$\begin{aligned}
 &= \left(\frac{273}{T_b}\right) \left(\frac{P_T}{1}\right) \left(\frac{1}{22400}\right) Y_{OB} \frac{dV_L}{dt} \\
 &= \frac{Y_{OB} dV_L}{R'' dt}
 \end{aligned} \tag{89A}$$

Rate of accumulation, due to the change of partial pressure of oxygen in the vessel

$$\begin{aligned}
&= \left(\frac{273}{T_V}\right) \left(\frac{P_T}{1}\right) \left(\frac{1}{22400}\right) V_g \frac{dY_{Ai}}{dt} \\
&= \frac{V_g}{R'} \frac{dY_{Ai}}{dt} \quad (90A)
\end{aligned}$$

Hence,

$$\frac{Y_{OB}}{R''} \frac{dV_L}{dt} = \frac{k_L^* A_r Y_{Ai}}{m} + \frac{V_g}{R'} \frac{dY_{Ai}}{dt} \quad (91A)$$

Volume of oxygen that has entered the vessel

$$= V_L Y_{OB}$$

Correcting for temperature variation, volume of oxygen in the vessel at time t

$$\begin{aligned}
&= V_g Y_{Ai} = V_{O1} + (V_L Y_{OB} - V_L) \frac{T_v}{T_b} \\
&= V_{O1} - \frac{T_v}{T_b} (1 - Y_{OB}) V_L \quad (92A)
\end{aligned}$$

$$\frac{dY_{Ai}}{dt} = - \left(\frac{T_v}{T_b}\right) \left(\frac{1}{V_g}\right) (1 - Y_{OB}) \frac{dV_L}{dt} \quad (93A)$$

Substituting (92A) and (93A) into equation (91A) one obtains.

$$\begin{aligned}
\frac{Y_{OB}}{R''} \frac{dV_L}{dt} &= \frac{k_L^* A_r}{V_g} \left(V_{O1} - \frac{T_v}{T_b} (1 - Y_{OB}) V_L \right) \\
&\quad - \left(\frac{1}{R'}\right) \left(\frac{T_v}{T_b}\right) (1 - Y_{OB}) \frac{dV_L}{dt} \quad (94A)
\end{aligned}$$

Rearranging equation (94A) and integrating,

$$\left(\frac{k_L^* A}{V_m} \right) \frac{1}{\frac{Y_{OB}}{R''} + \frac{1}{R'} \left(\frac{T_v}{T_b} \right) (1 - Y_{OB})} \int_0^t dt$$

$$= \int_0^{V_L} \frac{dV_L}{V_{O1} - \left(\frac{T_v}{T_b} \right) (1 - Y_{OB}) V_L}$$

Thus,

$$\left(\frac{k_L^* A}{V_m} \right) \frac{1}{\frac{Y_{OB}}{R''} + \frac{1}{R'} \left(\frac{T_v}{T_b} \right) (1 - Y_{OB})} t = - \frac{T_b}{T_v} \frac{(2.303)}{(1 - Y_{OB})}$$

$$\log \left(V_{O1} - \frac{T_v}{T_b} (1 - Y_{OB}) V_L \right) + \frac{T_b}{T_v} \frac{2.303}{(1 - Y_{OB})} \log (V_{O1}) \quad (95A)$$

Plotting $\log \left(V_{O1} - \frac{T_v}{T_b} (1 - Y_{OB}) V_L \right)$ Vs t a straight line is obtained and k_L^* is given by

$$k_L^* = - \left(\frac{2.303V}{A T_v} \right) \frac{273m}{22400} \left(\frac{Y_{OB}}{1 - Y_{OB}} + 1 \right) (\text{slope}) \quad (96A)$$

As T_v was kept constant equation (96A) could be reduced to

$$k_L^* = - (BB) \text{ slope} \quad (97A)$$

The values of (BB) for corresponding values of Y_{OB} were tabulated in Table 2A.

Mole fraction of O ₂ in burette Y _{OB}	V _{O1} ml	BB
1.0	423	14.63
.75	318	
.50	212	7.32
.21	89	4.63

TABLE 2A MULTIPLICATION CONSTANTS FOR CALCULATING k_L^*

AT VARIOUS PARTIAL PRESSURES

Sample Calculation: Experiment No. 48

$$m = 1.025 \times 10^2 \text{ (atm.)(litre)/moles}$$

$$T_v = 277^\circ\text{K}$$

$$V_g = 474 \text{ ml}$$

$$A_r = .0475 \text{ ft}^3$$

Log $(V_{O1} - \frac{T_v}{T_b} (1 - Y_{OB}) V_L)$ versus t was plotted in figure

9A.

$$Y_{OB} = .75 \quad T_b = 298^\circ\text{K}$$

$$\text{slope} = .0388$$

$$k_L^* = .0388 (14.63) = .545 \text{ ft/hr.}$$

III.4 Reaction Rate Constants from Unsteady - State Absorption Data

Experiment No. 109

Volume of oxygen absorbed versus time was plotted in Figure 10A.

$$N_A = 3.005 \text{ moles/ft}^2 \text{ hr.} \times 10^{-2}$$

$$C_{Ai} = .209 \text{ moles/ft}^3$$

$$D_A = 20.0 \times 10^{-5} \text{ ft}^2/\text{hr.}$$

First Order Reaction

Using equation (63A)

$$k_{c1} = \left(\frac{N_A}{C_{Ai}} \right)^2 / D_A = \left(\frac{3.005 \times 10^{-2}}{.206} \right)^2 / 20.0 \times 10^{-5}$$

$$= 103.7 \text{ (hr)}^{-1}$$

Zeroth Order Reaction

Using equation (82A)

$$k_{Co} = (N_A)^2 / 2D_A C_{Ai} = (3.005 \times 10^{-2})^2 / .206 \times 2 \times 20.0 \times 10^{-5}$$

$$= 10.85 \text{ moles/ft}^3 \text{ (hr)}$$

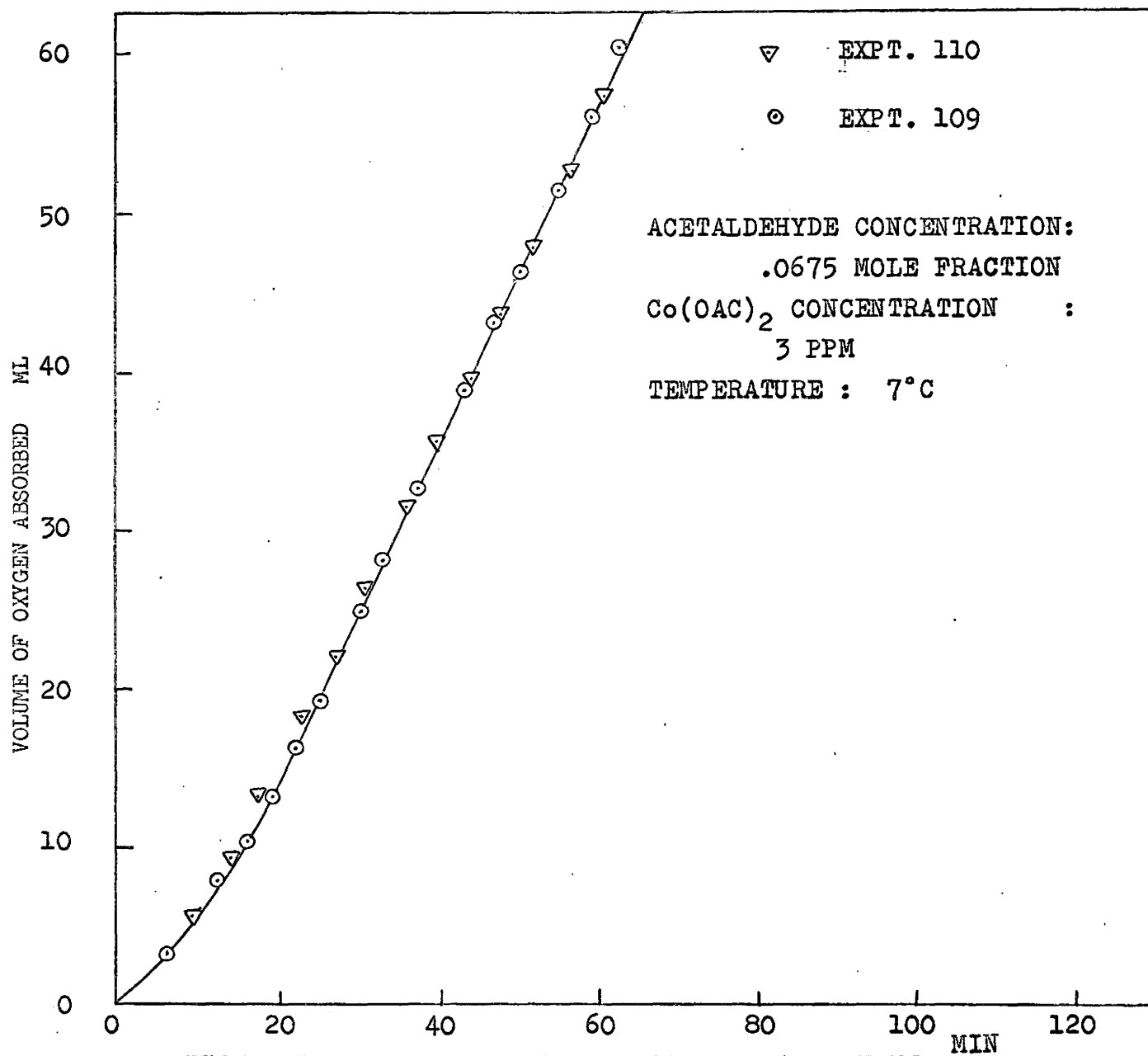
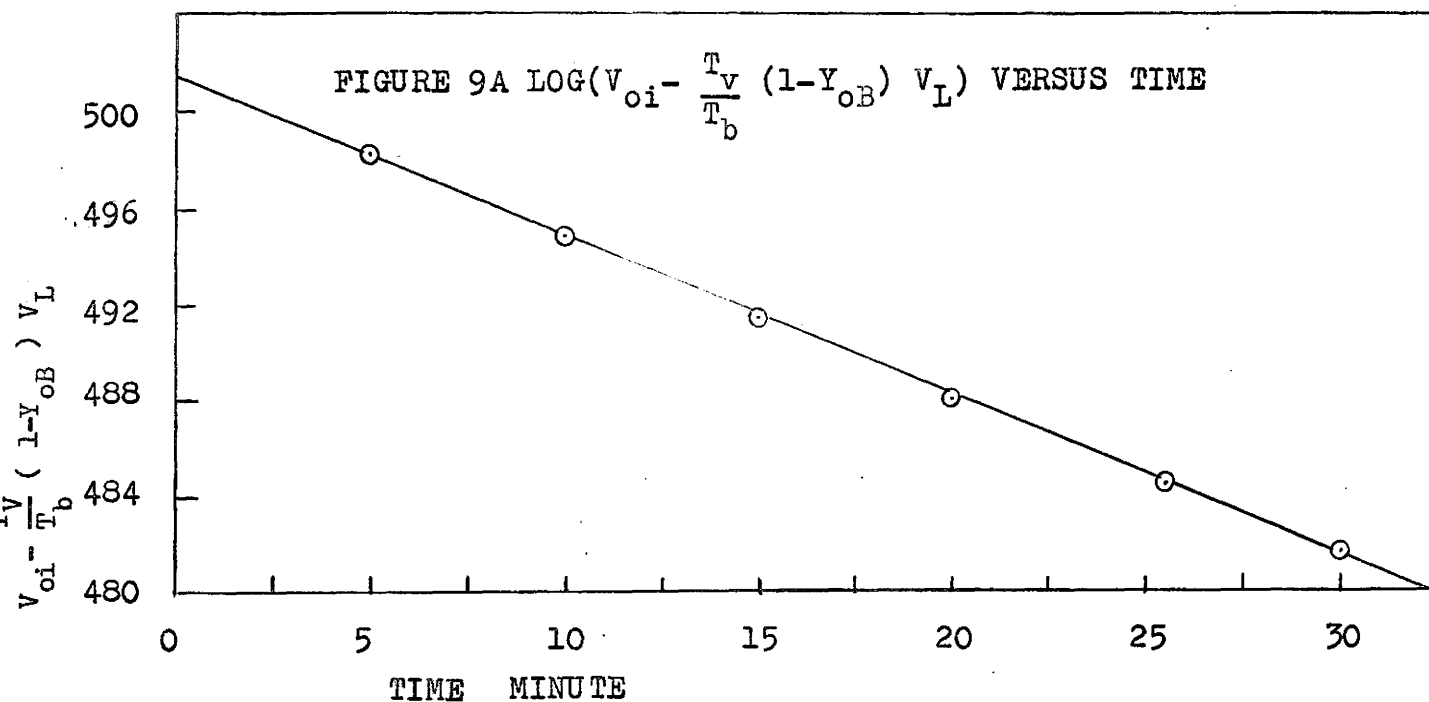


FIGURE 10A UNSTEADY STATE ABSORPTION OF OXYGEN

APPENDIX IV TABLES OF EXPERIMENTAL OBSERVATIONS

Expt. No.	Stirring Speed r.p.m.	Apparatus	V _{Ai}	V _L	Temperature °C	Slope hr ⁻¹ x 10 ²	k _L ft/hr x 10 ²
			ml				
6	509	Akehata	77.2	400	4	-.862	7.62
7	509	"	77.2	"	"	-1.112	9.60
9	"	"	77.2	"	"	-.806	7.13
13	"	"	39.4	200	"	-.985	8.80
14	"	"	39.4	"	"	-.963	8.50
102	"	"	41.0	"	0	-.460	4.10
98	395	"	41.0	"	"	-.466	4.16
103	"	"	39.2	"	4	-.462	4.12
104	"	"	39.2	"	"	-.517	4.60
95	"	"	36.3	"	10	-.533	4.55
99	"	"	36.3	"	"	-.553	4.83
123	120	Modified	39.2	"	5	-.803	3.90
35A	"	"	39.2	"	"	-.845	4.10

$$A_r(\text{Akehata}) = .0475 \text{ ft}^2$$

$$A_r(\text{Modified}) = .0873 \text{ ft}^2$$

TABLE 3A MASS TRANSFER COEFFICIENTS WITHOUT CHEMICAL REACTION

Expt. No.	Composition		Absorption rates N_A $\frac{\text{gm-moles}}{\text{ft}^2 \text{ hr.}}$	C_{Ai} $\frac{\text{gm-moles}}{\text{ft}^3}$	P_{O_2} Atm.	k_L^* ft/hr.	$\bar{\delta}$ $= k_L^*/k_L$
	AcH	Ethyl Acetate					
81	.0173	.976	.0249	.224	.953	.107	2.46
84	.0173	.976	.0234	.224	.953	.105	2.41
82	.0422	.950	.0980	.223	.940	.441	10.12
83	.0422	.963	.103	.222	.940	.465	10.67
80	.0675	.925	.165	.218	.930	.705	16.20
85	.123	.869	.162	.211	.903	.768	17.65
79	.162	.830	.168	.208	.883	.807	18.81
78	.236	.860	.168	.200	.852	.840	19.20

Temperature of Bath = 4°C.
 Co(OAC)_2 = 3.0 ppm.
 Speed of Stirrer = 395 rpm.
 k_L = .0436 ft./hr
 Apparatus = Akehata
 A_r = .0475 ft²

TABLE 4A MASS TRANSFER COEFFICIENT AND ENHANCEMENT FACTOR AT
VARIOUS ACETALDEHYDE CONCENTRATIONS

Expt. No.	Conc. of $\text{Co}(\text{OAc})_2$ p.p.m.	N_A moles $\text{ft}^2 \text{hr}$	k_L^* ft./hr.	$\Phi = k_L^*/k_L$
23	0	.0258	.123	1.48
37	4.3	.154	.737	8.86
29	5.0	.258	1.230	14.80
39	5.4	.299	1.425	17.15
41	6.4	.256	1.220	14.65
40	8.5	.273	1.300	15.65
38	10.7		.827	9.94
30	15.0	.181	.860	10.35
26	18.3	.219	1.043	12.55
24	27.7	.197	.340	11.55
25	55.4	.161	.767	9.22
27	55.4	.1443	.685	8.24
28	110.8	.1065	.507	6.10

Speed of stirrer = 509 r.p.m.

Acetaldehyde concentration = .10 mole fraction

Temperature of bath = $4.0 \pm .2^\circ\text{C}$

Apparatus - Akehata

k_L = .0832 ft./hr.

A_r = .0425 ft^2

TABLE 5A MASS TRANSFER COEFFICIENT AND ENHANCEMENT FACTOR AT
VARIOUS CATALYST CONCENTRATIONS

Expt. No.	Temperature °C.	Composition		Absorption rates N_A $\frac{\text{gm-moles}}{\text{ft}^2 \text{ hr.}}$	C_{A1} $\frac{\text{gm-moles}}{\text{ft}^3}$	P_{O_2} atm.	k_L^* ft/hr	k_L ft/hr $\times 10$	\bar{g}
		Mole fraction AcH	Mole fraction Ethyl Acetate						
88	0	.0675	.925	.100	.230	.942	.436	.413	10.55
91	"	.123	.869	.153	.225	.920	.682		16.50
89	"	.236	.756	.154	.219	.895	.703		17.00
90	"	.236	.756	.160	.219	.895	.728		17.60
86	10	.0422	.950	.130	.201	.910	.648	.457	14.20
92	"	.0675	.925	.151	.199	.903	.751		16.47
93	"	.123	.869	.157	.192	.872	.815		17.87
97	"	.162	.830	.154	.187	.848	.823		18.05
96	"	.214	.782	.161	.178	.811	.850		18.63

$\text{Co}(\text{OAc})_2$ = 3.0 ppm

Speed of Stirrer = 395 rpm

Apparatus = Akehata

A_r = .0475 ft^2

TABLE 6A MASS TRANSFER COEFFICIENT AND ENHANCEMENT FACTOR AT
VARIOUS TEMPERATURES AND ACETALDEHYDE CONCENTRATIONS

Expt. No.	Temp. °C.	$N_A \frac{\text{moles}}{\text{ft}^2 \text{ hr}} \times 10^2$	$D_A \text{-Mixt.} \frac{\text{ft}^2}{\text{hr}} \times 10^2$	D_{O_2} atm	$O_{A1} \frac{\text{mole}}{\text{ft}^3}$	$k_{cl} \text{ hr}^{-1}$	$\frac{1}{T} (\text{°K})^{-1} \times 10^3$
109	7.0	3.01	20.0	.917	.2085	103.7	3.57
110	7.0	2.96	20.0	.917	.2085	100.5	3.571
105	10.0	3.13	21.2	.902	.1990	117.0	3.533
106	10.0	3.28	21.2	.902	.1990	128.0	3.533
107	10.0	3.34	21.2	.902	.1990	133.0	3.533
108	10.0	3.22	21.2	.902	.1990	123.3	3.533
111	15.0	3.56	22.70	.881	.1872	159.4	3.472
112	15.0	3.49	22.70	.881	.1872	153.5	3.472

TABLE 7A FIRST ORDER REACTION RATE CONSTANTS
FROM UNSTEADY STATE ABSORPTION DATA

Expt. No.	Temperature °C	$k_{Co} \frac{\text{moles}}{\text{ft}^3} (\text{hr})^{-1}$	$\frac{1}{T} \times 10^3$	reducing to 1st order $k'' (\text{hr})^{-1}$
109	7.0	10.85	3.571	.538
110	7.0	10.50	3.571	.522
105	10.0	11.62	3.533	.577
106	10.0	12.75	3.533	.633
107	10.0	13.22	3.533	.657
108	10.0	12.26	3.533	.608
111	15.0	15.00	3.472	.745
112	15.0	14.45	3.472	.717

$Co(OA)_2 = 3 \text{ ppm}$

Acetaldehyde concentration:

(before experiment) = .0675 mole fraction

(after experiment) = .0655 mole fraction

TABLE 8A ZEROth ORDER REACTION RATE CONSTANTS FROM UNSTEADY - STATE
ABSORPTION DATA

Expt.	C_{BL} $\frac{\text{gm-moles}}{\text{ft.}^3}$	C_{CL} $\frac{\text{gm-moles}}{\text{ft.}^3}$	C_{Bi} $\frac{\text{gm-moles}}{\text{ft.}^3}$	C_{Ci} $\frac{\text{gm-moles}}{\text{ft.}^3}$	$\bar{C}_B = \int C_B dx / x_L$ $\frac{\text{gm-moles}}{\text{ft.}^3}$	$k'' \times 10^{-2}$ hr^{-1}
24	3.55	1.16	2.75	2.30	3.02	.0326
25	3.94	.793	2.90	1.80	3.29	.0281
26	4.01	.687	2.90	1.70	3.29	.0277
16	4.02	1.09	2.71	2.90	3.29	.0681
18	4.37	1.20	2.90	3.00	3.49	.0779
19	4.47	.92	3.00	3.10	3.60	.0839
33	5.45	1.74	3.95	4.60	4.63	.0891
34	5.50	1.70	3.85	4.30	4.52	.0891
13	6.48	1.87	4.30	7.00	5.34	.2710
15	6.76	1.73	4.45	7.00	5.65	.2490
14	6.91	1.96	4.65	7.00	5.86	.2280
22	7.67	3.35	5.45	8.90	6.53	.2400

TABLE 9A REACTION RATE CONSTANTS USING BAWN'S MECHANISM

Using Bawn's mechanism, but let

$$k'' = k_1^W + k_2^W C_B$$

where

$$k_1^W = -44.40(\text{hr})^{-1}, \quad k_2^W = 15.95 \frac{\text{ft.}^3}{\text{gm-moles hr}}$$

Equations (19), (20) and (21) become

$$D_A \frac{d^2 C_A}{dx^2} = k_1^W C_B + k_2^W C_B^2$$

$$D_B \frac{d^2 C_B}{dx^2} = \frac{k_1^W C_B^2}{C_c} + \frac{k_2^W C_B^3}{C_c}$$

$$D_C \frac{d^2 C_C}{dx^2} = -k_1^W C_B - k_2^W C_B^2$$

Results are tabulated in Table 10A

Expt. No	C_{Bi} <u>gm-moles</u> <u>ft³</u>	C_{Ci} <u>gm-moles</u> <u>ft³</u>	N_A (Expt) <u>gm-moles</u> <u>ft² hr</u>	N_A (predicted) <u>gm-moles</u> <u>ft² hr</u>
25	2.95	1.90	.0277	.0276
26	2.96	1.90	.0275	.0299
16	2.98	2.50	.0418	.0310
18	3.10	2.91	.0460	.0369
19	3.13	2.70	.0486	.0394
20	3.72	5.40	.0572	.0725
21	3.65	5.10	.0562	.0692
33	3.95	6.20	.0786	.0802
34	3.85	5.90	.0762	.0750
13	4.35	7.25	.1025	.0995
15	4.45	7.15	.0995	.1040
14	4.53	7.50	.0980	.1072

TABLE 10A PREDICTED ABSORPTION RATES USING FIRST
CORRELATION (Bawn's Reaction Mechanism)

Expt. No.	C_{BL} $\frac{\text{gm-moles}}{\text{ft}^3}$	C_{CL} $\frac{\text{gm-moles}}{\text{ft}^3}$	C_{ACOH} $\frac{\text{gm-moles}}{\text{ft}^3}$	C_{Ai} $\frac{\text{gm-moles}}{\text{ft}^3}$	$\frac{dC_A}{dx} \times 10^{-2}$ $\frac{\text{gm-moles}}{\text{ft}^4}$	$N_A \times 10$ $\frac{\text{moles}}{\text{ft}^2 \text{ hr}}$	$C_{BL} \text{ feed}$ $\frac{\text{gm-moles}}{\text{ft}^3}$	% lost or gained
26	4.01	.687	.343	.237	-1.416	.275	5.06	-.40
25	3.94	.793	.416	.237	-1.422	.277	5.06	+3.73
24	3.55	.877	.47	.237	-1.495	.291	5.06	+2.31
16	4.02	1.09	.19	.237	-2.150	.418	5.63	-5.78
18	4.37	1.20	.21	.237	-2.37	.461	5.63	+5.67
19	4.47	.92		.237	-2.50	.486	5.63	
34	5.45	1.74	.85	.273	-3.92	.763	7.60	-6.31
33	5.50	1.70	.45	.237	-4.04	.786	7.60	+ .71
14	6.91	1.96	.76	.236	-5.03	.980	9.39	+2.56
15	6.76	1.73	.55	.236	-5.12	.995	9.39	-3.73
13	6.48	1.87	1.00	.236	-5.26	1.025	9.39	- .43
12	6.05	2.36	1.06	.236	-5.93	1.155	9.39	+ .85

TABLE 11A PRODUCT DISTRIBUTION AND ABSORPTION RATES

Expt. no.	Experimental		Predicted	
	$\frac{dC_A}{dx}\bigg _{x=0}$ $\frac{\text{gm-moles}}{\text{ft}^4}$	N_A $\frac{\text{gm-moles}}{\text{ft}^2 \text{ hr}}$	$\frac{dC_A}{dx}\bigg _{x=0}$ $\frac{\text{gm-moles}}{\text{ft}^4}$	N_A $\frac{\text{gm-moles}}{\text{ft}^2 \text{ hr}}$
26	-141.6	.0276	-127.9	.0249
25	-142.2	.0277	-158.5	.0309
24	-149.5	.0291	-152.0	.0296
16	-215.0	.0418	-217.0	.0422
18	-237.0	.0462	-257.0	.0500
19	-250.0	.0486	-225.0	.0438
34	-392.0	.0762	-410.0	.0798
33	-404.0	.0786	-407.0	.0792
14	-503.0	.0980	-553.0	.1076
15	-512	.0995	-522.0	.1015

TABLE 12A PREDICTED ABSORPTION RATES USING SECOND CORRELATION

(Bolland's Reaction Mechanism)

APPENDIX V EXPERIMENTAL ERRORS AND STATISTICAL EVALUATION

V.1 Estimation of Experimental Errors (55)

$$u = f(x, y, z) \quad (98A)$$

$$du = \frac{\partial f}{\partial x} dx + \frac{\partial f}{\partial y} dy + \frac{\partial f}{\partial z} dz \quad (99A)$$

$$\Delta u \doteq \left(\frac{\partial f}{\partial x}\right) \Delta x + \left(\frac{\partial f}{\partial y}\right) \Delta y + \left(\frac{\partial f}{\partial z}\right) \Delta z \quad (100A)$$

Equation (100A) is the basic equation for estimating relative errors.

Throughout the first part of the experimental work the measurements of acetaldehyde, cobaltous acetate and ethyl acetate concentrations were by weight. The relative errors were very small. Other quantities involved in this section are k_L^* , k_L and \bar{E} .

(1) Errors in k_L^*

$$k_L^* = N_A / C_{Ai} = \alpha \frac{V_L}{t} / C_{Ai}$$

where α is a constant and C_{Ai} is estimated by Hildebrand's formula.

$$\ln k_L^* = \ln \alpha - \ln C_{Ai} + \ln V_L - \ln t$$

Using equation (100A),

$$\left| \frac{\Delta k_L^*}{k_L^*} \right| = \left| \frac{\Delta V_L}{V_L} \right| + \left| \frac{\Delta t}{t} \right| \quad (101A)$$

V_L was measured to the nearest .2 ml by gas burette. However, temperature change within the period of 2 hr is approximately $\pm .25^\circ\text{C}$ and the volume of the gas space of the reaction vessel is 600 ml. Thus, ΔV_L , due to temperature change, is equal to $600 \times \left(\frac{.25}{277} \right) = .55 \text{ ml}$.

Time was measured to nearest 5 sec.

For higher absorption rates, say, 150 ml per half hour

$$\frac{\Delta k_L^*}{k_L^*} = \frac{.55 + .2}{150} + \frac{5}{1800}$$

$$\frac{\Delta k_L^*}{k_L^*} = .008$$

when $k_L^* = 1 \frac{ft}{hr}$, $\Delta k_L^* = \pm .008 \text{ ft/hr}$.

For lower absorption rates, say, 15 ml every half hour.

$$\frac{\Delta k_L^*}{k_L^*} = \frac{.75}{15} + \frac{5}{1800} = .053$$

when $k_L^* = .1 \frac{ft}{hr}$, $\Delta k_L^* = \pm .0053 \text{ ft/hr}$

(2) Errors in k_L

$$k_L = \beta \log \left(\frac{V_{Ai}}{V_{Ai} - V_L} \right) / t$$

$$\log k_L = \log \beta + \log \left(\log \left(\frac{V_{Ai}}{V_{Ai} - V_L} \right) \right) - \log t.$$

$$\left| \frac{\Delta k_L}{k_L} \right| = \left| \frac{\Delta V_L}{\log \left(\frac{V_{Ai}}{V_{Ai} - V_L} \right) (V_{Ai} - V_L)} \right| + \left| \frac{\Delta t}{t} \right|$$

$$\Delta V_L = .2 + .55 = .75 \text{ ml}$$

Letting $V_{Ai} = 38 \text{ ml}$, $V_L = 10 \text{ ml}$ $t = 1/2 \text{ hour}$

$$\left| \frac{\Delta k_L}{k_L} \right| = \frac{.75}{(.51)(35)} + \frac{5}{1800}$$

$$=.076$$

when $k_L = 0.040 \frac{ft}{hr}$ $\Delta k_L = .076 (0.04) = \pm 0.003 \text{ ft/hr}$

(3) Error in \bar{Q}

$$\bar{Q} = \frac{k_L^*}{k_L}$$

$$\left| \frac{\Delta \bar{Q}}{\bar{Q}} \right| = \left| \frac{\Delta k_L^*}{k_L^*} \right| + \left| \frac{\Delta k_L}{k_L} \right|$$

$$\text{when } k_L^* = .10 \frac{\text{ft}}{\text{hr}}, \left| \frac{\Delta \bar{Q}}{\bar{Q}} \right| = .053 + .073 = .126$$

$$\text{when } k_L^* = 1.0 \frac{\text{ft}}{\text{hr}}, \left| \frac{\Delta \bar{Q}}{\bar{Q}} \right| = .073 + .008 = .081$$

$$\text{when } \bar{Q} = 2.50, \Delta \bar{Q} = \pm .31$$

$$\text{when } \bar{Q} = 25.0, \Delta \bar{Q} = \pm 3.1$$

V.2 Statistical Evaluation of the Correlations (56)V.2.1 Linear Correlation of Two Variables by the Least Squares Method

The straight line through the data points (x_i, y_i) is expressed by

$$\hat{y} = a + bx \quad (102A)$$

where \hat{y} is the estimated value for an observed value of x .

The values of a and b corresponding to the line with the minimum squared deviation of y from \hat{y} are given by

$$a = \bar{y} - b\bar{x} \quad (103A)$$

$$b = \frac{\sum' xy}{\sum' x^2} \quad (104A)$$

where

$$\sum' xy = \sum (x - \bar{x})(y - \bar{y})$$

$$\sum' x^2 = \sum (x - \bar{x})^2$$

and $\bar{x} = \frac{\sum x_1}{N}$, $\bar{y} = \frac{\sum y_1}{N}$

N is the number of data points.

The significance of the correlation is given by the correlation coefficient γ_c , which ranges from ± 1.0 for a perfect correlation to 0 for the case where there is no correlation. For a straight line correlation, γ_c is given by

$$\gamma_c = \frac{\sum' xy}{(\sum' x^2 \sum' y^2)^{1/2}} \quad (105A)$$

To determine whether the correlation is significant at certain probability level, γ_c estimated by equation (105A) is compared with the values of correlation coefficient in standard tables (56).

The variance of estimates may be used to set the confidence limits on the least squares line

$$\text{Variance of slope } S^2(b) = \frac{(1-\gamma_c^2) \sum' y^2}{(N-2) \sum' x^2} \quad (106A)$$

$$\text{Variance of } \bar{y} \text{ } S^2(\bar{y}) = \frac{(1-\gamma_c^2) \sum' y^2}{N} \quad (107A)$$

$$\text{Confidence limit of } \bar{y} = \bar{y} \pm ts(\bar{y})$$

$$\text{Confidence limit of } b = b \pm ts(b)$$

where t is selected at the proper degrees of freedom and the desired probability level from standard t-table.

Curves through the extremes of \bar{y} are drawn asymptotic to the lines with minimum and maximum slopes. The area between two curved lines is the confidence range of the correlation.

V.2.2 Statistical Evaluation of First Correlation (Bawn's Reaction Mechanism)

$$N = 12$$

$$\text{Degrees of freedom} = 10$$

$$\gamma_c = .962$$

$$b = 1.078$$

$$a = -.00390$$

$$\bar{y} = .0602$$

The tabulated value of γ_c for 10 degrees of freedom at the .001 level is .823.

$$S(b) = .0963$$

$$S(\bar{y}) = .00774$$

$$t_{10,.05} = 2.228$$

$$\begin{aligned} \text{confidence range of } b &= 1.078 \pm 2.228 (.0963) \\ &= .863 \text{ to } 1.293 \end{aligned}$$

$$\begin{aligned} \text{confidence range of } \bar{y} &= .0602 \pm 2.228 (.00774) \\ &= .0429 \text{ to } .0775 \end{aligned}$$

$$\text{Prescribed value of } b = 1.0$$

V.2.3 Statistical Evaluation of Second Correlation (Bolland's Reaction Mechanism)

$$N = 12$$

$$\text{Degrees of freedom} = 12 - 2 = 10$$

$$\gamma_c = .981$$

$$b = .948$$

$$a = -.00299$$

$$\bar{y} = .0655$$

The tabulated value of γ_c for 10 degrees of freedom at the .001 level is .823.

$$s(b) = .0592$$

$$s(\bar{y}) = .00189$$

$$t_{10,.05} = 2.228$$

$$\text{confidence range of } b = .948 \pm 2.228 (.0592)$$

$$= .816 \text{ to } 1.080$$

$$\text{confidence range of } \bar{y} = .0655 \pm 2.228 (.00189)$$

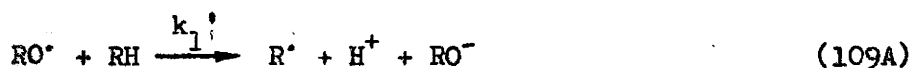
$$= .0613 \text{ to } .0697$$

prescribed value for $b = 1.0$

APPENDIX VI DERIVATION OF REACTION RATE EQUATIONS

VI.1 Bolland's Rate Equation for the Oxidation of Hydrocarbons

Initiation:



Propagation:



Termination:



Using the standard steady state approximation for free radical reactions, the following rate equations for all free radicals can be equated to zero.

$$\frac{dC_{\text{RO}}}{dt} = k_1 C_{\text{ROOH}} - k_1' C_{\text{RO}} C_{\text{RH}} = 0 \quad (116\text{A})$$

$$\frac{dC_{\text{OH}}}{dt} = k_1 C_{\text{ROOH}} - k_2' C_{\text{OH}} C_{\text{RH}} = 0 \quad (117\text{A})$$

$$\begin{aligned} \frac{dC_R}{dt} = & k_1' C_{RO} C_{RH} + k_2' C_{OH} C_{RH} - k_2 C_R C_{O_2} + k_3 C_{RO_2} C_{RH} - k_4 C_R^2 \\ & - k_5 C_R C_{RO_2} = 0 \end{aligned} \quad (118A)$$

$$\frac{dC_{RO_2}}{dt} = k_2 C_R C_{O_2} - k_3 C_{RO_2} C_{RH} - k_5 C_R C_{RO_2} - k_6 C_{RO_2}^2 = 0 \quad (119A)$$

From equations (116A) and (117A),

$$C_{RO} = \frac{k_1 C_{ROOH}}{k_1' C_{RH}} \quad (120A)$$

$$C_{OH} = \frac{k_2 C_{ROOH}}{k_2' C_{RH}} \quad (121A)$$

Substituting equations (120A) and (121A) into (118A), one obtains

$$2k_1 C_{ROOH} - k_2 C_R C_{O_2} + k_3 C_R C_{O_2} + k_3 C_{RO_2} C_{RH} - k_4 C_R^2 - k_5 C_R C_{RO_2} = 0 \quad (122A)$$

Assuming $k_5 = k_4^{1/2} k_6^{1/2}$ and adding (119A) and (122A), one obtains

$$2k_1 C_{ROOH} = k_4 C_R^2 + 2k_4^{1/2} k_6^{1/2} C_R C_{RO_2} + k_6 C_{RO_2}^2 \quad (123A)$$

The left hand side of (123A) is the rate of initiation. In order that the final equation is independent of the method of initiation, let $\gamma = 2k_1 C_{ROOH}$.

The right hand side is a perfect square and thus,

$$k_4^{1/2} C_R = \gamma^{1/2} - k_6^{1/2} C_{RO_2} \quad (124A)$$

Substituting (124A) into (122A) and rearranging, one obtains

$$C_{RO_2} = \frac{k_2 \gamma^{1/2} C_{O_2}}{k_2 k_6^{1/2} C_{O_2} + \gamma^{1/2} k_6^{1/2} k_4^{1/2} + k_3 k_4^{1/2} C_{RH}} \quad (125A)$$

The rate of oxygen uptake is given by:

$$-\frac{dC_{O_2}}{dt} = k_2 C_R C_{O_2} - k_6 C_{RO_2}^2 \quad (126A)$$

From equation (119A)

$$-\frac{dC_{O_2}}{dt} = k_3 C_{RO_2} C_{RH} + k_5 C_R C_{RO_2} \quad (127A)$$

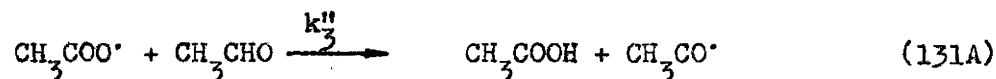
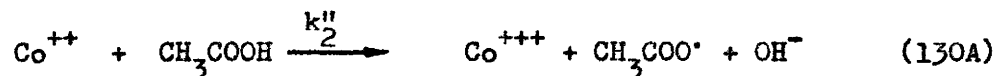
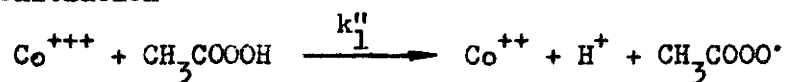
By substituting (119A) for C_{RO_2} and neglecting the second term in (127A)

Bolland's result is obtained as follows:

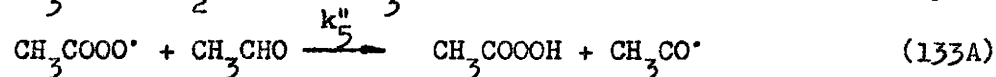
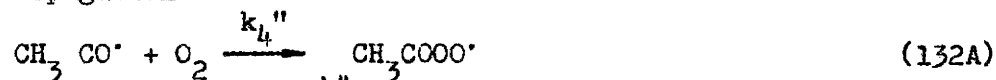
$$-\frac{dC_{O_2}}{dt} = \gamma^{1/2} \frac{k_3}{k_6} C_{RH} \frac{k_2 k_6^{1/2} C_{O_2}}{k_3 k_4^{1/2} C_{RH} + k_2 k_6^{1/2} C_{O_2} + k_4^{1/2} k_6^{1/2} \gamma^{1/2}} \quad (128A)$$

VI.2 Bawn's Rate Equation for the Oxidation of Acetaldehyde.

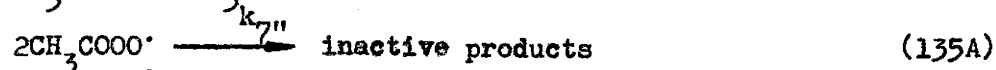
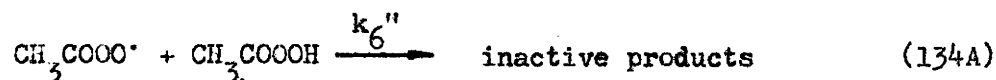
(1) Initiation



(2) Propagation



(3) Termination



(4) Equilibrium



Assuming only reactions (129A), (132A), (133A) and (134A) control the overall reaction and that the rate of initiation is negligible compared with that of propagation, the following expressions are derived:

$$\begin{aligned} \frac{dC_{f1}}{dt} = & k_1'' C_a C_c + k_4'' C_{f2} C_a \\ & - k_5'' C_{f1} C_B - k_6'' C_{f1} C_C \end{aligned} \quad (137\text{A})$$

$$\frac{dC_{f2}}{dt} = k_4'' C_{f2} C_a + k_5'' C_{f1} C_B \quad (138\text{A})$$

$$\frac{dC_A}{dt} = -k_4'' C_{f2} C_a \quad (139\text{A})$$

where C_{f1} is the concentration of $\text{CH}_3\text{COOO}^\cdot$ free radical; and C_{f2} the concentration of $\text{CH}_3\text{CO}^\cdot$ free radical.

In steady state, it is assumed that the concentrations of these free radicals are unchanged and thus,

$$\frac{dC_{f1}}{dt} = \frac{dC_{f2}}{dt} = 0 \quad (140\text{A})$$

From equation (138A), one obtains

$$C_{f2} = k_5'' C_{f1} C_B / k_4'' C_a \quad (141\text{A})$$

Substituting (141A) into (137A), the following expression results:

$$C_{f1} = \frac{k_1''}{k_6''} C_a \quad (142\text{A})$$

The rate of oxygen uptake as expressed by equation (139A) can now be written in terms of molecular concentrations as:

$$\frac{-dC_A}{dt} = \frac{k_5'' k_1''}{k_6''} C_{Ca} C_B \quad (143A)$$

The rate of change of C_C and C_{AMP} can be expressed as:

$$\begin{aligned} \frac{dC_C}{dt} = & -k_1'' C_{Ca} C_C - k_6'' C_{fl} C_C + k_5'' C_B C_{fl} - k_8'' C_B C_C \\ & + k_9'' C_{AMP} \end{aligned}$$

$$\frac{dC_{AMP}}{dt} = k_8'' C_B C_C - k_9'' C_{AMP} \quad (145A)$$

If instantaneous equilibrium is reached so that $\frac{dC_{AMP}}{dt} = 0$, then

$$\frac{C_{AMP}}{C_B C_C} = K \quad (146A)$$

where K is the equilibrium constant.

Substituting equation (142A) into (144A) and assuming k_1'' and k_6'' are small compared with k_5'' , one obtains

$$\frac{dC_C}{dt} = \frac{k_3'' k_1''}{k_4''} C_B C_{Ca} \quad (147A)$$

Differentiating equation (146A) and rearranging, the following equation is obtained:

$$\begin{aligned} \frac{dC_{AMP}}{dt} &= K \left(C_B \frac{dC_C}{dt} + C_C \frac{dC_B}{dt} \right) \\ &= 0 \end{aligned}$$

Hence

$$\frac{dC_B}{dt} = -\frac{C_B}{C_C} \frac{dC_C}{dt} = -\frac{k_3'' k_1''}{k_4''} \frac{C_B^2}{C_C} C_{Ca} \quad (148A)$$

The final rate equations are:

$$\frac{dC_A}{dt} = k' C_{Ca} C_B \quad (149A)$$

$$\frac{dC_B}{dt} = k' \frac{C_{Ca} C_B^2}{C_C} \quad (150A)$$

$$\frac{dC_C}{dt} = - k' C_{Ca} C_B \quad (151A)$$

$$\text{where } k' = \frac{k_3'' k_1''}{k_4''} \quad (152A)$$

APPENDIX VII SOLUBILITY OF OXYGEN IN ETHYL-ACETATE

As the International Critical Tables (57) give the solubility of oxygen in ethyl acetate at only one temperature and pressure, attempts to measure these values experimentally had been tried, but none of them proved to be very successful.

Winkler's method consisted of saturating the solution with oxygen and determining the amount of dissolved gas by titration. Oxygen being very slightly soluble in ethyl acetate only a very small amount of impurity in the form of an oxidant would cause considerable inaccuracies. Furthermore, the presaturation of the liquid with oxygen presented another problem.

In the absorption method the difficulty lay in the fact that the present gas burette was simply not precise enough to measure small volumes.

The experimental values obtained were only very approximate, and moreover, they did not show any definite variations with temperature and pressure.

A semi-empirical equation (53) for calculating solubilities of gases in non-electrolytes developed by Hildebrand and Scott is given by

$$-\log x_2 = \log P_2^0 - \log P_2 + V_2(\delta_1 - \delta_2)^2/2.303 RT. \quad (153A)$$

where x_2 is the solubility in mole fraction, P_2^0 , P_2 are vapor

pressure and partial pressure: and V_2 is the molal volume at the normal boiling point of the solute.

δ_1 and δ_2 are the solubility parameters of the solvent and the gas.

The basis of the equation is the energy of mixing and the Clausius - Clapeyron equation:

$$\frac{d \ln P^\circ}{d\left(\frac{1}{T}\right)} = \frac{\Delta H}{R} \quad (154A)$$

where ΔH is the enthalpy of vaporization.

Equation (141A) is the same equation derived from Raoult's Law except for the last term which can be considered as a correction for different solvents.

It was shown by Hildebrand that by extrapolating the plot of $\log P^\circ$ versus $\frac{1}{T}$ linearly, a hypothetical value of P° above the critical temperature could be used.

$$\delta, \text{ called the solubility parameter, is defined as } \delta = \frac{Z(\Delta H_{\text{app}} - RT)^{1/2}}{V_\ell} \quad (155A)$$

where ΔH_{app} is the apparent enthalpy of vaporization evaluated, according to Clausius - Clapeyron equation, by the slope of the $\log P^\circ$ versus $\frac{1}{T}$ plot, and V_ℓ is the molal volume of the liquid at its boiling point.

Using equation (141A) the solubility of oxygen evaluated for 25°C and atmospheric pressure agrees very well with that given in the International Critical Tables (57) and the experimental value. Table 13A shows a comparison of solubility of oxygen in ethyl - acetate by various methods.

Pressure	Temperature	Solubility		
atm.	°C	gm-moles/litre $\times 10^3$		
		Hildebrand	experimental	Int. Crit. Table
1	20	7.04		6.95
1	0	8.60		
1	4	8.20	8.4 (average of 8 samples)	

TABLE 13A COMPARISON OF SOLUBILITY OF OXYGEN IN
ETHYL-ACETATE BY VARIOUS METHODS

Expt. No.	Temperature ° ± .25	Solubility <u>moles</u> $\times 10^2$ litre	Vol. of Samples Used For Titration (ml)
1	0	.72	5
2	0	.69	5
3	0	.59	10
4	0	.85	10
5	4	.80	5
6	4	1.30	5
7	4	.55	10
8	4	1.13	10

TABLE 14A SOLUBILITY OF OXYGEN IN ETHYL - ACETATE
BY WINKLER'S METHOD

SAMPLE CALCULATION OF SOLUBILITY BY

HILDEBRAND'S FORMULA

Temp. °K	Vapor pressure of O ₂ (atm.) P ₂ ^o	$\frac{1}{T}$ (°K) ⁻¹ x 10 ²
89.9	1	1.111
97.0	2	1.030
108.5	5	.923
119.8	10	.834
133.0	20	.752
142.3	30	.703
148.99	40	.672

TABLE 15A VAPOR PRESSURE OF OXYGEN

SLOPE OF LOG P₂^o VERSUS $\frac{1}{T}$ BY LEAST SQUARE METHOD = 361°K

$$\Delta H_{app} / 2.303 = 361$$

$$\Delta H_{app} = 1655 \text{ cal/mole}$$

	T _R	P _R	Z	V cc	$\Delta H_{app} \frac{\text{cal}}{\text{moles}}$	δ
Oxygen	1.9	.0205	1.0	30.8 (Hildebrand)	1655	5.91
ethyl-acetate	1.17	.0265	1.0	97.7 (Perry)	10201 (Perry)	9.92

$$\text{Temperature} = 293^{\circ}\text{K}$$

TABLE 16A SOLUBILITY PARAMETERS BY EQUATION (155A)

From equation (154A),

$$p_{20}^o = \frac{1655}{4.575} (1.111 - .341) \times 10^{-2}$$

$$= 2.787$$

From equation (153A),

$$- \log x_2 = 2.787 + 3.08 (9.92 - 5.91)/4.58(293)$$

$$= 3.144$$

$$x_2 = 7.01 \times 10^{-4} \text{ mole fraction}$$

$$\doteq 7.08 \times 10^{-3} \frac{\text{gm-moles}}{\text{litre}}$$

APPENDIX VIII ESTIMATION OF DISPLACEMENT TIME

Before each experiment the reaction vessel was flushed with the gas in use. The flushing time necessary to displace 99.5% of the air in the vessel was estimated in the following way.

Assuming the gas in the vessel was completely mixed, and making a material balance of oxygen around the vessel then

$$V_g \frac{dy_{A1}}{dt} = F(Y_{OB} - Y_{A1})$$

where V_g is the volume of gas space in vessel, Y_{A1} and Y_{OB} are the mole fractions of oxygen in the vessel and the gas burette; F is the gas flow rate.

$$\frac{F}{V_g} \int_0^t dt = \int \frac{dy_{A1}}{(Y_{OB} - Y_{A1})}$$

$$\frac{Ft}{V_g} = -\ln(Y_{OB} - Y_{A1}) + \text{constant} \quad (156A)$$

$$\text{At } t = 0 \quad Y_{A1} = Y_{\text{air}}$$

Therefore,

$$\text{constant} = \ln(Y_{OB} - Y_{\text{air}})$$

Equation (156A) becomes

$$\frac{Ft}{V_g} = 2.303 \log \left(\frac{Y_{OB} - Y_{\text{air}}}{Y_{OB} - Y_{A1}} \right) \quad (157A)$$

The following table summarizes the displacement time for pure oxygen as well as mixtures of nitrogen and oxygen.

gas %		Approximate Displacement time minutes
N ₂	O ₂	
0	100	4
25	75	4
50	50	4
80	20	0

TABLE 17A DISPLACEMENT TIME

$F = 10.0$ litre/min

$V_g = .9$ litre

$Y_{air} = .2$

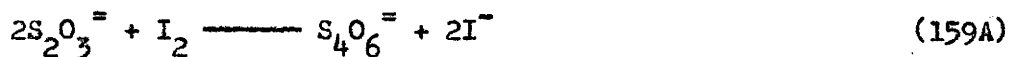
APPENDIX IX ANALYTICAL METHODS

As it was pointed out before, the oxidation of acetaldehyde by molecular oxygen gives rise to a number of products. The ones that are in significant quantities and thus of most interest to this study are peracetic acid, AMP, acetic acid and acetaldehyde. Analytical methods used by Shawinigan Chemicals (23) were adopted to determine the concentrations of these compounds, while Bawn's (25) method was used for total peroxide (peracetic acid and AMP) estimation.

IX.1 Peracetic Acid

Theory

The method of D'ans and Grey (30) is used for peracetic acid determination. The method is based on the oxidation of potassium iodide to iodine in aqueous acidic medium. Iodine liberated is titrated with sodium thiosulfate.



Procedure

(1) Add 1 ml of sample with stirring into 250 - ml erlenmeyer flask containing 50 ml of ice-cold H_2O and 10 ml of 15% KI solution which is freshly prepared.

(2) Quickly add 10 ml of cold N H_2SO_4 .

(3) Rapidly titrate the liberated I_2 with .02N thiosulfate to near the end point.

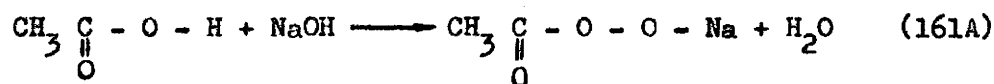
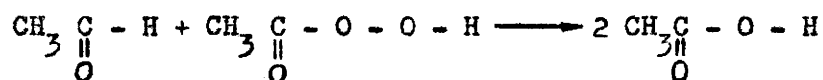
(4) Add starch and complete the titration.

IX.2 Acetic acid

Theory

The sample is allowed to react with excess acetaldehyde. Peracetic acid will then be converted to acetic acid. The concentration of the total acid is now determined by acid - base titration and peracetic acid is found by difference.

The reactions are:



Procedure

(1) 10 ml of 13% aqueous acetaldehyde solution is placed in 250 - ml flask.

(2) Add phenolphthalein, just neutralize with NaOH solution to the end point.

(3) Add 1 ml sample and allow it to react with stirring for five minutes.

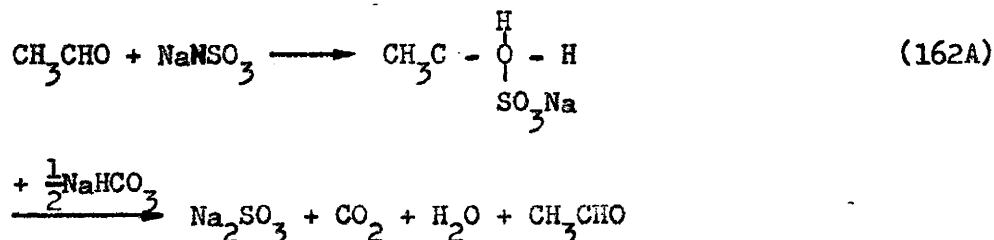
(4) Titrate with .1N NaOH solution.

IX.3 Acetaldehyde

Theory

Tomoda's method (23) is used to determine the acetaldehyde

contents. The compound is allowed to go through a series of reactions as represented by the following equations:



Finally the Na_2SO_3 formed is titrated with iodine solution and the equivalent amount of acetaldehyde can then be estimated.

The acetaldehyde analysis should be done after peracetic acid has been destroyed on account of the reaction between the peracetic acid and bisulfite.

Furthermore, as AMP is an addition compound of acetaldehyde and peracetic acid, acetaldehyde will be generated during the titration. The result of this analysis, therefore gives the sum of C_{ACH} and C_{AMP} and thus,

$$C_{\text{ACH}} = (C_{\text{ACH by titration}} - C_{\text{AMP}}) \quad (163A)$$

IX.4 Acetaldehyde Monoperacetate

Theory

It was found by Bawn that AMP does not liberate iodine from iodide solution in mineral acids nor in acetic acid containing some water. However, it does liberate iodine from KI powder in glacial acetic acid.

Procedure

The procedure is the same as IX.1 except 10 ml of glacial acetic

acid and 2 gm of KI powder are used instead of aqueous KI solution in H_2SO_4 . The flask has to be absolutely dry.

IX.5 Precision of Analytical Methods

In the second part of the experimental work the determination of the concentrations of acetaldehyde, peracetic acid, acetic acid and AMP by titration was involved. Standard solutions of these organic compounds except AMP were made up to test the analytical methods.

The precision of the measurements are shown in the following table.

Compound	No. of Sample	Max. Deviation From Mean
acetaldehyde	10	$\pm 2\%$
acetic acid	10	$\pm 10\%$
peracetic acid	10	$\pm 2\%$

TABLE 18A PRECISION OF ANALYTICAL METHODS

APPENDIX X ESTIMATION OF REACTION RATE CONSTANT
FROM BAWN'S EXPERIMENTAL DATA

The following data was taken from Trans. Fara. Soc. 1951.

737 Fig. 3. (25)

Temperature = 25°C

$$C_{Ca} = 3.8 \times 10^{-5} M \div \frac{3.8 \times 10^{-5} M}{1000 \text{ gm}} \times \frac{249 \text{ gm}}{M} \times 10^6 \div 9.0 \text{ ppm}$$

$$\text{Slope of } \frac{dC_A}{dt} \text{ versus } C_B \text{ plot} = k \quad C_{Ca} = k "$$

$$\therefore k " = 1.535 \text{ (hr}^{-1}\text{)}$$

Experiment no. 111

$$C_{Ca} = 3.0 \text{ ppm}$$

$$C_B = 20.2 \text{ moles/ft}^3$$

$$k_{Co} = 15.0 \text{ moles/ft}^3 \text{ hr} = k " C_B$$

$$k " = 15.0/20.2 = .745 \text{ hr}^{-1}$$

Extrapolating the curve of $\log k "$ versus $\frac{1}{T}$ to 25°C, $k " = .962 \text{ hr}^{-1}$

APPENDIX XI ESTIMATION OF DIFFUSIVITIES OF LIQUIDS

Wilke's relation (58),

$$D_{AB} = \frac{7.4 \times 10^{-8} (\rho_B M_B)^{1/2} T}{\eta_B V_A^{0.6}} \quad (164A)$$

and the equation (59),

$$\frac{1}{D_{A-Mixture}} = \frac{Y_B}{D_{AB}} + \frac{Y_C}{D_{AC}} + \frac{Y_D}{D_{AD}} \dots \quad (165A)$$

were used to estimate diffusivities in multicomponent mixtures, where

ρ is the association parameter;

V , the molal volume at the normal boiling point of liquid;

η , the viscosity

M , the molecular weight.

Table 19A tabulated the estimated value of diffusivities of dissolved oxygen in a mixture of ethyl acetate and acetaldehyde at various temperatures.

T °C	Viscosity (60) N _B N _D		D _{AB} $\frac{ft^2}{hr} \times 10^5$	D _{AD} $\frac{ft^2}{hr} \times 10^5$	D _{A-Mixture} $\frac{ft^2}{hr} \times 10^5$
7	.252	.550	30.3	19.55	20.00
10	.246	.525	31.3	20.70	21.20
15	.236	.500	33.3	22.10	22.70

A = Oxygen; B = Acetaldehyde; D = ethyl-acetate

$V_A = 25.6$ cc/gm-moles (p.27, Ref. 60)

$\rho_B = 1.0$ $M_B = 44$ (Ref. 58) $\rho_D = 1.0$ $M_D = 88$ (Ref. 58)

TABLE 19A DIFFUSIVITIES OF LIQUIDS

APPENDIX XII PRELIMINARY STUDIES ON PRODUCTION OF PERACETIC
ACID BY VERTICAL COCURRENT REACTOR

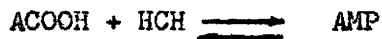
XII.1 Summary

While fundamental studies were carried out using the batch reaction - vessel, a laboratory scale cocurrent reactor was set up to simulate the commercial process for the production of peracetic acid by the autoxidation of acetaldehyde.

With a liquid flow rate of 4.5 ml/min. and a gas flow rate of .075 cu. ft/min. the yield of peracetic acid reached a steady state in approximately two hours.

With increasing catalyst concentration the yield of peracetic acid increased, then reached a maximum of 35%. Further increase of catalyst concentration only caused the decomposition of peracetic acid to acetic acid.

The concentrations of peracetic acid, acetaldehyde and the complex AMP, showed a consistent relation of $C_B C_C / C_{AMP} = K$ indicating the equilibrium of



may exist as it was reported in literature (25, 26, 27).

The average value of the equilibrium constant estimated from experimental data at 13°C is 3.45 litre/moles while that obtained by Bawn at 25°C is 3.7 litre/moles

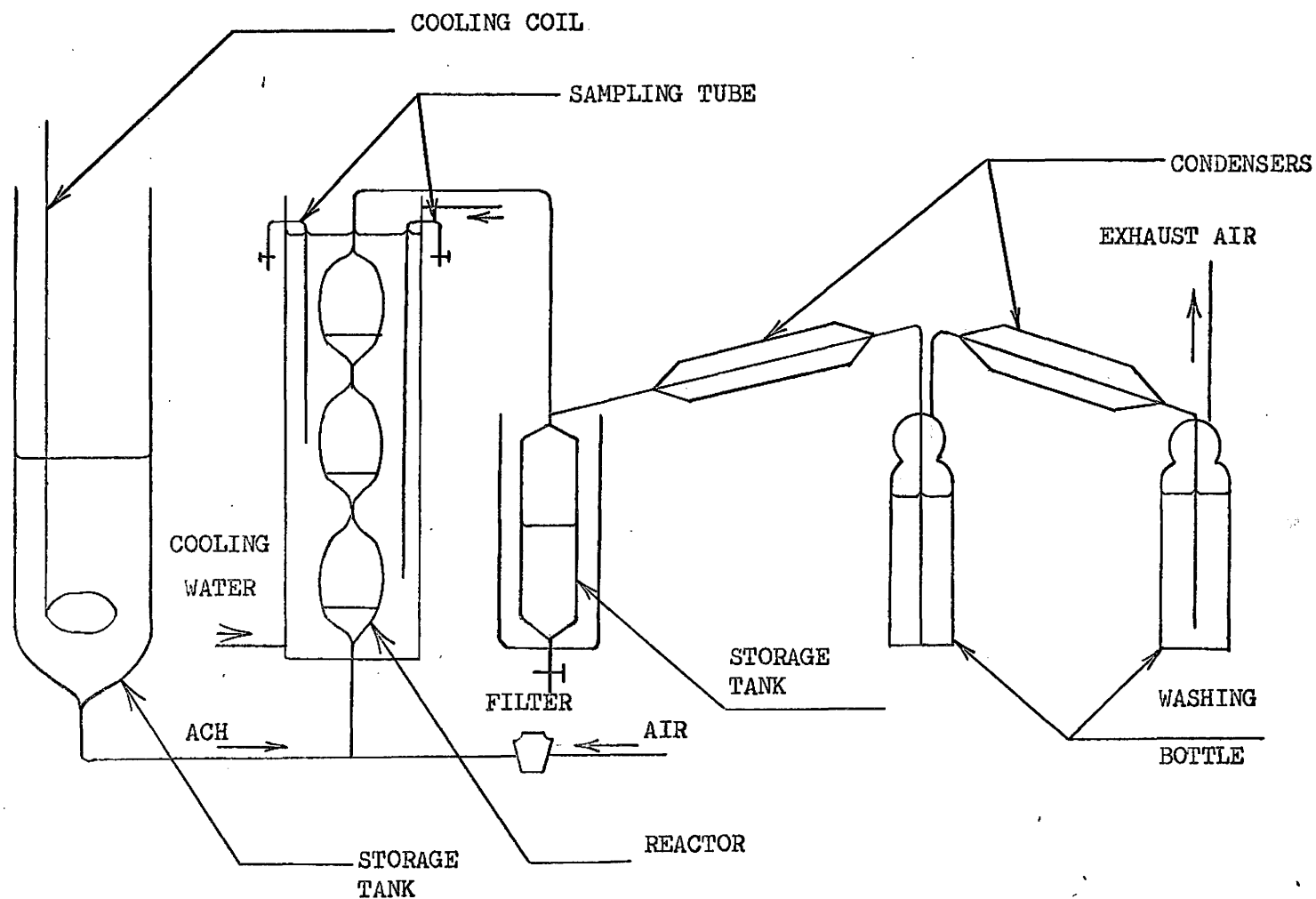


FIGURE 11A SCHEMATIC DIAGRAM OF VERTICAL COCURRENT REACTOR

XII.2 Apparatus and Experimental Details

Apparatus

The apparatus is shown in Figure (11A)

The reactor consists of three stages separating one from the other by sintered glass which serves two purposes:

- (1) to prevent back mixing of the liquid
- (2) to allow the gas entering the reactor as tiny bubbles, thus providing a large contacting surface for absorption and ensuring complete mixing of the liquid.

The reactor is provided with two sampling capillary tubes from the lower two stages and is jacketed by flowing tap - water.

Experimental Procedure

Acetaldehyde solution stored in a nitrogen atmosphere, kept cold by immersing into it a cooling coil, was pumped into the reactor by an accurately calibrated piston - type solution pump. Filtered air, after passing through a rotameter, entered the bottom of the reactor cocurrently with the liquid.

The product was collected in a storage flask while the gas was allowed to pass through two condensers where most of the organic vapors were trapped. The coolant used was ethylene - glycol - water mixture at -5°C

Several experiments were run with constant acetaldehyde concentration, gas and liquid flow rates, but various catalyst concentrations. The extent of oxidation was followed by analysing the products for peracetic acid, acetaldehyde, AMP and acetic acid at convenient intervals.

XII.3 Results

In the following experiments, the feed compositions with the exception of the catalyst were kept approximately constant. Acetic acid formed^o was estimated by material balance*

Feed Composition

Acetaldehyde: 75.5 gm = 96 ml.

Acetic acid: 77.0 gm = 75 ml.

Make up to 1000 ml with ethyl-acetate

$$\% \text{ yield} = \frac{\text{moles of (peracetic acid + AMP)}}{\text{moles of acetaldehyde in feed}}$$

Tables and Graphs

Table (18A) and Figure (12A) show results of a typical run.

The percentage yield of peracetic and acetic acid at various catalyst concentrations are tabulated in Table (18A) and plotted in Figure (13A)

Experiment No 3 Amount of catalyst = 0.066 gm in 1000 ml of feed solution.

Sample No.	Time Hr	ACOOH Wt %	ACH Wt %	ACOH Wt %	PA + AMP Wt %	Yield %	T °C
1	1.00	2.36	2.55	1.51	4.33	30.0	14
2	1.50	2.51	2.53	1.15	4.71	32.6	"
3	2.00	2.585	2.51	1.17	4.71	32.6	"
4	2.50	2.585	2.49	1.19	4.71	32.6	"
5	3.75	2.625	2.49	1.46	4.44	30.5	"
6	4.50	2.66	2.49	1.46	4.44	30.5	"

TABLE 20A ANALYTICAL RESULTS OF A TYPICAL EXPERIMENT

* It was assumed that loss by evaporation was the same for all the runs. The estimated values of the acetic acid concentration may be used only for qualitative interpretation.

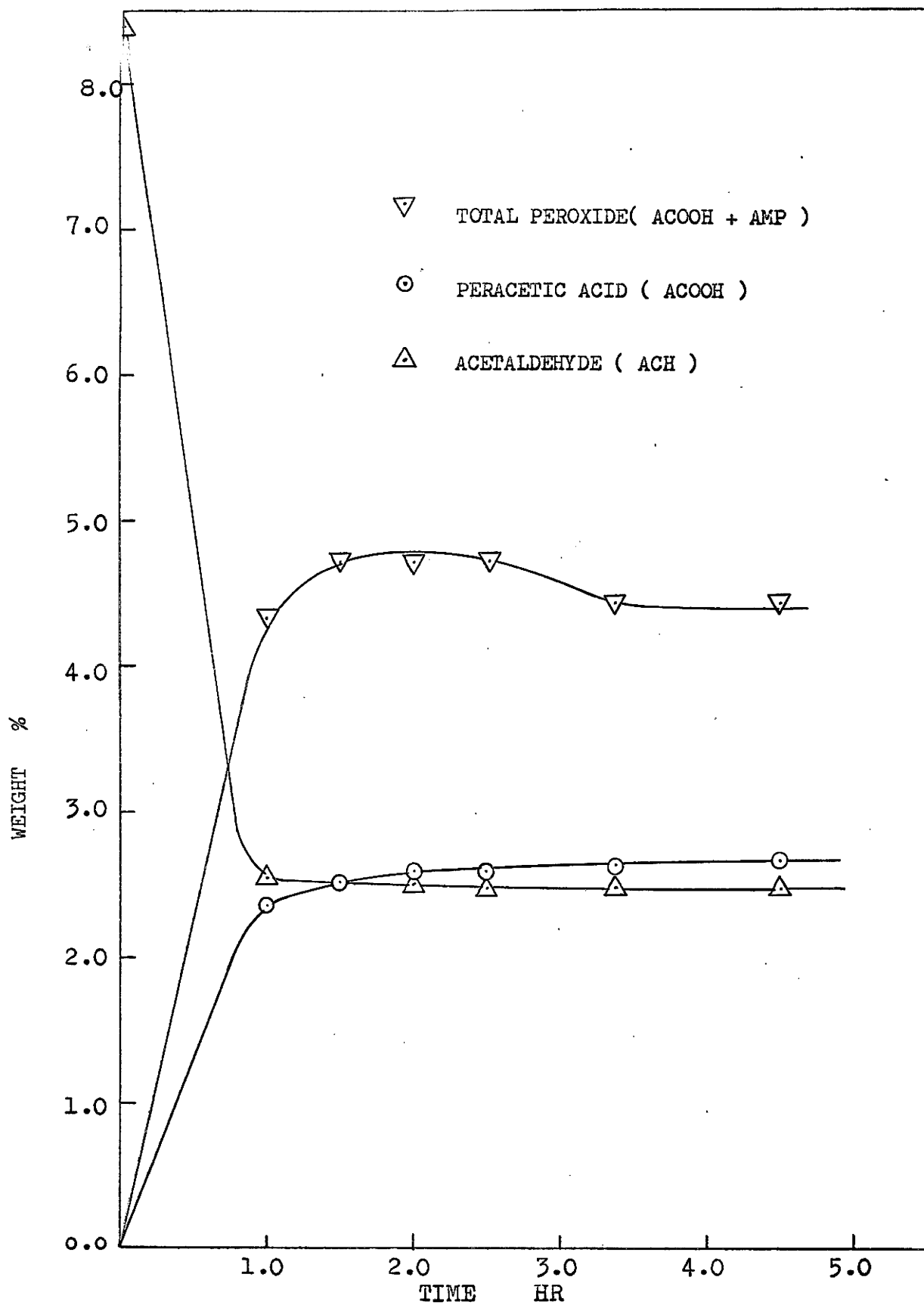


FIGURE 12A WEIGHT % OF PRODUCTS AND REACTANT
VERSUS TIME

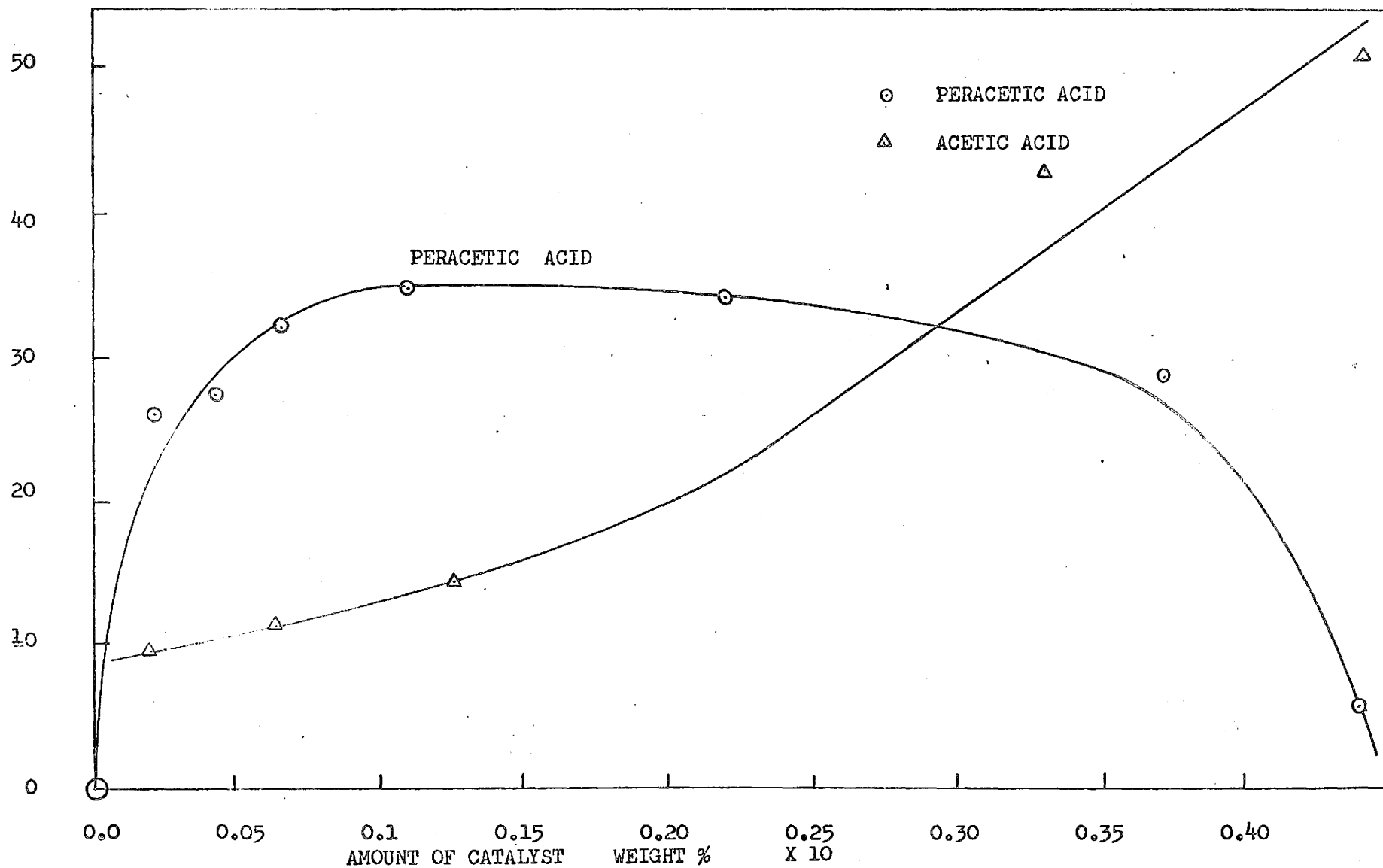


FIGURE 13A % YIELD OF PERACETIC ACID AT VARIOUS CATALYST CONCENTRATIONS

Catalyst % Wt	% Yield		T°C
	Peracetic Acid	Acetic Acid	
0.00244	26.0	9.0	12°
0.00488	27.0		14
0.00732	32.0	10.1	14
0.00988	31.0		13
0.0122	34.6	13.4	13
0.0244	34.0		13
0.0369	28.7	43.2	21
0.0488	5.0	50.7	10

TABLE 21A YIELD OF PERACETIC ACID AND ACETIC ACID AT VARIOUS CATALYST CONCENTRATIONS

The equilibrium constant K estimated from experimental data are tabulated in Table (20A). The value of K at 25°C obtained from Bawn's experimental data was 3.7 litre/mole.

Temperature	K $\frac{\text{litre}}{\text{mole}}$
12.5	3.71
13.0	4.03
13.0	2.38 = Average 3.45
14.0	3.87
12.0	3.26

TABLE 22A EQUILIBRIUM CONSTANT

XII.4 Discussions of Results

Figure (14A) shows that the production of peracetic acid increases with time, reaches a maximum, then decreases slightly to a steady - state

value.

The occurrence of the maximum is due to the fact that at the beginning of each run, the filling up of the reactor by the liquid took approximately 45 minutes. Hence, some of this liquid would have a slightly longer contact time with the gas than the average, leading to a higher yield of peracetic acid.

Figure (15A) illustrates the effect of catalyst concentration on product distribution. The increase of peracetic acid production at the beginning of the curve was expected as the rate of its formation was reported to be proportional to catalyst concentration. However, peracetic acid, which is itself an initiator of the reaction, may reach a steady - state*, after which a further increase of catalyst concentration may only accelerate the decomposition of peracetic acid to acetic acid.

The equilibrium constant K estimated showed reasonable consistency indicating the equilibrium



may have existed.

The values of K agreed fairly well with that estimated from Bawn's experimental data (25).

* See I.1.4 "the role of catalyst".

APPENDIX XIII DIGITAL COMPUTER PROGRAMMES

XIII.1 Correlation Using Bolland's Mechanism.

The basic differential equations to be solved are:

$$D_A \frac{d^2 C_A}{dx^2} = RK C_B C_C^n \quad (166A)$$

$$D_B \frac{d^2 C_B}{dx^2} = RK C_B C_C^n + RKK C_B C_C \quad (167A)$$

$$D_C \frac{d^2 C_C}{dx^2} = - RK C_B C_C^n + RKK C_B C_C \quad (168A)$$

The programme consists of two parts:

- (1) Determining the values of n , RK and RKK that best fit the experimental data.
- (2) Predicting the concentration profiles in the film under the experimental conditions and thus the absorption rates using the values of n , RK and RKK determined previously.

The first part of the programme involved a trial-and-error process.

The step-by-step procedure was outlined as follows:

- (1) choose $n = 0.5$
- (2) choose $RKK = 0.0$
- (3) solve equations (166A), (167A) and (168A) for RK using one set of experimental data as boundary conditions. For example,

$$x = 0, C_A = C_{Ai}, \left(\frac{dC_A}{dx} \right)_{x=0} = \frac{-N_A}{D_A} \quad (169A)$$

$$C_A = 0, \quad \frac{dC_A}{dx} = 0, \quad X = X_R, \quad (170A)$$

$$D_B \frac{d^2 C_B}{dx^2} = RKK C_B C_C,$$

$$D_C \frac{d^2 C_C}{dx^2} = RKK C_B C_C$$

$$X = X_L, \quad C_A = 0, \quad C_B = C_{BL}, \quad C_C = C_{CL} \quad (171A)$$

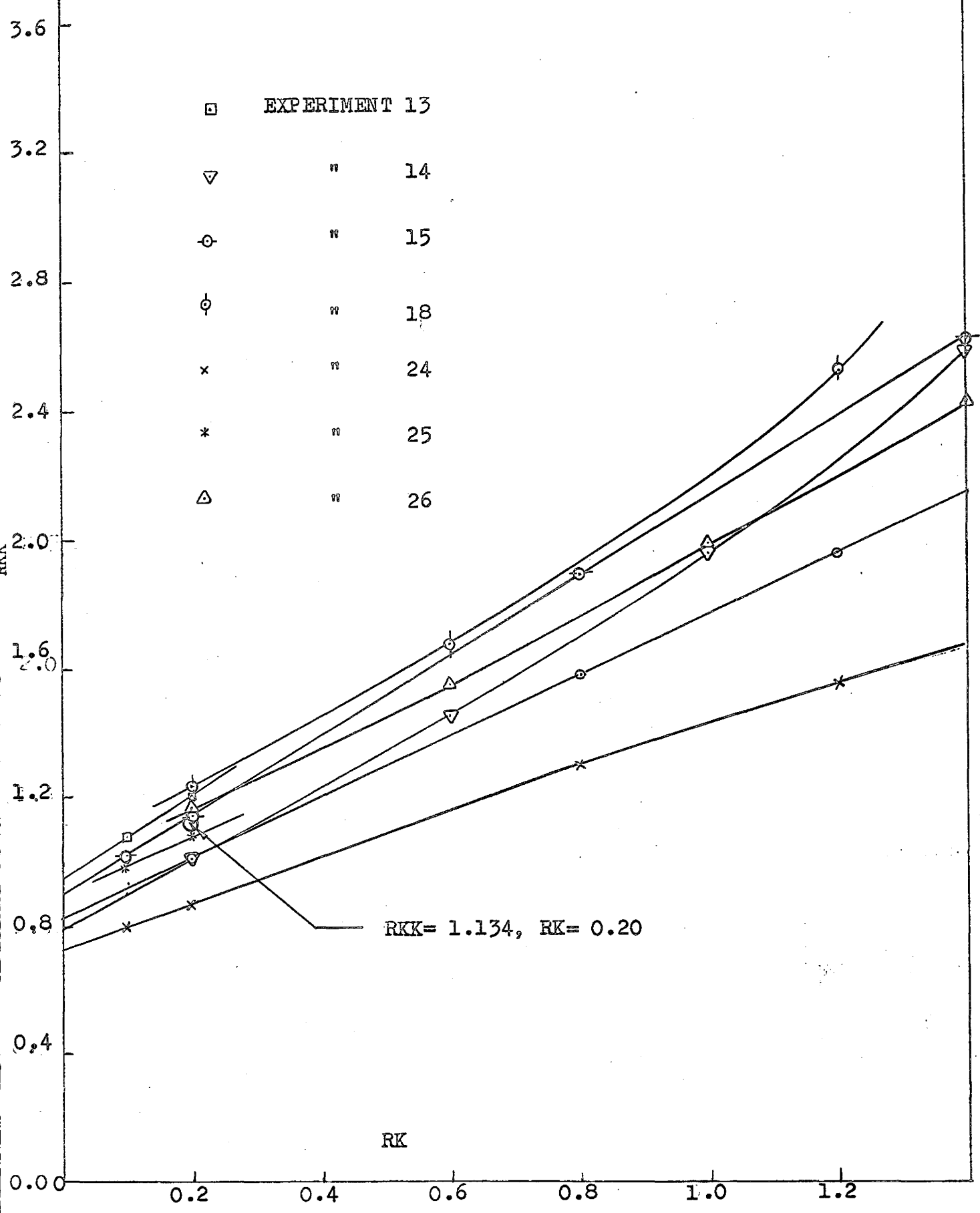
N_A was measured by the gas burette; C_{A1} and D 's were estimated by semi-empirical formulae; C_{BL} and C_{CL} were determined by analytical methods.

Differential equations (166A) to (171A) were solved using the Runge Kutta method. The step-wise trial-and-error procedure for the determination of RK was as follows:

- (a) Choose values for C_{B1} and C_{C1} , concentrations of component B and C at the interface.
- (b) Vary RK by the marching technique until the boundary condition as represented by equation (169A) was satisfied.
- (c) Vary C_{B1} C_{C1} by the marching technique and repeat procedure (b) until the boundary condition as represented by (171A) was satisfied
- (4) increase RKK in steps of 0.2 and solve for RK
- (5) repeat (2), (3), and (4) for all sets of data
- (6) plot RK versus RKK for each set of data as shown in Figure (14A).

Locate the position where the curves converge or lie closest

FIGURE 14A RKK VERSUS RK



together. The ordinate and abscissa will give the best values for RK and RKK

However, it was found that for $n = 0.5$ and 1.5 the RK versus RKK curves converge at negative values of RK. At $n = 2.0$, these curves become parallel. The best values for RK and RKK are found to be 0.2 and 1.134 respectively when $n = 1.9$

The second part of the programme was straightforward. Letting $n = 1.9$, $RK = 1.134$, $RKK = .2$ in equations (166A), (167A) and (168A) and using the bulk concentrations as the boundary conditions, $\frac{dC_A}{dx}$ at $x=0$ was found by a trial-and-error procedure.

The concentration profiles of the various components as predicted by the correlation are given in table 23A. The algorithm is shown in Figure 15A.

XIII.2 Diffusion with Second Order Chemical Reaction

The differential equations to be solved are:

$$D_A \frac{d^2 C_A}{dx^2} = k_{c2} C_A C_B \quad (172A)$$

$$D_B \frac{d^2 C_B}{dx^2} = k_{c2} C_A C_B \quad (173A)$$

The computer programme for the solution of (172A) and (173A) is essentially the same as given in XIII.1.

XIII.3 Computer Programme for Statistical Evaluation

Notation

$R = r_c$; $SY = S(\bar{y})$; $SB = S(b)$; $BETA = b$; $ALPHA = a$;

N = number of data points

x	C _A	C _B	$\frac{dC_A}{dx}$	$\frac{dC_B}{dx}$	C _C	$\frac{dC_C}{dx}$
EXPERIMENT 13						
0.	0.236000	2.917500	-496.000000	0.	6.270000	0.
0.000200	0.146076	2.934095	-384.687832	166.106089	6.245622	-243.476189
0.000400	0.078398	2.983947	-273.568058	332.879795	6.172715	-484.670181
0.000600	0.032894	3.067128	-163.053545	499.701813	6.051833	-722.620026
0.000800	0.009401	3.183573	-53.647690	665.776276	5.883742	-956.154968
0.000900	0.006279	3.254195	0.173106	746.966873	5.782301	-1072.010468
0.001100	0.	3.404154	0.	752.670494	5.568766	-1063.363205
0.001300	0.	3.555258	0.	758.411865	5.356967	-1054.655594
0.001500	0.	3.707513	0.	764.175621	5.146914	-1045.911728
0.001700	0.	3.860921	0.	769.946442	4.938610	-1037.155624
0.001900	0.	4.015483	0.	775.709038	4.732056	-1028.411285
0.002100	0.	4.171195	0.	781.448135	4.527248	-1019.702652
0.002300	0.	4.328051	0.	787.148476	4.324176	-1011.053642
0.002500	0.	4.486042	0.	792.794823	4.122825	-1002.488159
0.002700	0.	4.645156	0.	798.371941	3.923176	-994.030113
0.002900	0.	4.805376	0.	803.864586	3.725207	-985.703407
0.003100	0.	4.966685	0.	809.257515	3.528887	-977.531975
0.003300	0.	5.129062	0.	814.535454	3.334183	-969.539772
0.003500	0.	5.292481	0.	819.683121	3.141058	-961.750809
0.003700	0.	5.456915	0.	824.685181	2.949468	-954.189156
0.003900	0.	5.622334	0.	829.526276	2.759365	-946.878952
0.004100	0.	5.788703	0.	834.190979	2.570697	-939.844437
0.004300	0.	5.955987	0.	838.663811	2.383406	-933.109955
0.004500	0.	6.124144	0.	842.929214	2.197429	-926.699974
0.004700	0.	6.293132	0.	846.971550	2.012700	-920.639114
0.004870	0.	6.437439	0.	850.775078	1.856678	-914.952164
EXPERIMENT 21						
0.	0.237000	2.645000	-217.500000	0.	2.793750	0.
0.000200	0.195310	2.648349	-195.777718	33.499779	2.789167	-45.800900
0.000400	0.157961	2.658395	-174.095665	66.982998	2.775443	-91.363439
0.000600	0.124939	2.675123	-152.534386	100.331013	2.752644	-136.509003
0.000800	0.096212	2.698494	-131.174828	133.423578	2.720870	-181.059095
0.001000	0.071734	2.728444	-110.098761	166.138212	2.680258	-224.834604
0.001200	0.051440	2.764886	-89.389047	198.349764	2.630983	-267.655403
0.001400	0.035250	2.807706	-69.129731	229.930296	2.573252	-309.340393
0.001600	0.023068	2.856765	-49.405894	260.749329	2.507312	-349.708080
0.001800	0.014779	2.911897	-30.303236	290.674492	2.433444	-388.577736
0.002000	0.010251	2.972912	-11.907372	319.572639	2.351967	-425.771198
0.002150	0.009290	3.022400	1.296036	340.318607	2.286075	-452.534637
0.002350	0.	3.090670	0.	342.388943	2.195886	-449.362782
0.002550	0.	3.159350	0.	344.422153	2.106326	-446.249004
0.002750	0.	3.228433	0.	346.415428	2.017382	-443.197720
0.002950	0.	3.297911	0.	348.365944	1.929042	-440.213360
0.003150	0.	3.367774	0.	350.270870	1.841292	-437.300373
0.003350	0.	3.438013	0.	352.127361	1.754117	-434.463234
0.003550	0.	3.508618	0.	353.932560	1.667501	-431.706432
0.003750	0.	3.579579	0.	355.683590	1.581428	-429.034489
0.003950	0.	3.650885	0.	357.377567	1.495880	-426.451942
0.004150	0.	3.722523	0.	359.011589	1.410840	-423.963364
0.004350	0.	3.794482	0.	360.582729	1.326288	-421.573353
0.004550	0.	3.866749	0.	362.088051	1.242203	-419.286541
0.004750	0.	3.939309	0.	363.524590	1.158565	-417.107594
0.004870	0.	3.983014	0.	364.889362	1.108637	-415.041210

TABLE 23A CONCENTRATIONS AND CONCENTRATION GRADIENTS VERSUS DISTANCE FROM INTERFACE

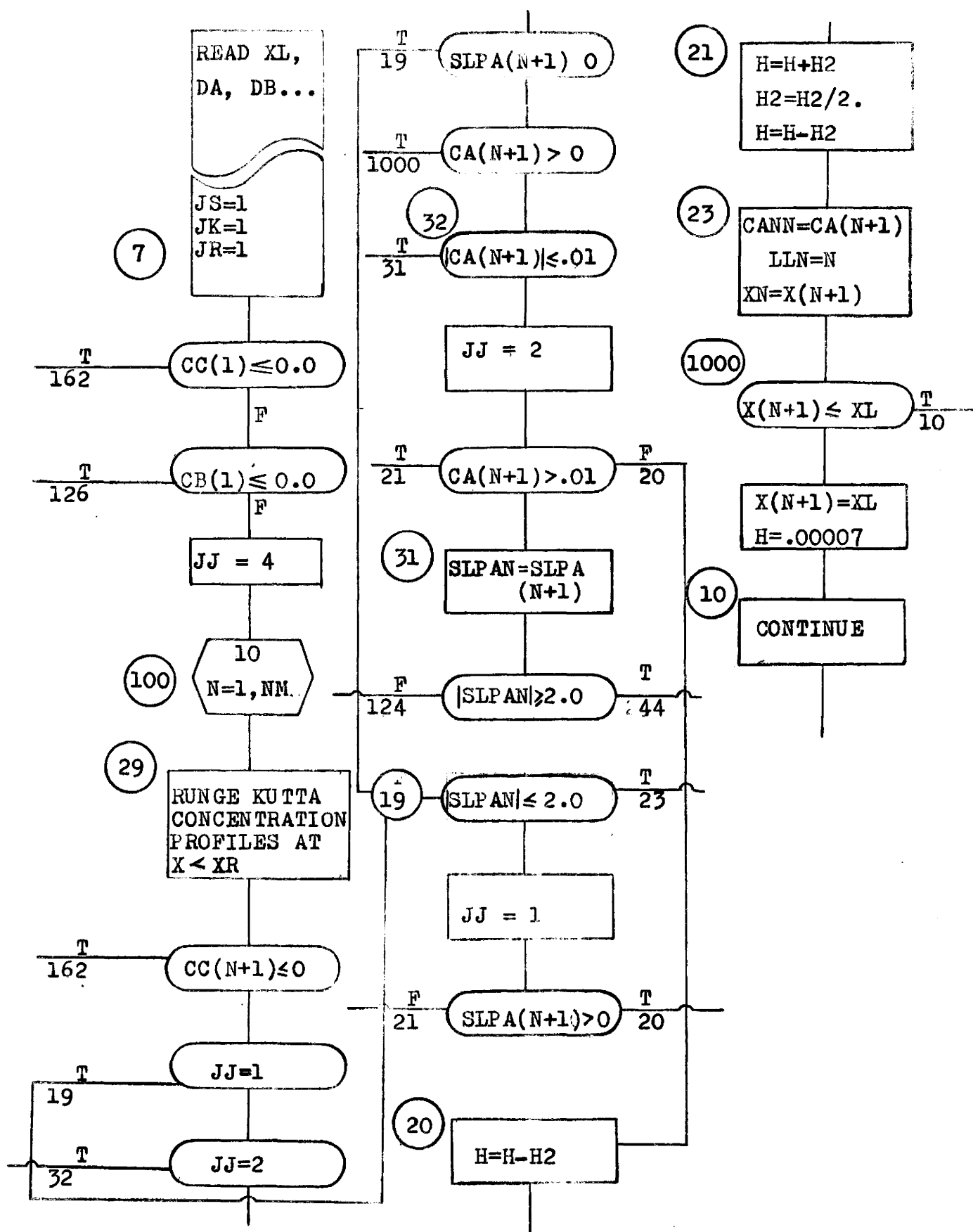


FIGURE 15A ALGORITHM--DIGITAL COMPUTER PROGRAMME

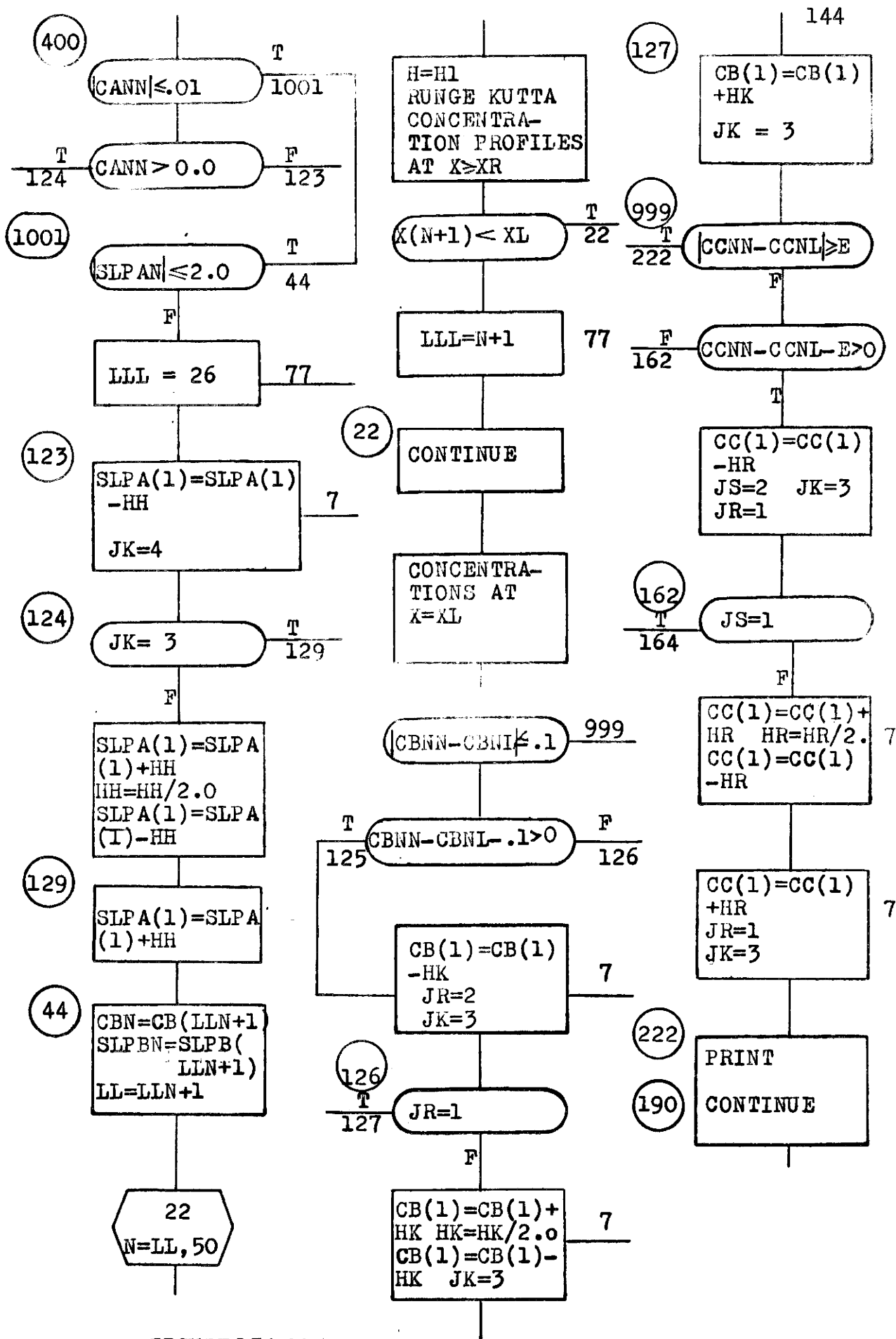


FIGURE 15A CONTINUED

C DIFFUSION INTO A FILM WITH CHEMICAL REACTION

C BOLLAND'S MODIFIED MECHANISM

C FILM THICKNESS = 0.00487 FT

DIMENSION CA(55),CB(55),SLPA(55),SLPB(55),X(55) ,CC(55),SLPC(

15)

READ 6, XL, DA, DB, H1, SLPBO, NM ,DC

PRINT 6,XL, DA, DB, H1, SLPBO, NM ,DC

6 FORMAT (F10.6, 2E10.2, 2F10.5, I5,E10.2)

II=1

1 CONTINUE

READ 200,E

200 FORMAT (F10.5)

READ 9, M, SLPAO, CBNN, RK, CA(1), CB(1) ,CCNN,CC(1)

PRINT 9,M, SLPAO, CBNN, RK, CA(1), CB(1) ,CCNN,CC(1)

RK=1.134

RKK=0.2

191 CONTINUE

JS=1

JK=3

JR=1

9 FORMAT (I5, 7F10.4)

SLPA(1)=SLPAO

SLPB(1)=SLPBO

SLPC(1)=0.0

HR=1.0

HK=1.0

HH=10.

7 X(1)=0.0

IF(CC(1).LE.0.0) GO TO 162

IF (CB(1).LE.0.0) GO TO 126

JJ=4

100 DO 10 N=1,NM

H=H1

H2= .00005

29 CONTINUE

DUM3=RK*CB(N)*(CC(N)**1.9)/DA

TK1=H*(SLPA(N))

TM1=H*DUM3

TK2=H*(SLPA(N)+TM1/2.)

TM2=TM1

TK3=TK2

TM3=TM2

TM4=TM3

TK4=TK3

CA(N+1)=CA(N)+(TK1+2.*TK2+2.*TK3+TK4)/6.0

X(N+1)=X(N)+H

SLPA(N+1)=SLPA(N)+(TM1+2.*TM2+2.*TM3+TM4)/6.0

DUM2=RK*CC(N)**1.9/DB +RKK*CC(N)/DB

SK1=H*(SLPB(N))

SM1=H*(DUM2*CB(N))

SK2=H*(SLPB(N)+SM1/2.)

SM2=H*(DUM2*(CB(N)+SK1/2.))

SK3=H*(SLPB(N)+SM2/2.)

SM3=H*(DUM2*(CB(N)+SK2/2.))

SK4=H*(SLPB(N)+SM3)

SM4=H*(DUM2*(CB(N)+SK3))

CB(N+1)=CB(N)+(SK1+2.*SK2+2.*SK3+SK4)/6.

SLPB(N+1)=SLPB(N)+(SM1+2.*SM2+2.*SM3+SM4)/6.

DUM1=-RK*CB(N)/DC

```

DUM4=RKK* CB(N)/DC
RK1=H*(SLPC(N))
RM1=H*(DUM1*CC(N)**1.9+DUM4*CC(N))
RK2=H*(SLPC(N)+RM1/2.)
RM2=H*(DUM1*(CC(N)+RK1/2.))**1.9+DUM4*(CC(N)+RK1/2.)
RK3=H*(SLPC(N)+RM2/2.)
RM3=H*(DUM1*(CC(N)+RK2/2.))**1.9+DUM4*(CC(N)+RK2/2.)
RK4=H*(SLPC(N)+RM3)
RM4=H*(DUM1*(CC(N)+RK3)**1.9+DUM4*(CC(N)+RK3/2.))
CC(N+1)=CC(N)+(RK1+2.*RK2+2.*RK3+RK4)/6.0
SLPC(N+1)=SLPC(N)+(RM1+2.*RM2+2.*RM3+RM4)/6.0
CANN=CA(N+1)
SLPAN=SLPA(N+1)
XN=X(N+1)
IF (CC(N+1).LE.0.0) GO TO 162
IF (JJ.EQ.1) GO TO 19
IF (JJ.EQ.2) GO TO 32
IF (SLPA(N+1).GE.0.0) GO TO 19
IF (CA(N+1).GT.0.0) GO TO 1000
32 IF( ABS(CA(N+1)).LE..01 ) GO TO 31
JJ=2
IF (CA(N+1)-.01 ) 20,31,21
31 SLPAN=SLPA(N+1)
LLN=N
CANN=CA(N+1)
IF (ABS(SLPAN).LE.2. ) GO TO 44
GO TO 124
19 IF (ABS(SLPA(N+1)).LE.2. ) GO TO 23
JJ=1
IF (SLPA(N+1)) 21,23,20
20 H=H-H2
GO TO 29
21 H=H+H2
H2=H2/2.
H=H-H2
GO TO 29
23 CANN = CA(N+1)
FPT=CANN
LLN=N
XN=X(N+1)
IF (ABS(FPT)-.01 ) 44,44,400
1000 IF (X(N+1) .LE.XL ) GO TO 10
X(N+1)=XL
H=.00007
GO TO 29
10 CONTINUE
400 IF (ABS(CANN) .LE. 0.01) GO TO 1001
IF (CANN) 124,1002,123
1001 IF (ABS(SLPAN) .LE. 2.) GO TO 44
1002 LLL=26
GO TO 77
123 SLPA(1)=SLPA(1)-HH
JK=4
GO TO 7
124 IF (JK.EQ.3) GO TO 129
SLPA(1)=SLPA(1)+HH
HH=HH/2.
SLPA(1)=SLPA(1)-HH

```

```

      PRINT 41, SLPA(1)
      GO TO 7
129 SLPA(1)=SLPA(1)+HH
41  FORMAT (6H SLPA2, F20.10)
      GO TO 7
44  CONTINUE
      CBN= CB(LLN+1)
      CCN= CC(LLN+1)
      SLPBN= SLPB(LLN+1)
      SLPCN= SLPC(LLN+1)
      LL=LLN+1
99  DO 22 N=LL,50
      H=H1
      DUM2=RKK*CC(N)/DB
      SK1=H*(SLPB(N))
      SM1=H*(DUM2*CB(N))
      SK2=H*(SLPB(N)+SM1/2.)
      SM2=H*(DUM2*(CB(N)+SK1/2.))
      SK3=H*(SLPB(N)+SM2/2.)
      SM3=H*(DUM2*(CB(N)+SK2/2.))
      SK4=H*(SLPB(N)+SM3)
      SM4=H*(DUM2*(CB(N)+SK3))
      CB(N+1)=CB(N)+(SK1+2.*SK2+2.*SK3+SK4)/6.
      SLPB(N+1)=SLPB(N)+(SM1+2.*SM2+2.*SM3+SM4)/6.
      DUM4=RKK* CB(N)/DC
      RK1=H*(SLPC(N))
      RM1=H*(          DUM4*CC(N))
      RK2=H*(SLPC(N)+RM1/2.)
      RM2=H*(          DUM4*(CC(N)+RK1/2.))
      RK3=H*(SLPC(N)+RM2/2.)
      RM3=H*(          DUM4*(CC(N)+RK2/2.))
      RK4=H*(SLPC(N)+RM3)
      RM4=H*(          DUM4*(CC(N)+RK3/2.))
      CC(N+1)=CC(N)+(RK1+2.*RK2+2.*RK3+RK4)/6.0
      SLPC(N+1)=SLPC(N)+(RM1+2.*RM2+2.*RM3+RM4)/6.0
      SLPA(N+1)=0.0
      CA(N+1)=0.0
      X(N+1)=XN+H*FLOAT(N-LLN)
      IF (X(N+1).LT.XL) GO TO 22
      LLL=N+1
      GO TO 77
22  CONTINUE
77  FRR=(XL-X(LLN-1))/H
      X(LLN)=XL
      CBNL=CB(LLN-1)+(CB(LLN)-CB(LLN-1))*FRR
      CCNL=CC(LLN-1)+(CC(LLN)-CC(LLN-1))*FRR
      CB(LLN)=CBNL
      CC(LLN)=CCNL
      IF (ABS(CBNN-CBNL).LE..10) GO TO 999
      IF (CBNN-CBNL-.10) 125,999,126
125 CB(1)=CB(1)-HK
      JR=2
      JK=3
      RH=RK
      HH=10.
      GO TO 7
126 IF (JR.EQ.1) GO TO 127
      CB(1)=CB(1)+HK

```

```

HK=HK/2.
  CB(1)=CB(1)-HK
RK=RH
HH=10.
JK=3
GO TO 7
127 CB(1)=CB(1)+HK
HH=10.
JK=3
RH=RK
GO TO 7
999 CONTINUE
  IF (ABS(CCNN-CCNL).LE.E ) GO TO 222
  IF (CCNN-CCNL-E ) 161,222,162
161 CC(1)=CC(1)-HR
JS=2
JK=3
RH=RK
HH=10.
JR=1
  HK=1.0
GO TO 7
162 IF (JS.EQ.1) GO TO 164
CC(1)=CC(1)+HR
HR=HR/2.
  CC(1)=CC(1)-HR
  HK=1.0
JK=3
RK=RH
HH=10.
JR=1
  GO TO 7
164 CC(1)=CC(1)+HR
JR=1
JK=3
RH=RK
  HK=1.0
HH=10.
GO TO 7
222 PRINT 888,M
PRINT 192, RKK
PRINT 111,RK
888 FORMAT (9H EXPT NO=, I10)
333 FORMAT (6H CANN=,2F20.5, I5)
PRINT 145
111 FORMAT (10X,4H RK=,F20.5)
PRINT 155, (X(I),CA(I),CB(I),SLPA(I),SLPB(I),
1CC(I),SLPC(I),I=1,LLL)
155 FORMAT ( 3X, 7F16.6)
145 FORMAT (10X,3H X,13X,3H CA,13X,3H CB,11X,5H SLPA,11X,5H SLPB,
113X,3H CC, 11X,5H SLPC)
192 FORMAT (4H RKK, F20.5)
190 CONTINUE
  IF (II.GE.2 ) GO TO 444
  II=II+1
GO TO 1
444 STOP
END

```

STATISTICAL EVALUATION OF CORRELATIONS

```

READ 10, N      ,M
SUM X = 0.0
SUM Y = 0.0
SUM XY = 0.0
SUM XX = 0.0
SUM YY=0.0
I = 1
1 READ 11, Y,X
  SUM X = SUM X + X
  SUM Y = SUM Y + Y
  SUM XY = SUM XY + X*Y
  SUM XX = SUM XX + X*X
  SUM YY=SUM YY+Y*Y
  IF (I - N) 3,2,2
3 I = I + 1
  GO TO 1
2 SIZE = N
  SUM1YY=SUM YY-SUM Y*SUM Y/SIZE
  SUM1XX=SUM XX-SUM X*SUM X/SIZE
  SUM1XY=SUM XY-SUM Y*SUM X/SIZE
  R=SUM1XY/(SQRT(SUM1XX*SUM1YY))
  PRINT 112,N,M
  PRINT 113,SUM X,SUM Y,SUM XY,SUM XX,SUM YY ,SUM1YY,SUM1XX,SUM1XY
  PRINT 14, R
  SY=(1.-R*R)*SUM1YY/(SIZE-2.)
  SB=SQRT(SY/SUM1XX)
  BETA = (SUMX * SUMY - SIZE * SUMXY)/(SUMX * SUMX - SIZE * SUMXX)
  ALPHA = (SUM Y - BETA * SUMX)/SIZE
  PRINT 12, ALPHA, BETA
  PRINT 13, SB
14 FORMAT (2HR=, F20.5)
111 CONTINUE
113 FORMAT (3X,8F12.3)
112 FORMAT (10HNO OF DATA,I10,5X,7HEXPT NO,I10//)
13 FORMAT (17HVARIANCE OF SLOPE, F20.5//)
10 FORMAT (2I5)
11 FORMAT (2F 10.6)
12 FORMAT (9HINTERCEPT,F20.5,5X,5HSLOPE,F20.6K//)
END

```

APPENDIX XIV ANALOG COMPUTER CIRCUIT

Equations to be solved are given in II.2.1.2. The method of solution is the same stepwise trial-and-error procedure outlined in XIII.1 except that the first two steps are omitted.

The analog computer circuits are shown in Figure (15A)

Scaling

The maximum values that all the variables may assume are listed in Table (24A)

Variable	Maximum Values
C_A	.25 gm-moles/ft ³
C_B	10 gm-moles/ft ³
C_C	5 gm-moles/ft ³
dC_A/dx	-500 gm-moles/ft ⁴
dC_B/dx	2000 gm-moles/ft ⁴
dC_C/dx	2000 gm-moles/ft ⁴
$D's$	20×10^{-5}
k	100 hr ⁻¹

TABLE (24A) MAXIMUM VALUES OF VARIABLES

Let $C_A' = 10C_A$; $x' = 1000x$; $k_A' = k/10^2$; $D_A' = 1/D_A \times 10^{-4}$.

then,

$$\frac{d^2 C_A'}{dx'^2} = \frac{10 d^2 C_A}{10^6 dx^2} = 10 k_A' D_A' C_B$$

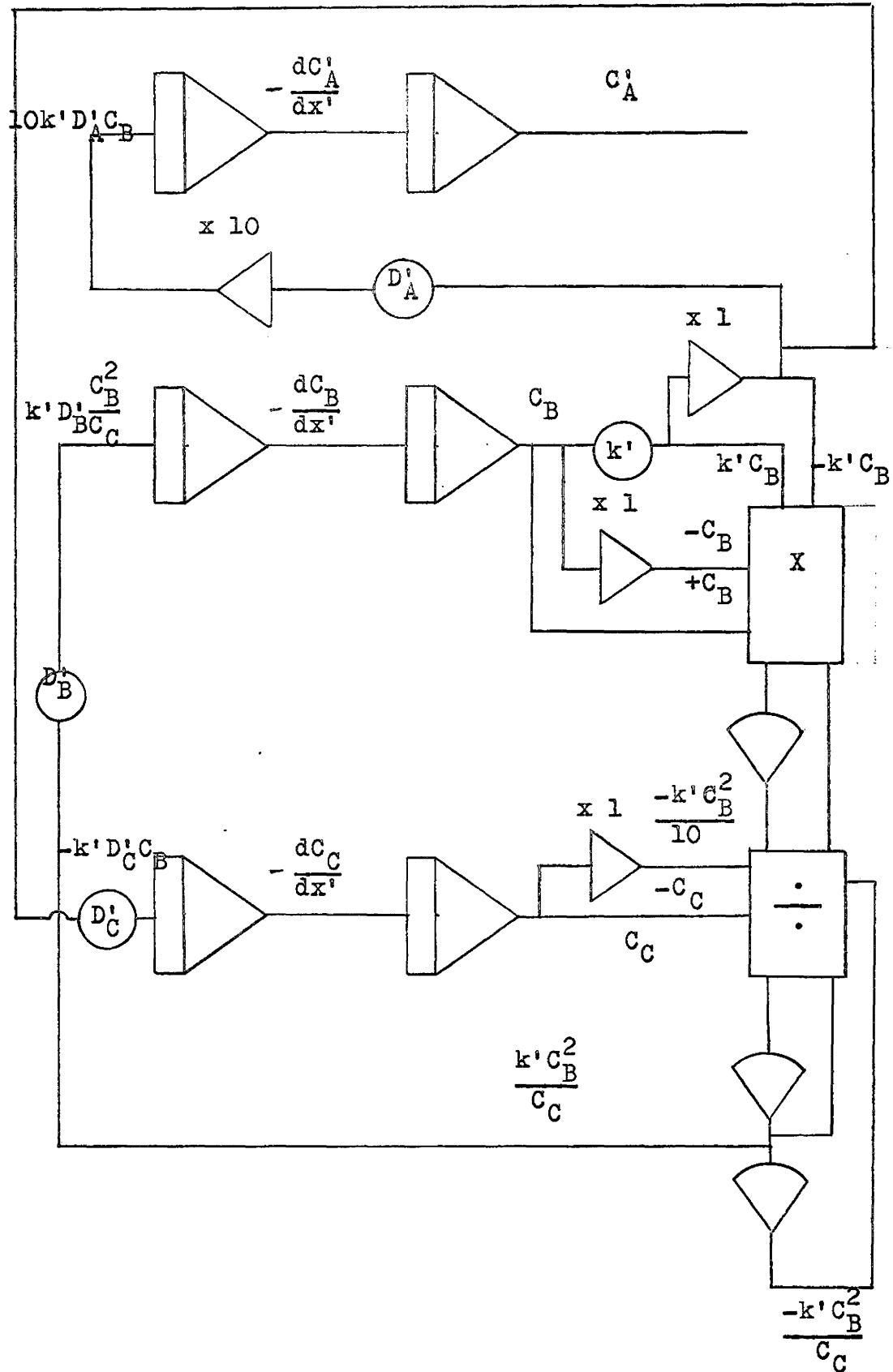


FIGURE 16A ANALOG COMPUTER CIRCUIT

$$\frac{d^2 C_B}{dx'^2} = \frac{1}{10^6} \frac{d^2 C_B}{dx^2} = k_A^{D_B} \frac{C_B^2}{C_C}$$

$$\frac{d^2 C_C}{dx'^2} = \frac{1}{10^6} \frac{d^2 C_C}{dx^2} = -k_A^{D_C} C_B$$

LITERATURE CITED

1. Hatta, S. Techol. Rept. Tohoku Imp. Univ. 8, 1 (1928-29)
2. Hatta, S, ibid., 10, 119 (1932)
3. Davis, H. S. and G. S. Crandall, J. Am. Chem. Soc , 52, 3757, 3709 (1930)
4. Whitman, W. G., Chem. and Met. Eng., 29, No. 4 (July 23, 1923)
5. Van Krevelen, D. W., and Hoftijzer, P. T., Rec. Trav. Chim. 67, 563, (1948)
6. Bawn, C.E. and Williamson, J.B., Trans. Fara. Soc., 47, 721 (1951)
7. Bawn, C. E., Hobin, T. P. and Raphael L., Proc. Roy. Soc. (London) A237, 313-24 (1956)
8. Higbie, R., Trans. Am. Inst. Chem. Engrs. 31, 365 (1935)
9. Danckwerts, Trans. Fara. Soc., 46, 300 (1950)
10. Astarita G., Marrucci, G., I & EC Fundamentals, Vol 2, 4, Feb., (1963)
11. Brian, P. L. T., A.I.Ch.E. J. 10, (1) 5, Jan. (1964)
12. Brian, P. L. T., Hurley, J. F., Hasseltine, E. H., ibid., 7, (2) 226, June (1961)
13. Carslaw and Jaeger, Conduction of Heat in Solid London Oxford Univ. Press, 1947, p. 64.
14. Van de Vusse, J. G., Chem. Eng. Sci. 16, 21 (1961)
15. Carpenter, B. H., I.E. & C. Proc. Design and Development, 4, (1), Jan. (1965)
16. Carslaw and Jaeger, Conduction of Heat in Solid London Oxford Univ. Press 1947 p. 62
17. Spalding, C. W., A.I.Ch.E. J. 8, (5), 685, Nov. (1962)
18. Gilliland, E. R., Baddour, R. E., Brian, P. L. T., ibid. 4, (2), 223, June (1958)
19. Emmert, R. E., Pigford, R. L., ibid., 8, (2), May (1962)

20. Liebig, Annalen, 14, 139, (1835)
21. Bach, Compt rend., 124, 951, (1897)
22. U. S. Patent, 2833814, May 6, 1958
23. U. S. Patent, 2830080, Apr. 8, 1958
24. U. S. Patent, 2804473, Aug. 27, 1957
25. Bawn, C. E., Williamson, J. B., Trans. Fara. Soc. 47, 721 (1951)
26. Starcher, P. S., Phillips, B., Frostick, F. C., Jr., J. Org. Chem. 26, 3568-71 (1961)
27. Twigg, G. H., Symposium. Oxidation Processes in Chemical Manufacture, Sept. (1961)
28. Swern, Chem. Rev., 45, 1, (1949)
29. M. P. Hahto, Peracetic Acid Method of Analysis P.R.R. Shawinagan Chem. Co. Ltd., July (1961)
30. D'an and Frey, Anorg. Che. 84, 145, (1914)
31. Tomoda, J. S. C. I. 48, 14, 76T - 77T (1929)
32. Akehata, Absorption of Ethylene by Chlorine Water, to be Published in Can. J. Chem. Eng.
33. Quarterly Review, Chem Soc., Vol 3-4, 1949-50
34. Nozaki, K. and Bartlett, P. D., J. Amer. Chem. Soc. 68, 1686, (1946)
35. Cass, W. E., ibid., 68, 1976, (1946)
36. Brown, D. J., ibid., 70, 1208, (1948)
37. Bolland, J. L., Gee Geoffrey Trans. Fara. Soc. 42, 236, (1946)
38. Bolland, J. L., Pten Have, ibid., 43, 201, (1947)
39. Sharp, Patton, Whitcomb, J. Am. Chem. Soc. 73, 5600 (1951)
40. Dastur, Lea, Analyst 66, 90, (1941)
41. Bateman, L., Trans. Fara. Soc., 42, 266, (1946)
42. Bateman, L., Gee G. Proc. Roy. Soc., A, 195, 376 (1948)
43. Bolland J. L. Proc. Roy. Soc., A, 186, 218, (1946)
44. Galtzenstein, E., U. S. Patent, 1179421 (1916)

45. Kimiya et. al and Ingold, Can. J. Chem. 41, 2020 (1963)
46. Tobolsky, A. V., India Rubber World, 118, 363 (1948)
47. Woodward, A. E., Mesrobian, R. B., J. Am. Chem. Soc., 75 6189 (1953)
48. Tobolsky, A. V., Metz, D. T., Mesrobian, R. B., ibid., 72, 1942) (1950)
49. Ridial, E. K., Robertson, A., Proc. Roy. Soc. (London) A185, 288 (1946)
50. Ingold, "Lipids and their Oxidation" edited by H. W. Schultz and E. A. Day. Publishing Co. Ind. Westport Conn. 1962, Chap. 5
51. Denisov., E. T., Usp. Khim, 29, 1409 (1960)
52. Hildebrand, J. H. and Scott, R. L. "Solubilities of non-electrolytes" Amer. Chem. Soc. Monograph Series Reinhold Publishing Corp. 3rd Ed. p. 244, 425 , 1959
53. Vassilatos, M. A. Sc. Thesis (1960) University of Toronto
54. Crank, J. "The Mathematics of Diffusion", Oxford Clarendon Press, 1959
55. Daniels, F., "Experimental Physical Chemistry" 6th Edition, p. 399
56. Volk, W., "Applied Statistics for Engineers" P. 225. McGraw-Hill Series in Chemical Engineering , 1958.
57. International Critical Tables, vol. 3, pp. 261-270
58. Wilke, C. R., Chem. Eng. Progr. 45, 218 (1949)
59. Treybal, R. E., "Mass Transfer Operation" McGraw-Hill Company Inc. p. 19, 1955
60. Perry, J. H. "Chemical Engineers' Handbook" p. 373 , 3rd Edition